CRANFIELD UNIVERSITY

TOBIAS-AKASH SHANKER

# WHOLE-BODY VIBRATION IN THE DEFENCE MARITIME ENVIRONMENT: ANALYSIS AND SIMULATION OF VERTEBRAL CANCELLOUS BONE

CRANFIELD DEFENCE AND SECURITY

PhD THESIS
Academic Year: 2014 - 2018

Supervisor: PETER ZIOUPOS
June 2018

CRANFIELD UNIVERSITY

CRANFIELD DEFENCE AND SECURITY

PhD

Academic Year 2014 - 2018

TOBIAS-AKASH SHANKER

# WHOLE-BODY VIBRATION IN THE DEFENCE MARITIME ENVIRONMENT: ANALYSIS AND SIMULATION OF VERTEBRAL CANCELLOUS BONE

Supervisor: PETER ZIOUPOS

June 2018

# ABSTRACT

Whole-body vibration has been shown to increase the risk of low back pain, especially during extreme exposures such as on marine craft which can reach peak loads of 20g during “slamming”. Wedge fractures and trabecular damage of vertebrae have been noted at these high acceleration events. There is a need of a quantitative link between whole-body vibration and spinal damage, with possible tools for prediction. There is currently little known about the role trabecular damage plays under damage from Whole-body vibration, as well as a lack of robust and repeatable trabecular fatigue FE techniques.

A fatigue model for trabecular vertebral bone was developed in four steps: Fatigue testing of porcine vertebral cores; validation of a novel element material method; fatigue simulation of a porcine core to select the failure method; prediction using the validated material mapping model with the best failure method on human vertebral cubes.

The fatigue tests were carried out on porcine trabecular cores loaded at 2Hz with varying normalised stress values until fatigue failure. Signal analysis was used to examine the vibrational statistics as per ISO 2631-1. This was done to both compare the statistical approaches used in measuring vibration and quantifying a link with in-vivo damage. Vibration Dose Value exposure was found to be the best predictor of failure within these tests. Its $4^{th}$ order averaging accounted for minute differences in acceleration that RMS could not, even at the low frequency tested. Fatigue of porcine bone has not been extensively examined in the literature and experimental results indicate that there are significant differences in its fatigue behaviour compared to human and bovine bone.

Currently there is a need to calibrate the material models used in finite element simulations to achieve parity with experimental testing. This thesis validates a novel greyscale mapping technique which does not require calibration. This was done on human trabecular cores taken at different orientations, with both experimental and finite element simulations. With these tissue material

properties the simulations showed good agreement in terms of mechanical response in all three directions.

Fatigue was calculated using finite element analysis on a porcine core which was validated against experimental results. Three methods were tested for this: A stress based model which bases the element failure criteria in respect to the cycle number; a model which calculates failure by the specific element stress and a strain model which fails elements based upon total element strain. This was conducted using a direct iterative approach using linear isotropic material properties with failure calculated after each cycle, keeping down computational costs. All methods took roughly the same amount of time for a load step. Failure was predicted much sooner in comparison to the experimental with the specific element stress and strain models. The method which varies failure based on cycle count was selected as it was the most accurate. As porcine fatigue testing has not been examined the results were difficult to compare and differed from previous experiments on human and bovine tissues.

Using the validated material model and the best performing fatigue method this was then applied to Human trabecular specimens to estimate the fatigue life. The cubes were then loaded in the main physiological direction from in-vivo loading. This predicted most of the expected mechanical behaviour during fatigue including a linear relationship between damage fraction and modulus reduction. It also highlights the importance of angular orientation in regards to trabecular fatigue life. Although it tended to underestimate the fatigue life of bone, it was in good agreement with the literature over the normalised stress range tested. The differences in simulated fatigue behaviour and the literature, seen previously with porcine tissue, were not apparent here. With further study and validation this model has the potential to improve the understanding of trabecular fatigue failure using vibration exposure as the model stimulus.

Keywords:

*Fatigue, Biomechanics, low back pain, Finite Element Analysis, ISO 2631, Spine, Micro-Computed Tomography, Control of Vibration at Work*

# ACKNOWLEDGEMENTS

This research was made possible by a grant from the Royal Centre for Defence Medicine.

This Thesis is dedicated to my family, friends and colleagues who supported me; new friends I've met along the way; and those who are no longer with us.

In Memoriam:

| | |
|---|---|
| Mrs. Pushpa Devi Singh | (1927 - 2017) |
| Dr. Michael Cleveland Gibson | (1981 – 2018) |

# TABLE OF CONTENTS

# LIST OF FIGURES

# LIST OF TABLES

# LIST OF EQUATIONS

# LIST OF ABBREVIATIONS

| | |
|---|---|
| AP | Anterior-Posterior |
| BMD | Bone Mineral Density |
| BSI | British Standards Institution |
| BV | Material Volume |
| CF | Crest Factor |
| Conn. | Connectivity |
| Conn. D | Connectivity Density |
| CT | Computed Tomography |
| CVWR | Control of Vibration at Work Regulations |
| DA | Degree of Anisotropy |
| DDD | Degenerative Disc Disease |
| DFT | Discrete Fourier Transform |
| DOF | Degree of Freedom |
| DRI | Dynamic Response Index |
| EAV | Exposure Action Value |
| EC | European Council |
| ELV | Exposure Limit Value |
| eVDV | Estimated Vibration Dose Value |
| FE | Finite Element |
| FEA | Finite Element Analysis |
| FFT | Fast Fourier Transform |
| FIOSH | Federal Institute for Occupational Safety and Health |
| FT | Fourier Transform |
| GS | Greyscale |
| HAV | Hand-arm Vibration |
| HGZ | Health Guidance Zones |
| HPC | High-performance computing |
| HSC | High Speed Craft |
| HU | Hounsfield Units |
| IS | Inferior-Superior |
| ISO | International Organisation for Standardization |

| | |
|---|---|
| IVD | Intervertebral Disc |
| LBP | Low Back Pain |
| MCA | Maritime and Coastguard Agency |
| ML | Mediolateral |
| MoD | Ministry of Defence |
| MRI | Magnetic Resonance Imaging |
| NASA | National Aeronautics and Space Administration |
| NDRI | National Disease Research Interchange |
| PSD | Power Spectral Density |
| RMS | Root Mean Square |
| RNN | Recursive Neural Network |
| SD | Standard Deviation |
| TbTh | Trabecular Thickness |
| TV | Total Volume |
| VDV | Vibration Dose Value |
| WBV | Whole-body Vibration |
| WIS | Wounded, Injured and Sick |

# CONFERENCE PRESENTATIONS – Main Author

*1.* Shanker T, Zioupos P (2017)

Can vibration statistics of an idealised sine wave be used to examine fatigue properties of porcine trabecular bone?

52nd UK Conference on Human Responses to Vibration (HRV2017), Shrivenham, 5-6 September 2017

*2.* Shanker T, Franceskides C, Gibson M, Clasper J, Adams G & Zioupos P (2016)

Finite element optimisation techniques applied to human vertebral cancellous bone

51st UK Conference on Human Responses to Vibration (HRV2016), Gosport, 14-15 September 2016

*3.* Shanker T, Franceskides C, Gibson M, Clasper J & Zioupos P (2016)

Effects of μCT and FE resolution in expressing anisotropic properties in vertebral cancellous bone.

13th International Symposium on Computer Methods in Biomechanics and Biomedical Engineering (CMBBE), Montreal, September 2015

# CONFERENCE PRESENTATIONS – Associated Author

1. Gibson M, Shanker T, Zioupos P (2017)
   Representation of structural response to vibration in micro-FEA model of trabecular bone
   52nd UK Conference on Human Responses to Vibration (HRV2017), Shrivenham, 5-6 September 2017

2. Franceskides C, Leger T, Horsfall I, Shanker T, Adams GJ , Clasper J & Zioupos P (2016) Evaluation of bone excision on occipital area of simulated human skull.
   22nd Congress of the European Society of Biomechanics (ESB 2016), Lyon, 10-13 July 2016

3. Wood D, Appleby-Thomas G, Fitzmaurice B, Franceskides C, Shanker T, Zioupos P & Samra A (2016)
   On The Shock Behaviour And Response Of Ovis Aries Vertebrae
   22nd Congress of the European Society of Biomechanics (ESB2016), Lyon, 10-13 July 2016

4. Franceskides C, Shanker T, Gibson M, Clasper J & Zioupos P (2015)
   Input Optimisation for FEA of trabecular bone anisotropy in human thoracic-lumbar vertebrae.
   13th International Symposium on Computer Methods in Biomechanics and Biomedical Engineering (CMBBE), Montreal, September 2015

# INTRODUCTION

## 1.1 Low Back Pain

### 1.1.1 Prevalence and effect

Low back pain (LBP) is a medical condition defined as a “Local or referred pain at the base of the spine”. It will affect 60-80% of us at some point in our lives (Manchikanti, 2000). Most cases are acute and the symptoms dissipate after a few days with over 90% returning to work before 3 months (Andersson, 1999). However if it continues for longer than 7-12 weeks it is classified as chronic and can have severe implications (Duthey, 2013). Globally the prevalence is less in middle- and low-income economies than in high-income economies (Hoy et al., 2012) however with the increase of urbanisation and industrialisation this is speculated to increase (Volinn, 1997). As of 2013 LBP is the global leading cause of disability (Buchbinder et al., 2013).

To the individual LBP can be an ordeal, not just because of the physical pain it causes but also because of loss of earnings. It is the most common reason for people taking days off sick in the UK with approximately 31 million days lost in 2013 due to “Musculoskeletal Conditions” (Jenkins, 2014). This has a further effect on government spending: Mandiakis & Gray (2000) estimate the cost of LBP in the UK to be £1632 million of which only 37% is from treating the condition, the rest is from loss of earnings. This value is even higher in the US: Katz (2006) puts the figure at over $100 billion of which two thirds are indirect costs.

Military service personnel undergo extensive training so that their bodies can withstand the physical challenges required. This is shown in a lowered weighted incidence rate for low back pain per 1000 person-years for US military personnel (Knox et al., 2011) in comparison to the general population (Waterman, Belmont and Schoenfeld, 2012). In contrast to this, the incidence of LBP is higher in population studies of military veterans versus the general public (Groessl et al., 2008) even though they are generally younger and more active.

With such a large incidence rate and impact on society, a considerable amount of research has been conducted to assess the causes of LBP. Shown in Table 1-1 are the risk factors associated with low back pain taken from hundreds of sources including papers, surveys and statistics (Manchikanti, 2000).

| Causal | Probable | Possible | Nonrelated |
|---|---|---|---|
| None | Genetic | Lifting | Body height |
| | Age | Job dissatisfaction | Scoliosis |
| | Smoking | Psychosocial factors | Kyphosis |
| | | Gender | Leg-length discrepancy |
| | | Heavy physical work | Physical activity |
| | | Static work postures | |
| | | Back pain history | |
| | | Vibration | |

**Table 1-1: Risk factors of low back pain (redrawn from** (Manchikanti, 2000)**)**

In this table it can be seen that direct causes for LBP are largely unknown. This is still seen today as most cases are diagnosed as non-specific, i.e. having no distinct root cause.

There are three probable causes: Genetics, Age and Smoking. The role of genetics has been further researched with Battié et al (2007) concluding that *"disc degeneration is one pathway through which genes influence back pain"* with a heritability estimate ranging from 30% to 46%. This is further supported by a study on a population of elderly twins by Hartvigsen, Christensen and Frederiksen (2003) which put a conservative estimate of genetic effects at 25%.

Previous literature reviews have shown an epidemiological link between aging and the reported incidence of LBP. In two review papers it is suggested that the prevalence of chronic LBP increases from the age of 30 until 60 (Hoy et al., 2010; Meucci, Fassa and Faria, 2015).

Smokers have been shown to be at a higher risk to LBP even when accounting for age and social-economic factors such as employment status, level of education and amount of exercise (Deyo and Bass, 1989). Sufferers of LBP were statistically also more likely to be smokers (Frymoyer et al., 1983). A dose response relationship between frequency of smoking and LBP has also been shown (Alkherayf and Agbi, 2009).

This still leaves a majority of the factors for LBP as environmental. In 2010 a series of reviews were carried out by Roffey & Wai et al. which assessed the causality of manual handling (Roffey et al., 2010a), posture (Roffey et al., 2010b), pushing and pulling (Roffey et al., 2010c), sitting (Roffey et al., 2010d), standing or walking (Roffey et al., 2010e), bending or twisting (Wai et al., 2010a), carrying (Wai et al., 2010b) and lifting (Wai et al., 2010c) as independent factors of LBP using the Bradford-Hill criteria. In all the reviews independent causality was disproved. A point of note is that these reviews were conducted from selected epidemiological qualitative studies thus discounting a variety of laboratory studies. The usage of the Hill criteria in these papers have been debated in letters to the editor (Andersen, Haahr and Frost, 2011; Dagenais, Roffey and Wai, 2010, 2011; Kuijer et al., 2011; Takala, 2010; Talmage, 2010). Roffey & Wai et al. also mention that various sub-categories of occupational risk require further study and they only disprove independent causality; in real life combinations of risk factors may occur, such as sitting and poor posture, adding confounding variables to the risk of LBP.

Psychosocial factors cannot be discounted as they affect all qualitative studies on the phenomenon of LBP. The Institute for Work and Health in Canada (Institute for Work & Health, 2012) have shown that the desire to return to work can cause an increase of LBP complaints. Stress, job satisfaction and benefits are key influences in this decision. In a study on low back pain in British school children, Watson et al. (2003) found that emotional wellbeing was associated with LBP while physical factors were not. The importance of mental health and LBP was also investigated in a review paper by Andersson (1999) where the incidence of LBP was significantly in higher in patients abusing substances,

experiencing depression or anxiety disorders. Such a link between LBP and mental health could explain the high numbers of medical discharges from the military for these conditions.

Some people experiencing illness or pain will state they are healthy in order to stay in work, this may be due to various reasons which could be financial or more complex (Azaroff, Levenstein and Wegman, 2002). In the military environment the work culture also plays a factor; Smith et al. (2016) examined injury reporting in an American Army Infantry Brigade Combat Team and found that 49% of injuries went unreported. However, the number of unreported injuries are consistent with civilian jobs.

There also exists a bias known as the “healthy worker effect” which is also a factor in epidemiological studies. Baillargeon (2001) has suggested two components:

- Healthy worker hire effect: healthier workers are hired due to self-selection (having a positive health image) or employer selection (there is more risk hiring someone likely at risk of disease).
- Healthy worker survivor effect: less healthy workers more likely to leave a high-exposure job

If this occurs during sampling this leads to a conclusion that high exposure jobs are less dangerous than they really are.

Gender may also be a factor. Hoy et. al. (2012) found that the “*overall prevalence of low back pain was higher among females than males across all age groups*” this confirms research by LeResche (1999) who found that although the relationship between gender and reporting pain is complex, women are more likely to report it. This could be because of higher stimuli sensitivity, lower threshold for what is considered painful or the differences in upbringing which make it more acceptable for women to report pain. All of the psychosocial factors mentioned make it difficult to produce a completely unbiased qualitative epidemiological study.

The risk factor examined in this thesis is vibration. There are three main types of vibration: Noise, Hand-arm vibration (HAV) and Whole-body vibration (WBV). Of these three types only whole-body vibration has LBP as a diagnosable effect. Griffin (Griffin, 1990) defines Whole-body vibration to occur *"when the body is supported on a surface which is vibrating. There are three principal possibilities: sitting on a vibrating seat, standing on vibrating floor, or lying on a vibrating bed"*. Any sort of relationship between WBV and LBP is fraught with the issue of the large prevalence of LBP within the general population and that most occupational studies have only found a correlation between lifetime exposure duration and the incidence of back problems (Putz-Anderson, Bernard and Burt, 1997; Stayner, 2001).

### 1.1.2 Low back pain in the Military

Musculoskeletal conditions and mental health disorders are the primary reasons for medical discharge in the UK military (Ministry of Defence, 2017a) and in the Canadian armed forces (Poisson, 2015). From the UK Ministry of Defence (MoD) report, it can be seen that 62% of all medical discharges from the Royal Navy were due to Musculoskeletal Disorders, this was higher than the Army (59%) and the Royal Air Force (45%). The incidence risk of musculoskeletal related discharge was 22.1 per 1000 personnel for the Royal Marines; the elite commando troops of the Royal Navy. This is in comparison to 11.2 per 1000 personnel for the regular Royal Navy personnel.

Contrariwise, American marines have a lower incidence rate of LBP than other sectors of the military (Ernat et al., 2012; Knox et al., 2011). The authors suggest that this may be due to the enhanced training received making American marines less susceptible to musculoskeletal disorders, this is reinforced by the negative correlation of fitness level and incidence of musculoskeletal disorders in US army recruits (Jones et al., 1988). Ernat et al. suggest that there may be other factors in play such as *"differences in care-seeking behaviour"*, where marines are less likely to seek medical care due to being perceived as elite soldiers.

Carragee and Cohen (2009) showed that soldiers self-reporting as being without chronic LBP still stated episodes of back pain; they also returned to regular duties quickly suggesting that episodes of LBP are seen as normal occurrences within the armed forces and could therefore be underreported.

As with the general population, LBP in soldiers has been linked with age and psychological stress (Nissen et al., 2014). The military has a similar problem to the "healthy worker effect" known as the "healthy soldier effect" (Comstock, 1975; McLaughlin, Nielsen and Waller, 2008; Schram-Bijkerk and Bogers, 2011). This says that mortality rates for soldiers are lower than for the general population for reasons similar to those mentioned by Baillargeon (2001). There is evidence that more recently this effect is being eroded; a study of American soldiers from 2015 looking at veterans from Iraq and Afghanistan theatres (Bollinger et al., 2015) has seen the healthy soldier effect decrease to be close with the general population. Reasons for this could be the relaxed hiring criteria for recruits as the need for soldiers increased, resulting in more soldiers who have lower education levels who are more likely to be injured or mortally wounded (Montez, Hummer and Hayward, 2012).

The military environment is unique and has many confounding issues. These range from the healthy soldier effect, the reticence of soldiers to report LBP to comorbidity between instances of PTSD and chronic pain (Gauntlett-Gilbert and Wilson, 2013). A report into the Wounded, Injured and Sick (WIS) in the UK armed forces examines soldiers currently receiving military health care (Ministry of Defence, 2017b). Statistics are not directly comparable amongst the forces (Navy, Army, Royal Airforce) due to differences in eligibility. The definition used by the MoD for naval service health care eligibility is: "*Personnel who are WIS and unfit for Service in the maritime environment with a longterm sick absence or in a Military Treatment Facilities (MTF) for more than 28 days or those who can only be employed for limited duties ashore outside of their main trade or skill*". Since April 2016 there has been a significant increase in the percentage of trained regular naval service personnel in the recovery pathway. This is not because a sudden increase in injuries but rather a change in eligibility and a

subsequent uptake in support. The amount of personnel receiving enhanced support actually decreased over this time period suggesting that more people with less demanding health care needs are responsible for this. There is a corresponding growth in the number of WIS personnel returning to work (93%) and a reduction of personnel subsequently leaving the naval services (7%).

Marine craft have very high levels of vibration and shock which could be potential very damaging to operators of these craft (Gollwitzer and Peterson, 1995). Although Gollwitzer et al. did not examine injuries, there was a qualitative study (Ensign et al., 2000) of self-reported injuries among operators of special boats which operate under conditions similar to those mentioned by Gollwitzer and Peterson. Ensign et al. found an increased risk of special boat training and operations with the majority of injuries located in the lower back (33.6%) and the most prevalent injuries being sprains and strains (49.3%), disc problems and trauma were the both second most prevalent injury (7.9%). A study of Swedish marines found that being a crew member of combat craft (Monnier et al., 2016) strongly correlated with incidence of LBP. The authors also reported that marines with a height greater than 1.86m were at an increased risk of experiencing LBP; this is possibly due to poor adaption of equipment and tasks for their physiology.

From conversation with military operators of high speed planing boats, Gollwitzer et al. found that their primary concern was of "*discomfort, pain and decreased on-site mission effectiveness*" and that "*shock mitigation systems should not be used at the expense of payload capacity and other important mission capabilities*" (Gollwitzer and Peterson, 1995). This is more difficult to quantify than the effectiveness of shock isolation systems in reducing the high shocks experienced by the occupants. Reducing the incidence of LBP in the navy may require a holistic approach examining a wide range of factors. This is beyond the scope of this project which focuses on a greater understanding of the underlying systems behind LBP. In order to explain the incidence of LBP the first thing to do is to examine the human musculoskeletal system and the damage which can cause pain within it.

## 1.2 The Human Spine

### 1.2.1 An Overview

The human vertebral column is one of the main supports of the human body, contains and protects the spinal cord and, if damaged, is also the structure in which LBP arises. Figure 1-1 is an overview of the human spine showing its natural curvature and the different regions of the spinal sections.

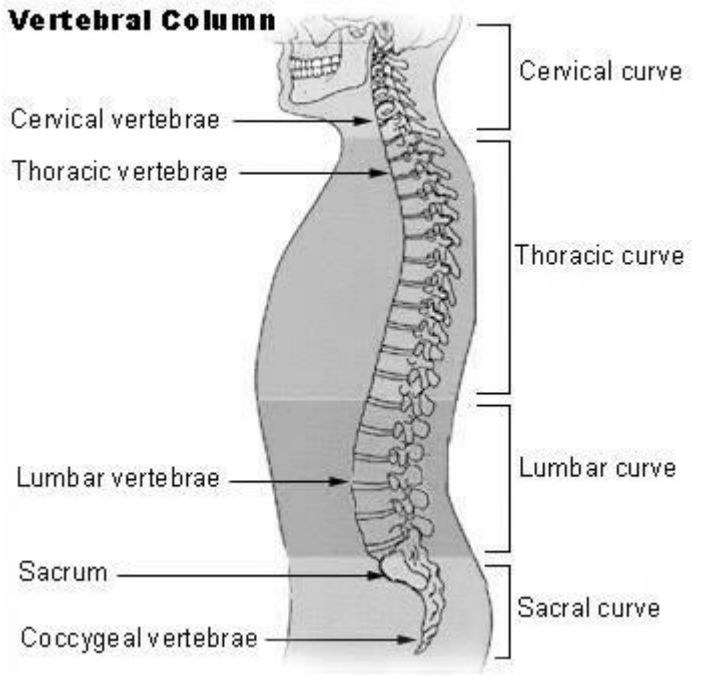


**Figure 1-1: Detail of Human Vertebral Column (Image in public domain accessed from** http://training.seer.cancer.gov/module_anatomy/unit3_5_skeleton_divisions.html**)**

The vertebral column consists of 7 cervical vertebrae, 12 thoracic vertebrae, 5 lumbar vertebrae, the sacrum and the coccyx. From the top cervical vertebrae to the sacrum the size of each successive vertebra increases and they are each separated by an intervertebral disc (IVD). This size increase is related to the weight bearing capacity of each vertebra; larger vertebrae are needed to bear larger forces within the human body due to our upright bipedal stance.

The support structure of the human body is composed of two main types: hard tissue and soft tissue. The hard tissue represents the bone and cartilage, while the soft tissue represents all the connective tissues, fat, blood vessels and

nerves. In the spine the bone is the hard tissue and the muscles, nerves, bone marrow and intervertebral discs are the soft. **Figure 1-2** shows a sagittal cross-section of a segment of the human spine highlighting several key features. For examining the hard tissue Computed Tomography (CT) scans are generally used while Magnetic Resonance Imaging (MRI) scans are used to examine the soft tissue.

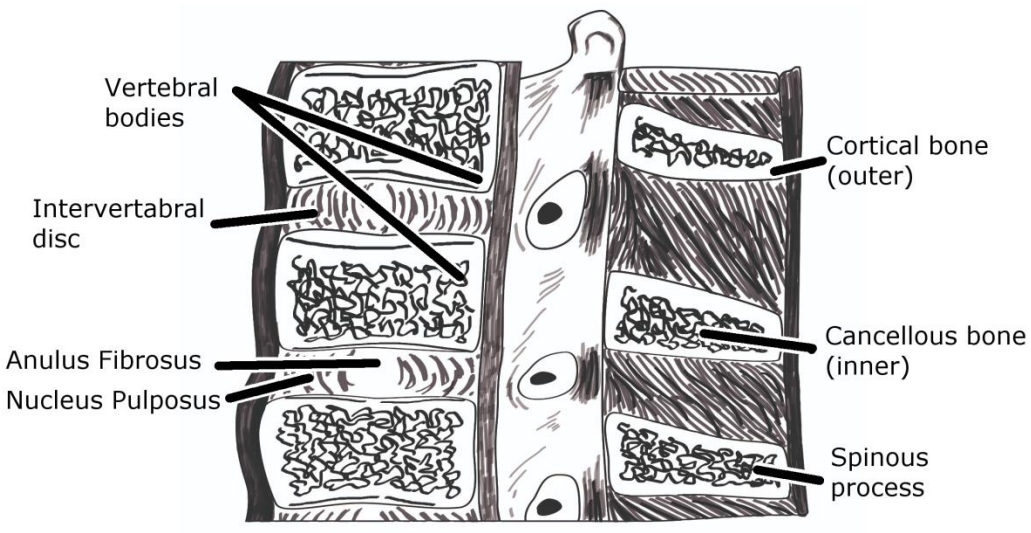


**Figure 1-2: Sagittal cross-section of human spine section redrawn from Snell (1986)**

### 1.2.2 Motion Segment

A motion segment is a biomechanical unit of the spine comprising of two adjacent vertebrae, the interconnecting disc and all ligaments between them. It exhibits biomechanical characteristics similar to the entire spine. For in vitro testing a motion segment (or a few motion segments) is often used.

### 1.2.3 Intervertebral Discs

Each vertebra is separated by an intervertebral disc which provides the spine with flexibility. The discs themselves are composed of concentric rings of fibrous tissue known as the annulus fibrosis. These surround the nucleus pulposus inside. The nucleus spreads the pressure within the IVD and distributes it onto the endplates to which they are attached. The nucleus absorbs water which allows it to recover height. During the course of an average day the human

spine is loaded, the nucleus expels water into the vertebrae and the annulus, and the IVD loses height (Zhu et al., 2015). This is then recovered when in a recumbent position (Paajanen et al., 1994) or through extension of the spine (Kourtis et al., 2004). MRI scans have shown that all the disc height lost within a day is recovered at night although the recovery time is much shorter (Malko, Hutton and Fajman, 2002). Malko et al. suggest that this is due to fluid in-flow into the IVD being greater than fluid out-flow into the vertebrae via the endplates, a view supported by the directionality of fluid flow through the endplate (Ayotte, Ito and Tepic, 2001).

As a unit the intervertebral disc has a damping effect on spinal motion, allowing the human body to absorb shocks without damage to the vertebrae. The discs themselves can be damaged in many ways which can lead to reduced functionality and mobility of the sufferer. IVD damage has several common diagnosable conditions:

- Degenerative Disc Disease (DDD)
- IVD Herniation
- Schmorl's nodes

Degenerative Disc Disease is caused by the natural deterioration, over time or through microdamage, of the IVD. Although aging causes changes with the structure of IVDs, it is more likely that the lifetime loading of the spine causes degenerative changes (Petit et al., 2015). Miller, Schmatz and Schultz (1988) have shown that lower located IVDs are more likely to be degenerate than discs at higher levels, even though the discs were all the same age. DDD is common (Cheung et al., 2009) especially in older individuals, which correlates with lifetime spinal loading.

There are many different methods for characterising disc degeneration using imaging techniques (Kettler and Wilke, 2006). One of the more commonly used methods was formulated by Pfirrmann et al (2001). It allows for the characterisation of DDD with T2-weighted MRI scans. **Figure 1-3** shows the different grades used to classify degenerated discs with the classifications listed in Table 1-2.

| | |
|---|---|
| Grade 1 | Bright white IVD visible |
| Grade 2 | IVD white but not as bright |
| Grade 3 | Difference between annulus and nucleus visible |
| Grade 4 | Not collapsed but no difference between IVD components |
| Grade 5 | Collapsed IVD space |

**Table 1-2: Pfirrmann Disc Degeneration Classification**

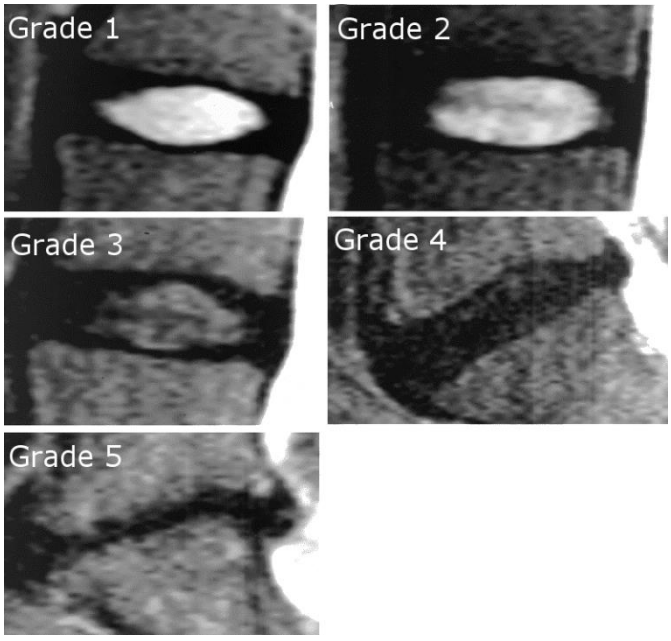


**Figure 1-3: Pfirmann Disc Degeneration Grading, Image adapted from (Pfirrmann et al., 2001)**

The Pfirrmann classification has been shown as a poor indicator of the mechanical properties of an IVD (Cheng and Hu, 2010; Schultz et al., 2009) however Cheng and Hu showed that the IVDs of self-reporting LBP sufferers have different energy dissipation characteristics than those from subjects not reporting pain. Although an increased risk of LBP with DDD exists the relationship is not well defined (Luoma et al., 2000).

Several authors have linked DDD with other physical changes to the human spine such as spondylophytes, also known as endplate bone spurs, which are regions of extraneous bone growth (Malmivaara, 1987; Vernon-Roberts and Pirie, 1977) and spinal stenosis (Ewald, Walter and Waschke, 2016).

Osteophyte formation (such as spondylophytes) in the spine can lead to serious health issues including difficulty breathing and vocal cord paralysis (van der Kraan and van den Berg, 2007). They have also been linked with Lumbar spine pain (Ackerman and Ahmad, 2000; Lamer, 1999).

Vertebral endplates allow for the transfer of fluids and nutrients into the IVD as shown in in vivo animal studies (Crock and Goldwasser, 1984; Giers et al., 2017; Holm et al., 1981; Ogata and Whiteside, 1981). An early study by Nachemson (Nachemson et al., 1970) showed a significant association between disc degeneration and endplate impermeability, suggesting that damage leads to degeneration. In this study, Nachemson et al. claimed that in adult human endplates only the middle of the endplate is permeable. These tests were carried out in vitro; a more recent study by van der Veen et al. (van der Veen et al., 2007) has shown that fluid in-flow to the IVD in vitro is less than in vivo. The discrepancy between the two studies is theorised to be caused by blockages in the endplate from blood clots or bone debris encountered post-mortem (Adams and Hutton, 1983a; Ayotte et al., 2000; Lee et al., 2006; van der Veen et al., 2005). The differences between in vivo and in vitro testing of the endplates mean defining a cause/effect relationship between in vitro endplate damage and in vivo health effects is difficult.

Discs can herniate in the horizontal plane. With disc degeneration the nucleus pulposus changes into a more fibrous tissue which can, over time, create a pathway for the nucleus to bulge out (Burke, 1964). A bulge on a herniated disc can be asymptomatic or can cause health issues if the nucleus impinges on the nerves. In this case it can cause numbness in extremities, paralysis or radiating pain.

A Schmorl's node is a vertical herniation of the nucleus pulposus into a neighbouring vertebral body. The causes for the development of Schmorl's nodes are not well defined however some researchers attribute them to spinal loading at a young age, however there are multiple theories and no agreement in the literature (Kyere et al., 2012) . They are generally asymptomatic though prevalence within the general population varies quite heavily from study to study

(Dar et al., 2010; Hamanishi et al., 1994; Pfirrmann and Resnick, 2001). Pfirrmann and Resnick link the incidence of Schmorl's nodes with degenerative changes within the spine; however, their presence does not preclude symptomatic pain or spinal injury.

### 1.2.4 Vertebra

The anterior element of the vertebra is the vertebral body. It is composed of two different types of bone: cortical and cancellous. These can be seen in Figure 1-2; the solid cortical bone surrounds the 'spongy' cancellous bone.

Cortical bone provides the main support and protection for the human body. In the vertebrae it provides the cortex for the cancellous bone. This cortex is covered by the periosteum, a vascular network which provides nutrients for the body through the red marrow found in cancellous trabecular bone. The periosteum also contains nociceptors: nerve endings which provide a sensation of pain. The presence of these within the spine could lead to the perception of lower back pain in the event of tissue damage (Jaumard, Welch and Winkelstein, 2011).

The functional unit of cancellous bone is a trabecula, a small beam of bone tissue. Cancellous bone is also known as trabecular bone because of this. Cancellous bone is anisotropic at the macro scale (Whitehouse, 1974). Trabeculae are often arranged in the direction of loading (Barak, Lieberman and Hublin, 2011). Within the human spine the primary orientation of these trabeculae is vertical, from the head towards the hip. The spine is strongest in the vertical direction which allows the spine to support the upper body.

The posterior elements of the spine include several processes; (spinous, articular, transverse) and pedicles. The spinous and transverse processes serve as the main attachment point for ligaments and joints in the human spine, allowing for movement of the back. The articular processes are the main contact points of the inferior and superior levels of the spine. It adds stability to the backbone, restricting its movement from that which could cause serious damage to a person (Adams and Hutton, 1983b). In between two articular

processes is a region of contact coated with cartilage to allow for smoother movement; this is known as the facet joint.

The facet joints themselves can become arthritic; this is caused from a bone to bone contact causing the formation of more bone on the affected area. Dunlop, Adams and Hutton (1984) have hypothesised that this may be due to disc space narrowing, causing the pressure contact on the facet joints to increase. This can lead to restricted movement (Fujiwara et al., 2000), as the facet joints help the spine distribute load, and can be very painful for sufferers of this condition (Gellhorn, Katz and Suri, 2013). Nociceptors are also present in the tissue surrounding the facet joints; this is another possible source of pain for LBP sufferers.

In a clinical study (Lewinnek and Warfield, 1986) sufferers of facet joint LBP felt a temporal relief from having anaesthetics and steroids injected to the affected area. A more recent study managed to relieve pain in-vivo by targeting arthritic facet joints with anaesthetic concluding that osteoarthritis can cause LBP (Borenstein, 2004).

The spinal cord is partly composed of nerves which allow the brain to control the body. The vertebral arch protects the spinal cord encasing it in bone; it is composed of the pedicles, the posterior face of the vertebral body and the spinous process.

The vertebral arch can be affected by degenerative changes such as spinal stenosis. This is a narrowing of the vertebral canal causing spinal cord nerve impingement which could lead to serious health issues; however most cases that are not severe do not progress to that stage (Djurasovic et al., 2010). Djurasovic et al. show that stenosis is generally caused from aging related spinal degeneration. Stenosis, as with most morphological changes, can be asymptomatic and not require treatment. Patients suffering from stenosis usually present with radiating pain from the back to the legs and/or buttocks (Weinstein et al., 2008).

Damage to the spinal cord can be catastrophic, severe injury can result in paralysation or even death. This kind of spinal trauma is generally attributed to road traffic incidents, sporting accidents, work place injuries or other such physical trauma. However in countries with an aging population incidence of spinal cord injury is increasing from low level falls (Lee et al., 2014).

The prevalence of LBP is increasing with an uptake in life expectancy (Fehlings et al., 2015). As well as an increased loading history in the lower back, the biochemical and physiological changes of aging contribute to incidents of LBP and injury. As cortical bone ages its elastic modulus, strength and fracture toughness decreases (Zioupos and Currey, 1998); similar trends have be noticed with cancellous bone (Ding et al., 1997). In their paper Ding et al. hypothesise that the decrease in these mechanical properties is due to a decrease of trabecular bone mass rather than changes in the bone material itself. This is due a natural process called bone remodelling.

### 1.2.5 Bone Remodelling

Decrease of bone mass is partly due to bone remodelling, which happens mostly between birth and 30 years of age and then later again at 60 (Frost, 1964). Bone remodelling is a biological process in which bone is resorbed by cells called osteoclasts and then new bone is laid by osteoblasts. As previously noted (section 1.2.4) bone is suggested to align trabecular to the primary direction of loading, bone remodelling also exhibits this behaviour (Ding et al., 2002). For vertebral bone this leads to bone loss in the horizontal axis, while bone orientated primarily in the vertical axis has no significant change with age (Mosekilde, 1988). Goldstein, Goulet and McCubbrey (1993) showed that trabecular orientation plays a significant role in the mechanics of cancellous bone. Metabolic diseases, such as osteoporosis and Paget's disease of bone, can cause significant morphological changes in bone making it more fragile (US Department of Health and Human Services, 2004).

Although it may seem that bone remodelling is degenerative in nature, it plays a very important role in early bone development, converting bone from a more ductile to a mechanically stronger material. Bone has also shown a reaction to

the stresses exerted upon it from daily life and exercise. This phenomenon was developed by Julius Wolff and is known as “Wolff’s law” (Wolff, 1892) which posits that bone will adapt to the loads exerted upon it; if the bone is under-stressed it loses density and if there is enough loading then it gains mass. Wolff’s law has been developed further into a model called the Mechanostat (Frost, 2001). This has been supported in studies and reviews (Barak, Lieberman and Hublin, 2011; Frost, 2004); therefore staying physically active is commonly suggested as a way of maintaining bone mass and consequently, bone health (Forwood and Burr, 1993; Hughes et al., 2016; Silva and Gibson, 1997).

### 1.2.6 Posture

The flexibility of the spine allows the human body to adopt many different postures; the main three are sitting, standing and recumbent. In addition to these positions the spine can also be under flexion or extension (bent forward and backward respectively), and twisted or bent laterally. All of these postures change the intradiscal pressures in the lumbar spine (Nachemson, 1966; Wilke et al., 1999), With Wilke et al. showing that standing flexed induces the highest pressure without external loading. Although Wilke et al. did not look at twisting nor sidewise leaning of the spine they concluded that being recumbent applies the lowest pressure between the L4-L5 vertebrae.

The study by Wilke et al. also supports the work of Adams and Hutton (Adams and Hutton, 1980) which found a reduction of loading in the facet joints of the spine while sitting, without lumbar support, in comparison to standing. In non-degenerated discs the forces of the spine are evenly distributed. This is not the case in degenerated discs where the vertebral arch bears a larger percentage of the load while standing erect, which shifts anteriorly with flexion (Pollintine et al., 2004).This protects the vulnerable part of the spine by changing the loading pathway, which is called stress-shielding. A similar effect for the posterior annulus of a lumbar disc was observed in extended postures (Adams et al., 2000).

Postural changes cause the IVD nucleus to move in the opposite direction to the bending moment (Fennell, Jones and Hukins, 1996), placing more pressure on the posterior element of the vertebral arch in flexion (Knutsson, 1944) and more pressure on the anterior while in extension. Such pressure on the posterior part of the spine has been linked to disc degeneration.

Flexion may not be entirely detrimental to the human spine, however, studies have shown that fluid flow into the IVD, and therefore disc nutrition, is increased while the spine is under flexion (Adams and Hutton, 1985, 1983a). Further work has also shown that flattening the natural lordosis of the spine through flexion is advantageous when lifting loads (Adams et al., 1994; Shirazi-Adl and Parnianpour, 1999).

Muscle responses are also different in people with LBP (Radebold et al., 2000) with delayed reactions commonly seen. If combined with unexpected loading this could cause damage as the body lacks the time to respond appropriately (Magnusson et al., 1996).

Whether posture is a contributing factor to LBP is complicated. Certain postures place greater stresses on the lumbar spine and it is postulated that should lead to degeneration and back pain. Indeed, in ex-vivo fatigue studies the spine fails rapidly under loading while in extension in comparison to the neutral position (Gallagher et al., 2005; Gooyers et al., 2012). Prolonged sitting causes the stiffness of the lumbar spine to increase (Beach et al., 2005), the authors also believe that there is an increased risk of damage if flexion is performed after this stiffness change but this has not been validated.

### 1.2.7 Morphology of back pain

When it comes to the imaging of the spine it can be difficult to ascribe any morphological changes in the spine to LBP; many of the changes seen in MRI and CT scans are considered part of the aging process and are seen in many asymptomatic individuals (Boden et al., 1990; Brinjikji et al., 2015).

As discussed in this section there are many changes in the spine which have been linked to LBP; due to the complex interaction between the changes spinal

degeneration, prevalence of non-specific LBP in the general population and the morphological differences between people; it is difficult to find a causative relationship. A study examining CT scans of 187 participants examining many degenerative changes only showed significance with stenosis in relation to LBP (Kalichman et al., 2010). There exists an occupational and task related risk to developing LBP and one factor for this is exposure to WBV.

## 1.3 Whole-Body Vibration

Whole-body vibration is capable of producing harmful effects upon the human body, whether it is independent of or due to a compound effect with, another physical stressor at lower levels. Therefore the study of vibrational events is important in understanding the mechanism of injury. The two main components of vibration are the frequency and the amplitude.

The amplitude of vibration is the distance from equilibrium to its peak value. In vibrational studies it is often noted in terms of acceleration, either $m/s^2$ or g. The frequency of a signal is the rate at which it repeats per unit time. The unit is Hz, where 1Hz is one cycle per second. The concepts are best understood with the example of a simple sinusoidal wave (sine wave) as shown in **Figure 1-4**. This sine wave has a frequency of 1Hz and its maximum amplitude is 10 $m/s^2$.

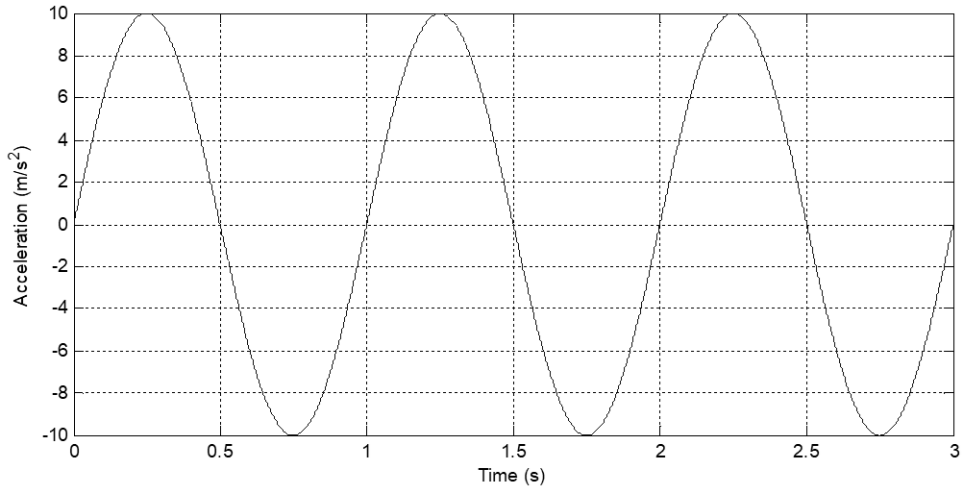


**Figure 1-4: Sinusoidal Vibration**

A sinusoidal wave is an example of a deterministic vibration; it can be accurately predicted from the previous data. The most common type of vibration experienced in everyday life is random; this is defined as a vibration in which magnitude cannot be precisely predicted at a particular instance. **Figure 1-5** shows an example of random vibration.

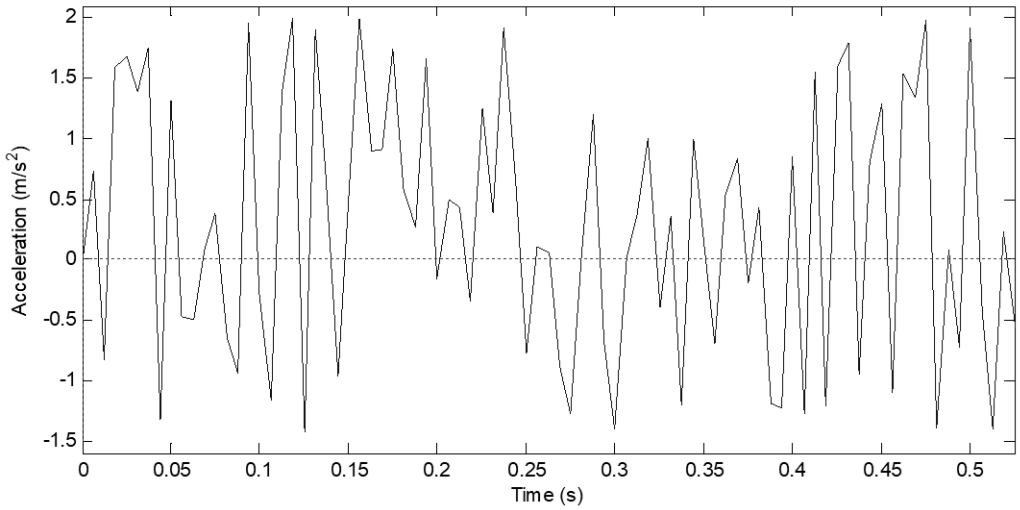


**Figure 1-5: Random Vibration**

Transient motion also frequently occurs as shown in **Figure 1-6**. It appears as an incongruous peak in the data. An example of this would be a boat slamming onto water.

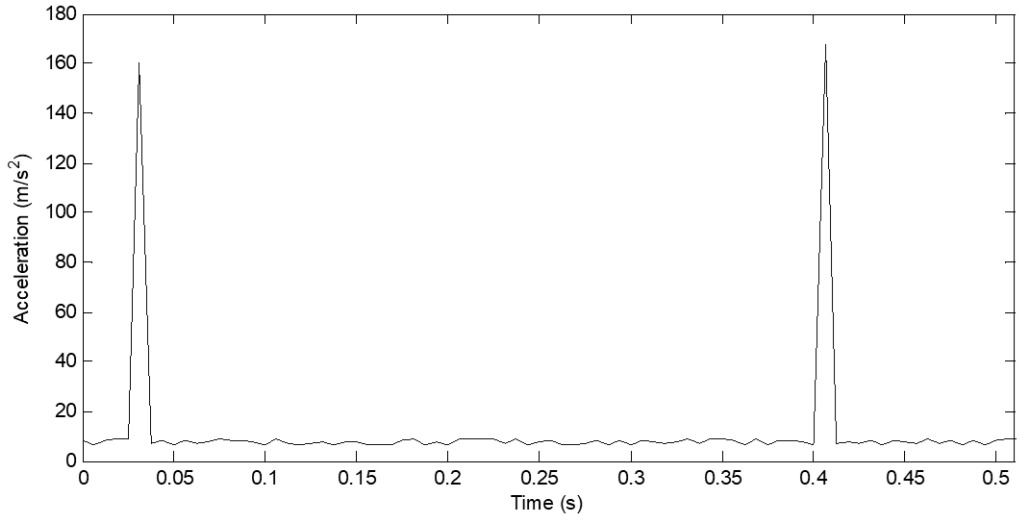


**Figure 1-6: Transient Vibration**

In the real world vibration can occur as a combination of all three vibration types therefore the measurement and analysis of the waveforms remains key to understanding vibrational effects.

### 1.3.1 Measurement of Vibration

The measurement of vibration is a task which is carried out using accelerometers. Multiple international standards exist which attempt to standardise the positioning and measurement of vibration in order prevent erroneous data acquisition. ISO 2631, Mechanical vibration and shock – Evaluation of human exposure to whole-body vibration (ISO, 1997) and its various addendums will be discussed as their methods are used extensively in the field of vibration mechanics.

The direction of vibration is measured in three directions which are oriented in relation to the human body; these are known as basicentric axes and are shown in **Figure 1-7**. When measuring vibration accelerometers should be placed at the vibration/body interfaces such as the feet, seat-surface and seat-back.

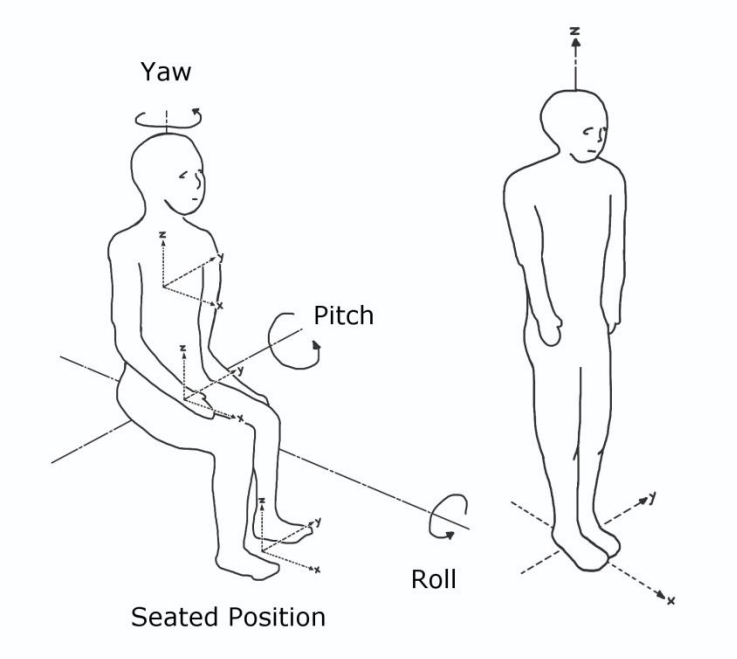


**Figure 1-7: Basicentric Axes redrawn from (ISO, 1997)**

Octave band filtering (ISO, 1997) is one technique during measurement which allows only energy of a specific frequency to pass through. This allows an analyst to focus on frequencies of interest. This is also done during measurement to prevent aliasing, a measurement error which causes vibrational signals to lose data. An octave change is achieved by either doubling or halving the frequency. Standard frequency bands are defined in ISO 266: Acoustics – Preferred frequencies (EN/ISO, 1997). If a higher resolution is required 1/3$^{rd}$ frequency bands can be used by splitting each band into 3. This is used in ISO 2631 as the basis for its frequency weighting criteria.

Frequency weighting in regards to vibration is a technique in which frequencies of interest are weighted by their effect on the human body. The weightings are shown in **Figure 1-8** in which $W_k$ relates to translation in the z-direction, $W_d$ the x and y directions and $W_i$ accounts for motion sickness.

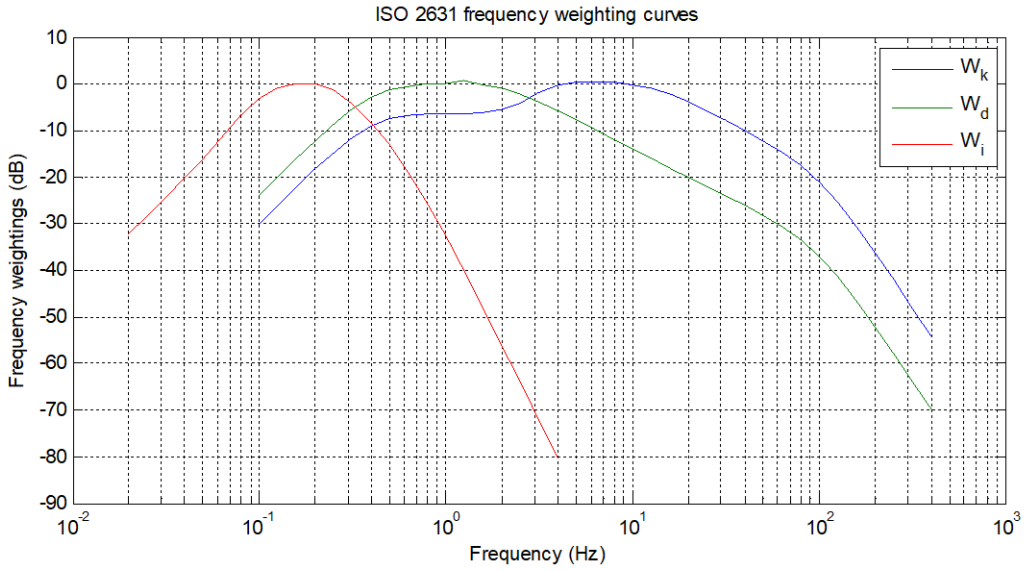


**Figure 1-8: ISO 2631 Frequency Weightings**

For motion sickness the peak is at 0.2Hz which is the frequency at which nausea is most quickly obtained based on qualitative studies carried out in vibration labs (Cheung and Nakashima, 2006; Golding, Mueller and Gresty, 2001; O'Hanlon and McCauley, 1974). In the z-axis there is a noticeable peak at 4-6Hz where resonance in the lumbar spine has previously been observed (Fairley and Griffin, 1989; Wilder et al., 1982)

In the principal basicentric axes (**Figure 1-7**) the derivation of the modern frequency weighting contours was inferred from qualitative studies based on perceived discomfort (Corbridge and Griffin, 1986; Griffin, 1976, 1980). The frequency weighting contours used in ISO 2631 have been debated since its inception in 1974 with researchers unclear of its source and its accuracy. (Morrison and Robinson, 2001; Oborne, 1978, 1983; Schust et al., 2010)

Although ISO 2631 has a list of references appended to it they are not clearly referenced in the text so it is hard to attribute the research to the text. It is possible that the original frequency weightings are also based upon research by Miwa (1967) on perceived comfort as the contours presented are very similar to first draft of ISO 2631 (ISO, 1974).

The perception of comfort as described by ISO 2631-1 is also based on frequency weighting where the weighted Root Mean Square (section 1.3.2) values correspond to different comfort levels. An alternative method proposed by Miwa (Miwa, 1968) in 1968 suggests the use of a measure of *"Vibration greatness"* when evaluating seat comfort, which was shown to have no dependence on frequency. Maeda, Mansfield and Shibata (2008) experimentally proved this method and found that it could be more suitable for predicting comfort than ISO 2631-1 and further expanded to look at other responses to vibration.

Lower back pain is a condition which can happen over an extended period of time and the origin of which is fraught with complications. Comfort is easier to measure in a laboratory environment and ethics generally allows for vibration at levels which are not detrimental to long-term human health. This is why comfort contours are the basis for the frequency weights seen in ISO 2631 today. A study by Griefahn and Bröde (1999) compared single-axis and dual-axis vibration in the lateral and vertical directions, they found that the comfort contours were *"qualitatively valid"* but not in the case of multi-axis loading.

Morioka & Griffin (2010) reported that comfort was magnitude dependant, so simple linear comfort curves are unsuitable for the evaluation of comfort and thus health as defined by ISO 2631-1. Non-linear biodynamic response of the

human body has been investigated in both the vertical (Mansfield and Griffin, 2000) and the horizontal axes (Nawayseh and Griffin, 2005). Mansfield and Griffin found there was a change in human resonant frequencies in the z-axis which depended on the magnitude of vibration.

A link between comfort and the health effects of vibration is not established but it is assumed that vibration subjects perceive as uncomfortable or intolerable are detrimental to human health. This assumption is troubling as many people find motion sickness quite uncomfortable but it is not known to cause long term health effects.

Frequency weightings are nevertheless used and they provide a basis for the health guidance of vibration as set out in the EC directive 2002/44/EC (Directive, 2002).

### 1.3.2 Vibration analysis methods

There are several methods on which the effects of vibration are analysed. These are:

- Root-Mean-Squared (RMS)
- Crest factor (CF)
- Vibration dose value (VDV)
- Estimated vibration dose value (eVDV)
- Vibration dose value exposure ($VDV_{exp}$)
- A $6^{th}$ order recursive neural network (Spinal Acceleration Dose)
- Power spectral density (PSD)
- Dynamic Response Index (DRI)

RMS used in the field of vibration analysis is the quadratic mean of the acceleration profile. Equation (1-1) shows how it is calculated:

$$x_{RMS} = \sqrt{\frac{1}{N}\sum_{i=1}^{i=N} x_{(i)}{}^{2}} \qquad (1\text{-}1)$$

Where,

$x_i$ = i$^{th}$ measurement of instantaneous acceleration (m/s$^2$)

$N$ = Number of data points

The RMS is a rudimentary measure which tends to underestimate the acceleration profile when used in conjunction with data with transient motion (ISO, 1997; Stayner, 2001)

The CF of a vibration signal is the ratio between Peak and RMS acceleration as shown in Equation (1-2)

$$CF = \frac{|x|_{peak}}{x_{rms}} \tag{1-2}$$

Where,

$|x|_{peak}$ = Peak, or maximum, acceleration measured

Profiles with a high crest factor contain a large amount of shocks. The current edition of ISO 2631-1 recommends against using RMS and suggests that vibration dose value be used instead when the CF is larger than 9. This is in contrast to BS 6841 (British Standards Institution, 1987) which suggests VDV be used when the CF exceeds 6.

VDV is the quadratic-root of vibrational magnitude over the measured time period T, calculated as in Equation (1-3)

$$VDV = \sqrt[4]{\frac{\mathrm{T}}{N}\sum_{i=1}^{i=N} x_{(i)}^4} \tag{1-3}$$

Using the 4$^{th}$ power VDV is more sensitive to high acceleration events in comparison to the RMS method. Boileau, Turcot and Scory (1989) compared 4$^{th}$ power methods and RMS. They found that RMS underestimates the vibration exposure dose in comparison to the VDV as the CF increases and continues to diverge.

ISO 2631-1 states that the VDV can be estimated as in Equation (1-4) to create an estimated vibration dose value when the CF is less than 9.

$$eVDV = \sqrt[4]{1.4 x_{rms} T} \quad (1\text{-}4)$$

This estimation is based on the RMS therefore the accuracy of this value depends highly on the acceleration profile used. Although it produces a value using the 4th power it is an estimate as it does not integrate the 4th power over the entire time period and as such is not a true 4th order statistic.

VDV is a cumulative measure therefore the longer the logged signal, the greater the VDV. It is useful to normalise the VDV against a constant exposure time for comparison. This is known as the $VDV_{exp}$ and defined as:

$$VDV_{exp} = VDV \left(\frac{T_{exp}}{T}\right)^{1/4} \quad (1\text{-}5)$$

Where,

$VDV_{exp}$ = the 4th order daily vibration exposure ($m/s^{1.75}$)

$T_{exp}$ = the length of time exposed to the vibration signal in a given day (s)

All the general techniques, apart from $VDV_{exp}$, described above are used by ISO 2631-1 in conjunction with the weightings depicted earlier in **Figure 1-8**. Where the acceleration profile is filtered in regards to axis of acceleration to produce the frequency weighted acceleration profiles, in these cases $x = a_{weighted}$.

ISO 2631-5 introduced another method for quantifying the risk of the health effects associated with WBV known as the spinal acceleration dose. This is calculated using a 6th order recursive neural network (RNN) for quantifying the human response to vibration. For the x and y directions it assumes a single degree of freedom and uses a simple linear equation to calculate the response. For the z-direction it uses computation to calculate the complex response of the human spine. The two equations are as follows:

$$a_{lz} = \sum_{j=1}^{7} W_j u_j(t) + W_8 \quad \textbf{(1-6)}$$

$$u_j(t) = \tanh\left[\sum_{i=1}^{4} w_{ji} a_{lz}(t-i) + \sum_{i=5}^{12} w_{ji} a_{sz}(t-i+4) + w_{j13}\right] \quad \textbf{(1-7)}$$

Where,

$a_{lz} = \text{z direction lumbar acceleration}$

$a_{sz} = \text{z direction seat acceleration}$

$W, w = \text{modelling coefficients described in ISO 2631-5}$

This calculates the lumbar response of the human spine from the seat acceleration data. It acts as a transfer function from the seat to the lumbar spine. Once this operation has been performed it is assumed that the peak loads in the lumbar region of the spine have the most effect, this leads to a 6$^{th}$ order summation of the peaks to calculate the acceleration dose $D_k$ which is defined by Equation **(1-8)**

$$D_k = \sqrt[6]{\left[\sum_i {A_{ik}}^6\right]} \quad \textbf{(1-8)}$$

Where,

$A_{ik} = \text{The i}^{\text{th}}\text{ peak of the lumbar response acceleration } a_{lk}(\text{t})$

$k = x, y, z$

In the Z-axis when the seat pad notes a tension event, such as an unloading of the seat pad, it is difficult to quantify the tensional loads within the spine especially when compared with a compressive event where the behaviour can be easily calculated. It is for this reason, and the assumption that compression is of primary concern when investigating spinal fatigue failure, that for the Z axis only positive peaks are counted. In the x and y directions both positive and negative peaks are included in the calculation of $D_k$.

ISO 2631-5 also assumes that peaks less than 3 times the magnitude of the highest acceleration event can be discounted from the $D_k$ summation.

This acceleration dose is currently only for the time period over which the data was collected, it can be further processed into a daily acceleration dose $D_{kd}$. The guidance provided in ISO 2631-5 continues to assess the health effects and the risk of adverse health effects from vibration containing multiple shocks.

There exist several problems with the model described in ISO 2631-5, one of which is the applicability of the model. The standard states: *"The RNN for the z-axis was trained using vibration and shocks in the range of −20 m/s$^2$ to 40 m/s$^2$ and 0,5 Hz to 40 Hz. As the model is non-linear, this constitutes the range of applicability of this part of ISO 2631"* (ISO, 2004). Therefore implementation of ISO 2631-5 requires that frequencies higher than 40Hz be filtered out; a large amount of shocks on military marine craft experienced in the z-axis are at frequencies higher than 40Hz (Serrao and Paddan, 2013) so the usage of ISO 2631-5 is questionable when used in this environment.

The model coefficients used for the neural network are based on a sampling rate of 160 samples per second, any data collected at sample rates higher than this must be resampled to the prescribed sample rate. This has an effect on the vibration profile generally reporting less accurate statistics (RMS, VDV, etc) of high acceleration events. Considering that this model was conceived to characterise such vibration profiles this is perplexing.

A possible reason for this is that neural networks require datasets to be trained on. Data which characterises extreme shock tends to be non-uniform and training a RNN on this data would be difficult due to the high variability between the data sets, by selecting a lower frequency cut off, this reduces the complexity of the consequent RNN.

Acceleration is recorded as a function of time. A Fourier transform (FT) can turn an acceleration profile from the time domain into the frequency domain, allowing an examination of the frequency content of a particular signal. Vibration data is normally sampled at a specific sampling rate for a limited time window, meaning that the data is stored on a discrete time axis. This means that a discrete Fourier transform (DFT) can be used to convert the signal into the frequency domain. A more efficient way of doing this is by using a fast Fourier transform

(FFT) algorithm which simplifies the DFT matrix reducing the computation cost of the transformation.

When performing a FFT the signal is “tested” for frequencies the same width of the frequency bin, the thinner these bins are the more “tests” are made improving the accuracy. The resolution of the frequency bin can be calculated as shown in Equation (1-9) and is dependent on the sampling rate and the length of time that the signal is recorded.

$$\text{Bin resolution} = F_s/N \tag{1-9}$$

Where,

$F_s = \text{Sampling frequency}$

$N = \text{Number of recorded points}$

The easiest way of increasing the frequency resolution is to record for a longer time, increasing N above and thus the bin resolution. This is not without problems; the longer you record a random vibration event, the higher the probability that the vibration environment may change. For example, if vibration of a band saw is logged longer than its operation it may pick up un-intended vibration events which may skew later analysis. There always exists a balancing act between the frequency resolution and the temporal resolution when measuring time varying vibration.

A useful tool when comparing vibration in the frequency domain is the power spectral density (PSD) which is a normalised function of the FFT. This normalisation allows the comparison of vibrational data with different time periods and frequency resolutions, given that care is taken to ensure accurate signal measurement and analysis. PSD assumes that the measurement has been taken over a long enough time as to be practically infinite. PSD is therefore the energy of an acceleration event per unit time in this context. It is important to note that the normalisation is done in reference to the bin resolution which affects the magnitude.

As an example of Fourier analysis a deterministic waveform given by 3 different frequency and amplitude sine waves with properties $a = 3\sin(2\pi t) + 2\sin(4\pi t) + \sin(8\pi t)$ where a = acceleration (m/s$^2$). In this function the standard sine function $(2\pi ft)$ has already been simplified, therefore the frequencies and amplitudes are 1 Hz at 3 m/s$^2$, 2 Hz at 2 m/s$^2$ and 4 Hz at 1 m/s$^2$ respectively. The time period was 50 seconds sampled at 1kHz. **Figure 1-9** shows an enlarged section of this.

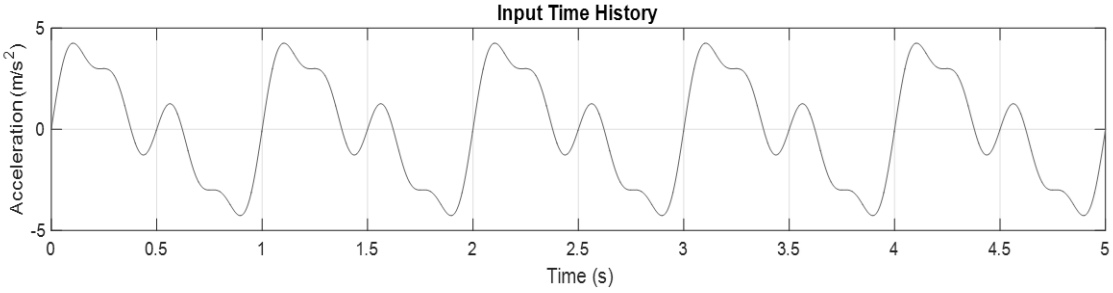


**Figure 1-9: Sine wave Combination Detail**

**Figure 1-10** shows the relevant FT, FFT and PSD of the signal.

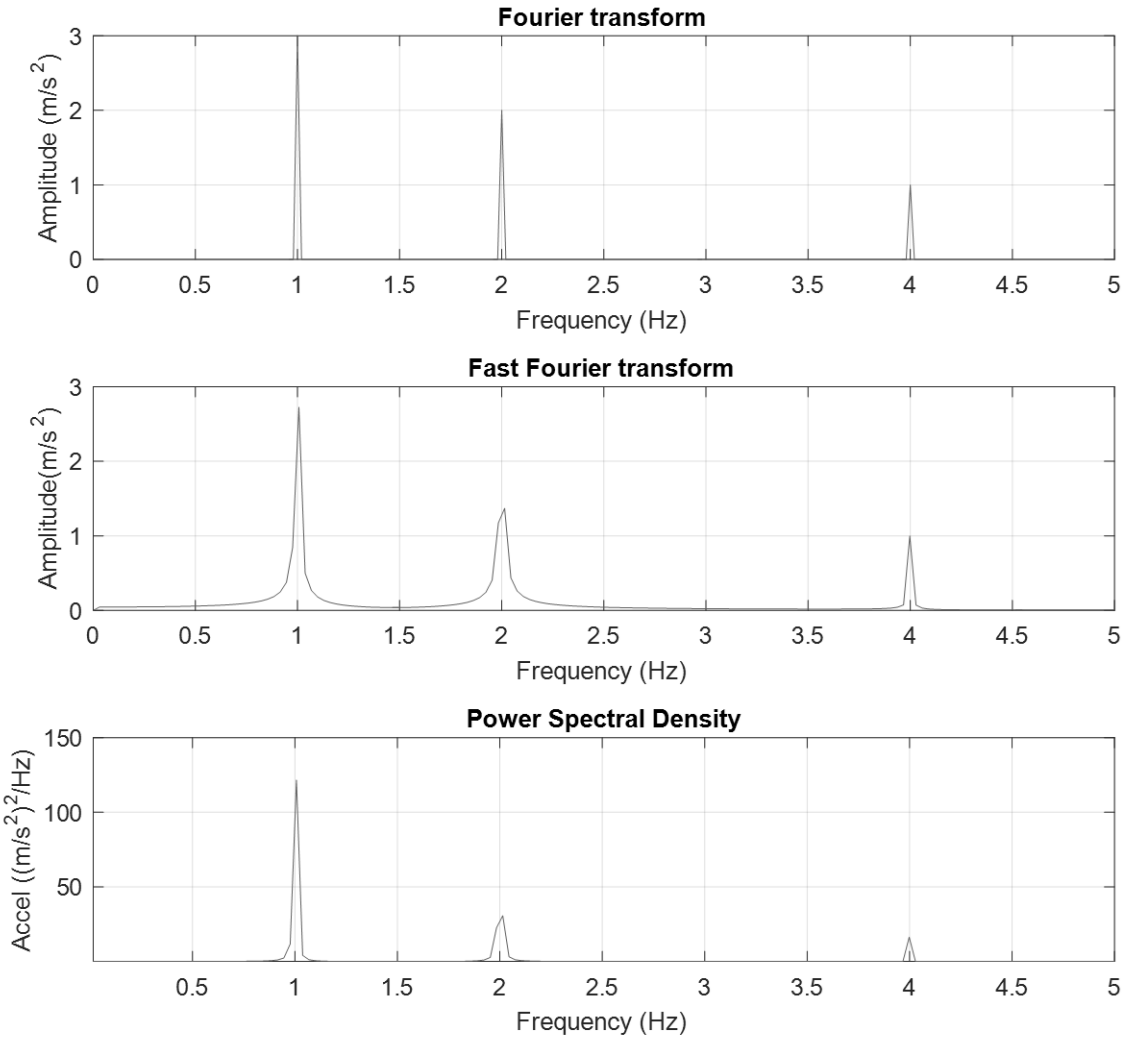


**Figure 1-10: Sine Combination Analysis**

From this analysis we can see that the FT gives the most accurate representation of the vibration signal in the frequency domain and the FFT provides a good agreement considering it is calculated using the discrete time domain. The PSD shows the distinct peaks at the correct frequencies of 1, 2 and 4Hz. When dealing with seat performance characteristics the PSD is most often supplied.

One additional method for examining health effects of shock loading on the human spine is the Dynamic Response Index (DRI) developed by Stech and Payne (1969) in a joint report for NASA and the United States Air Force. DRI was initially developed to deal with the risk of injuries from aircraft pilot

ejections, with accelerations around 20g. It treats the spine as a dampened spring-mass system with one degree of freedom and, using a differential equation, with pelvic acceleration (rather than seat base accelerations as in ISO 2631) to generate spinal deflection. This is used to generate a dimensionless number known as the DRI which indicates the severity of the acceleration event relating to spinal load and thus theoretical injury.

The spring constant for this model was acquired from the biomechanical response of cadaveric vertebrae while the damping ratio was ascertained from living individuals exposed to impact and vibration. It was verified against operational data vertebral fractures from ejections, where it was found to slightly overestimate the risk of spinal injury (Brinkley and Shaffer, 1971). The reason for this inconsistency is thought to be due to cadaveric tissue having a lower strength than that of a living person (Coltman et al., 1989). The DRI has influenced seat survivability design in American military aircraft but its use has been questioned; it is a poor indicator of lumbar load, human responses to vibration are nonlinear and it does not take into account the anthropometry of the occupant (Thyagarajan et al., 2014).

DRI has been shown to be a poor indicator for damage prediction in explosive blasts (Spurrier et al., 2015), this may be due to the fact that peak accelerations in blast can reach over 100g, in comparison to the 20g of ejection seats. The accelerations of an aircraft ejection are orders of magnitude higher than marine vibration. Usage of DRI also implies that the occupant remains seated with a restrained belt over the pelvis; this is not the case in marine craft as the occupants are free to stand and adapt to the loading experienced. This questions the suitability of applying the DRI method for marine environments.

### 1.3.3 Issues Arising from Vibration Measurement

There are four main issues when trying to measure WBV which can affect the data collected:

- Sensor positioning
- Instrumentation
- Aliasing
- Signal conditioning

In order to closely examine WBV in-situ sensors must be used to collect acceleration data. The correct positioning of these sensors is essential; if the human response to vibration is to be investigated then the sensor must be placed at the interface between the subject and the vibration source. For seated subjects this is straightforward; the accelerometer is attached to the seat. Getting robust data from marine craft is difficult as occupants often brace for impact from large waves by standing. In this case the subject being logged is no longer being monitored by the accelerometer and this data is lost.

Logged vibration from other positions than the subject and vibration interface point is difficult to transpose to examine the effects of vibration. In the marine environment however, some progress has been made to transpose data taken at the boat deck into seat pan data (interface point between the vibration and the subject) using a 2-Degree-of-freedom (DOF) model (Olausson and Garme, 2015) if the seat characteristics are known. However, this model assumes that the occupant remains in contact with the seat at all times.

Selection of equipment for vibration data logging is also very important. ISO 8041 (ISO/BS EN, 2017), which was recently revised, sets certain technical requirements for vibrational measuring devices used to examine the mechanical response of the human body to vibration. A device that conforms to this is more than capable of recording vibration events with sufficient accuracy. Aliasing is avoided with the use of filtering (Section 1.3.1) which also minimises errors caused by signal conditioning.

## 1.4 Standards and Legislation

### 1.4.1 ISO 2631 (1974)

Perhaps the most significant document on the matters of whole-body vibration is the international standard “ISO 2631: Guide for the evaluation of human exposure to whole-body vibration”. Commenced in 1966 and eventually published in 1974 it concerns “*Numerical values for limits of exposure for vibrations transmitted from solid surfaces to the human body in the frequency range 1 to 80Hz”* (ISO, 1974). Within the introduction it is noted that it is intended to be a general guide on the human response to vibration exposure rather than being a rigid set of limits.

A report from the committee chair H.E. Von Gierke (1975) gives an insight into the state of affairs during the writing period saying that the standard was a compromise of all the data collected up to this point which “*exhibited a considerable spread”* and acknowledged that “*humans judge vibration exposures differently depending the circumstances*”.

One of the aims of ISO 2631 was to *“encourage, in comparable and reproducible form, the collection of further and better data”* (Von Gierke, 1975). At this the standard succeeded with a large volume of papers produced in the years subsequent to publication. It set the usage of RMS as a simple way to measure vibration exposure magnitude.

The notion that vibration causes “fatigue-decreased proficiency” and “discomfort” is not a new one. An attempt to quantify it was made in the first edition of ISO 2631 using different boundaries for vibration exposure; Discomfort, fatigue and exposure. This was an effort to ascribe acceleration magnitude to effects of exposure where discomfort was the least harmful, fatigue would make tasks more difficult over a prolonged time, and exposure was considered harmful to health. The exposure boundary was twice that of the fatigue boundary which was 3.15 multiplied by the discomfort boundary.

It must be stated that this relationship is purely coincidental as Von Gierke denies that the ISO group created this value arbitrarily (Von Gierke, 1975). After

an amendment in 1985 the standard was later refined in 1997 and it is the first major revision along with the addition of the vibration dose value (VDV), which was first published in BS 6841.

### 1.4.2 BS 6841 (1987)

The United Kingdom voted against ISO 2631 on "*Technical grounds*" according to Von Gierke (1975). Although the ISO standard was still approved, the British Standards Institution (BSI) produced a similar document entitled "Guide to measurement and evaluation of human exposure to whole-body mechanical vibration and repeated shock" (British Standards Institution, 1987). The technical grounds alluded to become apparent when comparing ISO 2631 and BS 6841:

- Set limits and boundaries from ISO 2631 have been removed and replaced with guidance on the application of the standard
- $4^{th}$ power VDV estimation introduced
- Frequency weightings simplified and extended to a lower end of 0.5hz
- Seat discomfort quantification taking into account axial and vertical motion
- Quantification of motion sickness limits

BS 6841 was most recently confirmed in early 2012 and is still considered as current. Although the standard does not set limits for vibration it discusses a possible link between WBV and detrimental health effects giving 15 $m/s^{1.75}$ as a point at which epidemiological, field and laboratory studies have correlated VDV with LBP. Whereas BS 6841 gives guidance on the application of VDV, ISO 2631 and its modern revisions do not.

The revision of ISO 2631 in 1997 includes some of the analysis techniques first introduced by BS 6841 such as the VDV and simplified frequency weightings.

### 1.4.3 ISO 2631 (1997)

The current version of ISO 2631 was first released in 1997. The document is split into different parts:

- Part 1: General requirements,
- Part 2: Vibration in Buildings,
- Part 4: Guidelines for the evaluation of the effects of vibration and rotational motion on passenger and crew comfort in fixed-guideway transport systems
- Part 5: Method for evaluation of vibration containing multiple shocks.

Parts 1 and 5 are relevant to this thesis and thus will be examined further.

### 1.4.4 ISO 2631-1 (1997)

In addition to supplementing RMS analysis with VDV and the simplification of the weighting factors ISO 2631-1 extended the frequency range which the factors can be applied to 0.1-400 Hz in the z-axis in the basicentric coordinate system (**Figure 1-7**). This allows standardisation of reporting over a greater range of vibration. The limits suggested by ISO 2631-1 are calculated using time/dose relationships based on eVDV and RMS from the weighted acceleration as shown in Figure 1-11.

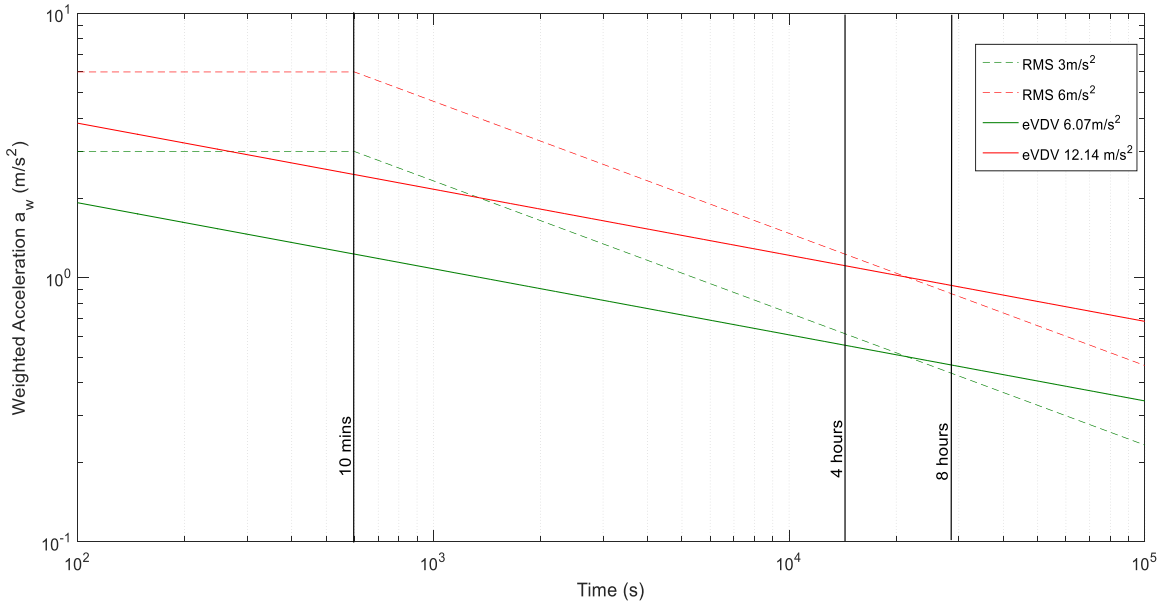


**Figure 1-11: Health guidance zones redrawn from ISO 2631-1 (1997, 2010)**

ISO 2631 advises using the health guidance zone (HGZ) where the two time dependencies are roughly equal, between the 4 and 8 hours mark, the

reasoning for this is unclear as the two dependencies vary considerably outside this area. In between the red and green lines is the “caution zone” where there could be health effects whereas above the red lines is the zone where “health risks are likely”. The limits set by ISO 2631-1 are considered arbitrary, difficult to apply and not based on studies concerned with measuring both the vibration exposure and incidence of lower back pain; therefore the usefulness of these limits is a source of considerable discussion (Griffin, 1998; Lewis and Griffin, 1998; Monaghan and Twest, 2004; Seidel et al., 1998) along with the debate around the applicability of weighting factors discussed earlier in section 1.3.1.

The usage of the $4^{th}$ power in the health guidance zone is contentious; as the limits are described in the standard they are calculated from a lower eVDV of $8.5m/s^{1.75}$ and an upper eVDV of $17\ m/s^{1.75}$ using a $4^{th}$ order time dependency. However, as they are shown in the HGZ they are converted into a standard acceleration measure with the same $2^{nd}$ order time dependency. Whether this is an attempt to standardise the limits on the y-axis of the HGZ is unknown but it is confusing for anyone trying to follow the standard.

The original document was amended in 2010 with the intention of clarifying the usage of the standard. EC directive (2002/44/EC) on the control of vibration in a work environment is heavily based on the information contained within ISO 2631-1.

Morrison and Robinson (2001) showed ISO 2631-1 $W_k$ filtering (Z-Axis vibration depicted in **Figure 1-8**) is unable to accurately model human spinal response to vibration with mechanical shocks of 0.5 to 4g amplitude. ISO 2631-5 attempts to address this by modelling the human spinal response to vibration rather than just an examination of the vibration signal.

### 1.4.5 ISO 2631-5 (2004)

ISO 2631-5 (ISO, 2004) is the standard produced by “Working group 10” mentioned in the HSE report on whole-body vibration (Stayner, 2001). This is the newest international standard which devises the $6^{th}$ order neural network

described above in 1.3.2 Vibration analysis methods. Part 5 of ISO 2631 describes the “Method for evaluation of vibration containing multiple shocks”

In the introduction it states: *“The assessment method described in this part of ISO 2631 is based on the predicted response of the bony vertebral endplate (hard tissue) in an individual who is in good physical condition with no evidence of spinal pathology and who is maintaining an upright unsupported posture.”* These are limitations that give an insight to the current state of this model. The effects of posture have been studied for many different populations and operating environments and although it has been shown to have a strong effect on lumbar loading (section 1.2.6) it is difficult to quantify and would only further complicate the model.

ISO 2631-5 mentions that *“the assessment method and related models described in this part of ISO 2631 have not been epidemiologically validated.”* Alem (2005) examined the application of ISO 2631-5 in a military ground vehicle environment but noted that the method used has not be verified.

This part to 2631-5 was introduced in 2004, 2 years after a European directive on exposure to vibration of employees and a year before the transposition of this directive into UK law. These directives have provisions for health monitoring of employees exposed to vibration. Data from this could be used to assess the model described in ISO 2631-5 if made available to researchers.

As of writing, ISO 2631-5 is currently being revised by ISO/TC 108/SC 4 Human exposure to mechanical vibration and shock.

### 1.4.6 Directive 2002/44/EC - On the minimum health and safety requirements regarding the exposure of workers to the risks arising from physical agents (vibration) (2002)

Directive 2002/44/EC (2002) refers to ISO 2631-1 when it comes to vibration measurement and analysis methods. The limits differ between ISO 2631-1 and Directive 2002/44/EC over an 8 hour period. The exposure action value (EAV), where health monitoring and best available methods for vibration isolation

should occur, is best compared with the lower bounds of the health guidance zone of ISO 2631-1 and the exposure limit value (ELV) compare with the upper bound. This is shown for WBV in **Table 1-3**.

| | Lower bound RMS $a_{w(8)}$ ($m/s^2$) | Upper bound RMS $a_{w(8)}$ ($m/s^2$) | Lower bound VDV $a_{w(8)}$ ($m/s^{1.75}$) | Upper bound VDV $a_{w(8)}$ ($m/s^{1.75}$) |
|---|---|---|---|---|
| ISO 2631-1 | 0.43 | 0.87 | 8.5 | 17 |
| 2002/44/EC | 0.5 | 1.15 | 9.1 | 21 |

**Table 1-3: Comparison of WBV Limits between ISO 2631-1 and 2002/44/EC**

This comparison shows that although the directive is based on ISO 2631 the bounds are higher than those in the international standard, further confusing the discussion of the link between LBP and WBV. BS 6841 has a VDV $a_{w(8)}$ value of 15 $m/s^{1.75}$ which *"will usually cause severe discomfort"* should be compared against the upper bound and is much lower than the values given by both ISO 2631-1 and 2002/44/EC.

In 2002/44/EC the lower bound is described at the *"Action value"* which is the point at which *"the employer shall establish and implement a programme of technical and/or organisational measures intended to reduce to a minimum exposure to mechanical vibration and the attendant risks"* (Directive, 2002), this is followed by a list of recommendations that employers can employ in order to do so. The Upper bound is the *"Limit value",* which should not be exceeded by workers. If it is exceeded the employer is required to take immediate action to reduce the exposure to vibration.

Although this directive seems lenient in regards to the vibration limits, it only sets out the maximum levels to which employees of a European union member state shall be exposed to vibration. A review by the European agency for safety and health at work (EASHW) (Donati et al., 2008) examined 6 member states; Belgium, Finland, France, Germany Poland and Spain and found that the implementation of directive 2002/44/EC varied between each. Certain countries

have transposed the directive with lower limits including Finland, Poland and Germany as discussed by EASHW. Germany's VDI 2057 Part 1 (VDI, 2002) is of particular interest as it brings the limit values in agreement with ISO 2631-1 and allows for the usage of alternative vibration calculations to calculate exposure to vibration where appropriate.

Even though the directive is relatively new in comparison to ISO 2631-1 it is still based on the assessment techniques described within the international standard, an area of considerable discussion within the vibration community (sections 1.4.1 and 1.4.4). Donati et al. (Donati et al., 2008) describe the requirement for more research in the analysis methods contained within ISO 2631-1 and their application in 2002/44/EC.

Directive 2002/44/EC also allows for derogations, especially in the fields of sea and air transport. This is of particular importance as this thesis is examining the role of vibration in the marine defence environment.

### 1.4.7 The Control of Vibration at Work Regulations (2005)

The control of vibration at work regulations (CVWR) (Regulations, 2005) is a transposition of 2002/44/EC into British law. The UK limits are the same values as set out in the original 2002/44/EC document. There is no usage of the VDV method as some other countries have decided to opt for, which is curious considering the history of BS 6841 in the UK.

Minor changes have been made to the document during transposition such as specifying that exemptions for emergency services, air transport and for the MoD can be applied for from the Secretary of state. For the MoD derogations can be made for any matters which are *"in the interests of national security".* Where the EAV cannot be met it must be documented and shown that the exposure to vibration has been reduced to "As low as reasonably practical" and regular health surveillance should be carried out by the employer.

Marine craft are also subjected to the 2007 regulations under MGN 353: merchant shipping and fishing vessels (Control of vibration at work) (Maritime and Coastguard Agency, 2007a) which is almost identical in content to the

CVWR but with specific mentions to commercial boats, their operation and their crew. MGN 353 identifies that the risks from WBV exposure are higher in poor sea conditions and in fast boats.

In a freedom of information request to the Navy Command Secretariat (Navy Command Secretariat FOI Section, 2016) it has been stated that the British Navy has received a derogation which is valid until the 6th of July 2020 and that *"No maritime user of these types of craft can currently meet the ELV set out in this legislation"* and that the *"MoD will therefore have to apply for rolling 5-year exemptions and derogations".*

This is troubling for many civilian and military personnel whose livelihoods depend on environments where exposure to vibration is an everyday occurrence. LITTLE published data exists from the health surveillance clauses of CVWR and the Merchant shipping and fishing vessels making a detailed analysis difficult.

### 1.4.8 Implications

Taking a critical look at the standards and legislation in regards to WBV reveals areas in which they are lacking:

- ISO 2631-1 performs analysis on the waveform itself and doesn't take into account the human biological response to vibration apart from comfort weighted frequency contours
- The application of frequency weighting is an issue of controversy
- The health guidance zone as described by ISO 2631-1 is thoroughly confusing
- ISO 2631-5, which attempts to model human biodynamic response has not been epidemiologically validated
- The sampling frequency of 160 samples per second used in ISO 2631-5 could adversely affect evaluation
- The EC directive 2002/44/EC has much more lenient vibrational limits than the ISO standards they are based on

- The UK navy do not have to reach the standards of the UK Control of vibration at work regulations or the merchant shipping and fishing vessels regulations
- Difference in those exposed to vibration are not taken into account (posture, body mass, height)

In addition to this there is no defined causal relationship between WBV and LBP, the general consensus is that if it makes you feel uncomfortable it is probably causing damage. This reasoning is not based on scientific evidence and is a cause for alarm when it is influencing laws and regulations in many countries.

## 1.5 The State of Whole-Body Vibration in Relation to the Lower Back

### 1.5.1 Early studies (Up to 1997)

Human response to extreme WBV is noted in papers from the 1950s such as Roman's (1958) report on experiments by White. In this report internal bleeding was noted at the extreme accelerations, whereas pain lasting for two days after experimentation was noted at the lower end. The ethics of this experimentation not-withstanding the subjects were subjected to vibration magnitudes at 1.5g up to 10g; which is significantly more than what would be experienced normally.

Roman also performed time to mortality sinusoidal studies on mice at 15g with mortality shortest in the range of 10-25Hz. Vertical vibration tests were carried out on domesticated cats with groups at 15g and 10g with varying times of exposure (Pape et al., 1963), the authors conclude that the decrease in vibration magnitude was more important in reducing the mortality rates than the time of exposure, stating there was a *"pathological correlation between the intensity of the forces applied and the response"*.

None of the studies allude to LBP and any such resulting pain from such short exposures could be entirely coincidental. Nevertheless, studies by Roman and Pape show notable damage in response to extreme vibration.

Through correspondence with orthopaedic surgeons, spinal disorders were attributed to "rough-riding" vehicles such as trucks and tractors (Fishbein and Salter, 1950) though the respondents were small in number and there was divergence from the surgeons on the contribution of vibration exposure to these disorders. Another epidemiological survey examining disc herniation put operating a motor vehicle as the greatest contributing risk to developing a herniated disc (Kelsey, 1975). Kelsey posits that it is a contribution of driving posture, lack of back support and exposure to vibration which leads to this elevated risk. This increased risk from driving a motor vehicle is supported in a papers by Frymoyer et al. (1983) and Walsh et al. (1989). Frymoyer also showed an increased risk with operating machine tools, another source of vibration in the workplace.

Bovenzi and Betta (1994) showed that posture as well as vibration exposure were significantly associated with low-back disorders; this is expected as it has been shown that posture affects peak loading within the spine. The operation of vehicles can lead to unfavourable postures of the spine when turning or reversing (Wikström, 1993), Wikström observed an increase of EMG-activity with vibration level. This relationship between posture and vibration could be a contributing factor not examined by earlier reviews. In a follow up review paper (Wikström, Kjellberg and Landström, 1994) the authors acknowledge the difficulty in defining the contribution of posture to discomfort under WBV.

Another review paper by the Seidel and Heide (1986) examined 78 epidemiological papers with vibration sources which included vehicles and stationary equipment. The main pathological conditions observed were in the lumbar part of the spinal column; however in this review the authors are critical of the non-standardised assessment of these health effects. Seidel and Heide are therefore careful not to link this directly to WBV but rather state an increase in risk of morbidity correlating with life-time WBV exposure or higher exposure intensity. This is consistent with other review papers of the time (Dupuis and Zerlett, 1987; Hulshof and Van Zanten, 1987; Pope and Hansson, 1992).

The focus on WBV has been mostly examining exposure in operators of land-based heavy machinery. Two reports from Japan examined the health effects of shocks in large marine vessels using the DRI method (section 1.3.2) (Kanda et al., 1980, 1982) where they found accelerations as high as 3g and frequently above 1g. The shocks are even higher for high speed planing boats (Gollwitzer and Peterson, 1995) where the shocks reported from sea trails were approximately 6g at their maximum. The sea state as reported by Gollwitzer et al. was calmer than that of Kanda et al. therefore we can assume that the accelerations would be even greater for a rougher sea state. Placement of the sensors is critical for examining the health effects caused by WBV (section 1.3.3), in both papers the sensors were positioned on the deck of the ship and not at the occupant/craft interface point; therefore any inferred health effects must be treated with caution.

The papers by Kanda et al. reported vertebral damage in the form of deformed IVDs through X-ray examination. The authors state that *"It is appropriate to assume that the primary cause of frequent occurrences of the low back pains is the excessive repeated compressive load exerted on the spinal vertebra…"* Through use of the DRI and the observed health effects, the authors assume that a spinal loading model can be used to predict damage and by extension, LBP.

In a review by Sandover (1983) the author applies fatigue models to estimate the fatigue life under dynamic loading that can be expected from vehicle vibrations. Using a fatigue model Lafferty (1978) found a high fatigue exponent of -9.95 in relation to applied stress; indicating that small variations in the ultimate material strength would have a very large impact on the calculated fatigue life. This is echoed by the large exponent of -14 seen in experimental tests (Hansson, Keller and Spengler, 1987) and in fatigue testing of vertebral samples tested at higher relative loads that are high compared to their predicted ultimate strength (Brinckmann et al., 1987). Sandover's (1983) application supports the theory that exposure to vibration can cause degenerative changes within the spine.

In assessing LBP as arising from fatigue damage through WBV, Seidel (1993) states *"The extent of peak forces is of decisive importance, because the peak rather than average (rms) values determine the fatigue failure of materials"*. ISO 2631 and BS 6841 are concerned with the average values of vibration which cannot accurately capture the loading profile.

### 1.5.2 Modern research (1997 - Present)

Sandover (1998) continued their work at applying fatigue damage principals with WBV with the prediction of fatigue life of vertebral endplates in operators of heavy vehicles exposed to WBV. Their conclusion agreed with Seidel (1993) on the importance of peak loading rather than the averaging methods used by ISO 2631 to predict damage in the spinal endplate.

With the development of ISO 2631-1 (ISO, 1997) more research was carried out to examine the effects of the new legislation in regards to health effects. A review paper (Bovenzi and Hulshof, 1999) compared the quality and design of epidemiological studies from an earlier review (Hulshof and Veldhuijzen van Zanten, 1987) and established that the data collected has improved in the intervening years. Although over ten years had passed since the first review paper with Hulshof, no dose-response relationship between WBV and LBP has been clearly identified. Bovenzi and Hulshof conclude that most of the industrial vehicles in the studies reviewed exceed the action level and sometimes even the limit value as proposed by ISO 2631-1. A report by the research group VIBRISKS echoed these remarks with data from epidemiological surveys in Italy, Sweden, the Netherlands and the United Kingdom (VIBRISKS, 2007a). These studies showed an increased occupational risk for professional drivers operating heavy machinery when assessed in accordance to 2002/44/EC.

VIBRISKS was created in 2003 to assess the risks arising from vibration, with HAV and WBV being the main factors examined; it was an EU research program lasting 4 years created under the Fifth Framework Programme (FP5) with EU funding. Collaborators included eminent researchers and organisations in the field of vibration and they examined vibration in relation to the limits set by 2002/44/EC (European Parliament, 2002). Of particular interest is the

conclusion that risk of LBP is multi-factorial and cannot be exclusively predicted from vibrational measurements (VIBRISKS, 2007b). This is of importance as the standardised ways of measuring WBV do not take this into account; body mass and posture have been shown to affect the risk factors for developing LBP.

Models have been used to describe the damaging response to movement for some time, DRI being a prime example of this. DRI uses the ultimate compressive load obtained from laboratory tests to inform the possible negative consequences of an aircraft ejection. Given the complexities of the human spine, general models such as the DRI have their limits. ISO 2631-5 is another example of such a generalised model. ISO 2631-5 attempts to model the risk of spinal damage through peak force accumulation similar to the methods by Sandover (1983) but does not take the importance of other confounding factors into account (Seidel et al., 2007a).

ISO 2631-5 is concerned primarily around a $50^{th}$ percentile male (by mass) seated upright with an unsupported posture; when compared against a linear-FE model developed as part of the VIBRISKS program (Seidel et al., 2007b), which takes into account variables such as posture and mass, the risk of incidence is higher than those calculated by the RNN of ISO 2631-5 (Seidel et al., 2007c). The risk of incidence was simulated taking, as input, seat cushion acceleration of heavy machinery. Incidence of risk was found to be higher at RMS values much lower than the 8-hour limit values described in Directive 2002/44/EC (European Parliament, 2002) and even the more restrictive ISO 2631-1 (ISO, 1997). The authors of this particular annex state that usage of this model is extremely complex as it requires model specific frequency weightings (Seidel, 2004) which would further complicate ISO 2631-1.

The data analysed and conducted as part of the VIBRISKS project were almost entirely ground based vehicles. It has been shown previously that high-speed marine vehicles operate in a highly demanding environment and the crew are exposed to extreme levels of vibration (Gollwitzer and Peterson, 1995; Kanda et al., 1980, 1982). A possible reason for the excessive levels of WBV on high-speed planing craft is discussed by Kearns and Vandiver (2001), when referring

to the Mark V Special Operations Craft (MkV SOC). Development of this craft was lacking resources, modified off-the-shelf designs which had catastrophic effects on the ships and their operators. In a statement Lt. Shearer, a senior Medical officer for the US Navy, said that: “The Mark V Special Ops vessel has produced slamming forces up to 20g’s, twenty times gravity”. Although unverified, this puts vibrations felt by operators of the MkV SOC similar to aircraft ejections (Sustained forces of ~20g’s). Ejections from aircraft have been shown to cause spinal damage from the force of the ejection gun (Read and Pillay, 2000) as well as limb injury on landing. Similar musculoskeletal problems are seen in the marine environment (Gollwitzer and Peterson, 1995; Ministry of Defence, 2017a) although not to the extremes of ejection; this could be due to the Mark V Special operations craft being an outlier in regards to vibration exposure.

Allen, Taunton and Allen (2008) conducted at sea vibration measurements on high-speed boats over two trials at various directions in respect to the wave motion. They showed the VDV was dominated by shocks and vibration in the Z axis and was highly influenced by the sea state (sea state 3 and 2, for trails 1 and 2 respectively) which the boat traversed. The crest factors measured (~24.3 and ~21.3) were much larger than the threshold value of 6 stated in ISO 2631-1 for the accurate measure of WBV using $4^{th}$ order techniques. VDV was used in these trials leading to values larger than the maximum daily dose (48.54 $ms^{-1.75}$ and 25.94 $ms^{-1.75}$) within a 90 minute exposure. These high exposure values in High Speed Craft (HSC) have been corroborated by military sea trials where 25% of HSC reached ELV within 10 minutes (McIlraith, Paddan and Serrao, 2014). The high vibration levels correlate with health effects as described by Ensign et al. (2000) in conditions of rougher seas and for longer periods than those measured by Allen et al.

The question then lies with how damage is translated into the spine within the marine environment. A report by the Marine Accident Investigation Branch (Branch, 2009) details a spinal injury sustained on a RIB during a thrill ride on board the “Celtic Pioneer”. The occupant was sitting towards the front of the

boat and a steep rise followed by a sharp slam caused a wedge compression fracture of the L2 vertebrae. This seating position has been known to have the highest vibration levels within RIBs (McIlraith, Paddan and Serrao, 2014).

Ergonomics and seat design plays a large role in the migration of shock inboard HSC. For example; the seats used in the MkV SOC mentioned above had two variants: V4 Semi-rigid and V5 suspension seats. The suspension seats proved to be much safer than the semi-rigid such that it *"would have been considered unethical to use a human test subject in the V4 semi-rigid seat"* (Dobbins, Rowley and Campbell, 2008).

Dobbins, Rowley and Campbell were the principal authors of the "High speed craft human factors engineering design guide" a collaborative project between the ABCD Working Group as well as the Royal National Lifeboat Institution (RNLI) and MoD. In this guide it was shown that proper ergonimically designed seats with 6-way adjustment were able to provide an average reduction of shock of 24%.

The principal component of the "High speed craft human factors engineering design guide" was that marine craft should be designed using a holistic approach to mitigate vibration and shocks. This view is shared by the Maritime and Costguard agency which has published guidance on "Mitigating Against the Effects of Shock and Impacts on Small Vessels" (Maritime and Coastguard Agency, 2007b) which not only provides guidelines for the design of small high speed craft but also the operation in more detail than MGN 353 (Maritime and Coastguard Agency, 2007a). For example: tailoring the voyage in regards to the occupants could reduce the likelihood of accidental injury avoiding a future incident like the "Celtic Pioneer".

If WBV is thought to induce spinal damage by way of fatigue, an examination of spinal fatigue failure and in particular the weakest element, trabecular tissue, may give more information.

## 1.6 Microdamage of Trabecular Tissue

An assumption can be made that fatigue is the primary method of damage within spinal column under WBV; this failure leads to microdamage in trabeculae and the development of LBP.

Although not exclusively trabecular bone, Hansson and Roos (1981) conducted an early examination of whole vertebrae using then current state of the art imaging techniques to examine microdamage. They used radiographs and dual photon absorptiometry; which is a precursor to the more accurate dual-energy x-ray absorptiometry used widely today (Wahner et al., 1988). They examined callus formations in 109 vertebrae, areas of subsequently repaired historical microdamage. The key findings were that more calluses were found in vertebrae with a lower bone mineral density (BMD) and that 90% of the lesions were found in the upper and lower thirds of the vertebrae, which is closer to the endplates and IVD. This is consistent with theory that damage is concentrated around the endplate region of vertebrae (Sandover, 1998).

Trabecular microdamage leads to the reduction of the apparent modulus, up to 60%, of cylindrical bone samples (Wachtel and Keaveny, 1997) showing the cumulative effect from bands of damage. Wachtel and Keaveny also argue that strain is the main driver to the amount and type of damage within trabeculae, a view shared by Moore and Gibson (2002). Moore and Gibson tested more strain values and at strains higher than Wachtel and Keaveny giving a more detailed view of how strain affects trabecular microdamage. Ultimate compressive strain was found to be around $\varepsilon$=-1.91% ± 0.55% after which microdamage increased quickly.

Nagaraja, Couse and Guldberg (2005) examined microdamage using a voxel based FE model from CT scans. Rather than examining the apparent level, as previous authors had, they examined the stresses and strains at a local level. They were in agreement with Moore and Gibson, (2002) who stated that complete trabecular fracture was rare, yet microdamage was extensive within the tested specimens.

A large body of literature has examined the effects of fatigue on trabecular bone and as such several well-established methods for assessment have been developed. Table 1-4 below shows some of the recent literature in examining cancellous fatigue failure; they are listed in reverse chronological order. There are two main groups prominently publishing in this field; Gibson et. al. (Cheng, 1992; Ganguly, Moore and Gibson, 2004; Moore, O'Brien and Gibson, 2004; Moore and Gibson, 2003a) and Hernandez et. al. (Goff et al., 2015; Lambers et al., 2013)

The testing has been carried out on bovine and human bone, with research groups using the same species. A reason for this may be because of the significant differences in moduli between human and bovine bone ($E_{human}$ = 77.36 ± 54.96 MPa, $E_{bovine}$ = 117.49 ± 61.53 MPa) (Poumarat and Squire, 1993), using the same species allows for a direct comparison between studies.

The locations at which bones are taken are also consistent, either the lumbar vertebrae or the Tibia; only one paper examined femoral trabecular bone (Dendorfer et al., 2008) and another paper also examined thoracic vertebral bone (Rapillard, Charlebois and Zysset, 2006). In combination with the species examined it is either the bovine tibia or the human vertebrae from which trabecular bone has been excised from. This is consistent within the research groups.

Most of the experimental work examined pertaining to the fatigue of trabecular bone has been performed with cylinders with a diameter to length ratio which conforms to the DIN testing standard (Diameter to Length ratio: 1-2) (Anon., 2016)

| *Author* | *Species* | *Geometry* | *Directional effects* | *Location* | *Dimensions (D x L) (approximate)* | *Rate* | *Testing conditions* |
|---|---|---|---|---|---|---|---|
| (Cheng, 1992) | Bovine | Cylinder | | Tibia | 6mm x 9mm | 2Hz | 10N to ε=-[0.29%,0.45%] |
| (Haddock et al., 2000) | Human | Cylinder | | Lumbar | 8.3mm x 40mm | 0.1 ε/s | $\sigma/E_0$=[0.4,0.5] |
| (Moore and Gibson, 2003b) | Bovine | Cylinder | | Tibia | 6.27mm x 9mm | 2Hz | $\sigma/E_0$=[0.005,0.008] |
| (Haddock et al., 2004) | Human | Cylinder | | Vertebral /Tibia | 8.3mm x 40mm | 0.0015 ε/s | $\sigma/E_0$=[0.026,0.070] |
| (Ganguly, Moore and Gibson, 2004) | Bovine | Cylinder | | Tibia | 6.27mm x 9mm | 2Hz | $\sigma/E_0$=[0.005,0.009] |
| (Moore, O'Brien and Gibson, 2004) | Bovine | Cylinder | | Tibia | 6.27mm x 9mm | 2Hz | $\sigma/E_0$=[0.0065,0.0095] |
| (Wang and Niebur, 2006) | Bovine | Cylinder | | Tibia | 8.2mm x 23mm | 0.5 ε/s | ε=4% (Torsion), ε=-2% (Compression) |
| (Rapillard, Charlebois and Zysset, 2006) | Human | Cylinder | | Thoracic Lumbar | 8mm x 10mm | 2Hz | 40% reduction of E |
| (Dendorfer et al., 2008) | Human Bovine | Cylinder Cube | (0,22,45,90°) | Vertebral Femoral | 11.2 x 15mm 7.75 x 7.75 x 15 mm | 0.015 ε/s | $\sigma/E_0$=[0.0022,0.0147] |
| (Lambers et al., 2013) | Human | Cylinder | | L3 | 8mm x 19mm | 4Hz | $\sigma/E_0$=0.0035 |
| (Goff et al., 2015) | Human | Cylinder | | L3 | 8mm x 25-30mm | 4Hz | $\sigma/E_0$=0.0035 |

**Table 1-4: Cancellous fatigue literature**

There is a difference in the method by which the forces are applied in response to fatigue: if the strain rate is set, the sample will deform over an increasing amount of time; if the frequency is set then the strain rate of the sample will increase throughout testing. At the strain rates examined here this effect is negligible (Carter and Hayes, 1977; Linde et al., 1991; Pal, 2014).

The testing conditions are either strain based or based upon "normalised stress". Normalising for stress is done to reduce the inter-specimen variability of samples caused by differences in morphology, allowing for a more generalised comparison between them. This is done by dividing the applied stress by the initial Young's modulus (Equation **(1-10)**).

$$\sigma_n = \frac{\Delta\sigma}{E_0} \qquad \textbf{(1-10)}$$

Where,

$\sigma_n = \text{Normalised Stress}$

$\Delta\sigma = \text{Applied stress}$

$E_0 = \text{Initial Young's Modulus}$

Trabecular microdamage under monotonic loading has been shown to be strain driven (Moore and Gibson, 2002; Wachtel and Keaveny, 1997); under fatigue loading these relationships have been shown to hold true (Moore and Gibson, 2003a) with strain/microdamage relationships which are stronger than strain/normalised stress.

Cheng (1992) examined the failure method of trabecular cores concluding that neither creep nor crack growth is solely responsible for failure under fatigue loading. After further examination by Moore, O'Brien and Gibson (2004) creep is considered to contribute little to fatigue in cancellous bone and that the plastic translation in strain is attributed to microdamage or diffuse damage. This is corroborated by Haddock et al. (2004) who state that crack propagation is the dominant source of damage and this appears as creep deformation.

Examining the relationship between bone architecture, mechanical properties and microdamage under fatigue leads to results which are expected; More microdamage accumulates before failure in high density bone or under low loading (Haddock et al., 2000) and cycles to failure increases with BV/TV (Rapillard, Charlebois and Zysset, 2006).

Orientation of bone is also important; a study by Dendorfer et al. (2008) demonstrated how sample orientation, in respect to the main axis of loading, affects the number of cycles to failure. As the sample orientation deviated from the main trabecular direction (0°) the cycles to failure decreases rapidly (following an almost logarithmic function) for a given normalised stress, such that the cycles to failure between 45° and 90° is practically constant. This is of importance to postural loads within the spine (section 1.2.6), which change where the load is applied thus modifying the orientation of applied load, and could contribute to in-vivo fatigue failure.

This is in agreement to a previous study (Öhman et al., 2007), where incorrect alignment accounted for an approximate 40% difference in Young's modulus and ultimate compressive stress between a 6° and a 21.6° misalignment. This has severe implications to the models and theories which have been developed through research conducted on cancellous samples, including the study by Dendorfer (Dendorfer et al., 2008) which measures how specimen angle affects the fatigue life without stating the deviation of orientation within the samples.

Animal bone specimens are used frequently as surrogates for human samples (Table 1-4) as they are easier to obtain and the usage of them is less ethically constrictive. The selection of the correct animal is difficult as the architecture and mechanical response varies between species. The need to examine the human spine means it is important to find an animal analogue with similar morphology and material properties to human vertebrae. A review (Sheng et al., 2010) taking into account over 500 papers published between 1980 and 2008, compared the shape and sizes of various animal spines with human vertebrae. They concluded that certain animal spines are better matches for different vertebral levels, such as sheep for the cervical level and calf/porcine for the

thoracic and lumbar levels. Porcine tissue was found to have similar micro and macrostructural properties to human bone with a bone composition only more closely matched by canine tissue (Pearce et al., 2007).

The mechanical properties of various animal intervertebral discs (including calves, pigs, baboons, sheep, rabbits, rats and mice) have been compared with humans. It was found that, when normalised for size and height, there is no significant difference under axial forces (Beckstein et al., 2008) and only calves and goats displayed significantly different torsional properties (Showalter et al., 2012). Porcine vertebrae have also been shown to be a good alternative for healthy young human spines in terms of damage location under compressive and shear loading (Yingling, Callaghan and McGill, 1999).

## 1.7 Finite Element Models

The development of various fatigue damage prediction models for the human spine signifies a shift from the assumption that health effects caused by WBV can be measured through averaged vibration exposures. The modern thinking is that LBP is more accurately described by a multi-factorial fatigue based damage model.

The use of animals in scientific studies is fraught with ethical difficulties, the use of the “3Rs” (Replacement, Reduction and Refinement) in EU Directive 2010/63/EU (European Parliament, 2010) has the aim to replace the use of animals in research. As a result of this there has been a recent shift in examining bone using FE methods.

With the advent of high performance computing (HPC) examining bone at the microscopic level has become feasible. Voxel meshing from high-resolution micro-CT is typically used as it significantly reduces computational time while still retaining computational accuracy (Baumann et al., 2016).

There is also a need to validate the data against mechanical testing; with trabecular bone this is difficult as mechanical testing is highly specimen

dependant. In a monotonic compression study, the sample donor highly influenced the amount of microdamage generated (Lambers et al., 2014).

There remains considerable discussion on how to account for this discrepancy. Some authors (Niebur et al., 2000; van Rietbergen et al., 1995) assign a starting value for Young's modulus at the microscopic level which is adjusted to agreement with validated data either from mechanical testing or values in the literature.

As apparent modulus ($E_{app}$) of bone is a function of architecture rather than location (Morgan, Bayraktar and Keaveny, 2003) assigning accurate material properties which reflect bone as a continuum is of critical importance; especially if there is to be a standardised method to simulating bone with finite element (FE) techniques.

There have been several models describing a relationship between apparent density ($\rho_{app}$) and the mechanical properties of cancellous bone (Carter and Hayes, 1977). These models are sensitive to changes such as species, testing methodology and specimen location as shown to differ in a literature review by Helgason et al. (2008). Helgason states that because of differences in the experimental procedures: *"all studies cannot be assumed equally valid and cannot be pooled together statistically, to derive an average elasticity-density relationship"*.

The relationship between BMD and apparent density is not monotonic (Zioupos, Cook and Hutchinson, 2008) and therefore attempting to ascribe a mechanical property based upon BMD is fraught with difficulty.

Ash density ($\rho_{ash}$) is a better predictor than apparent density of the mechanical properties of bone (Keller, 1994) but this is a destructive technique which may be influenced by prior mechanical testing.

While apparent density cannot give accurate microscopic mechanical properties of bone, CT imaging allows for a non-invasive characterisation of bone at the material level. This is currently the most common way of applying material specific mechanical properties.

Calibration to a standardised value is important; this can be done from scanning a bone density phantom in and applying a transformation to Hounsfield units (HU), or by mapping the known material densities to the corresponding greyscale range (Helgason et al., 2016).

Hounsfield units are a linear measure of a sample's attenuation in relation to air and water. Calibration to Hounsfield in accordance to scanned grayscale values has been shown to be difficult using clinical cone beam CT scans (Pauwels et al., 2015). Scanning a phantom with known densities allows for a direct comparison between CT greyscale (GS) and material density without prior transformation into Hounsfield units.

Authors have shown that mineralisation of bone is significantly correlated with its microhardness which is linked to Young's modulus (Boivin et al., 2008). Using CT techniques mineralisation is clearly visible and quantifiable (Rüegsegger et al., 1976). Adams (2017) used micro-CT scans and nanoindentation of trabecular tissue from a range of animals, this gives large density range and a generalised model for determining Young's modulus based on micro-CT calibrated density using a scanned density phantom.

This model attempts to fix an inherent problem with the FE of trabecular tissue; most models in the literature are very specimen specific and there is no universally accepted material model for the mechanical properties of bone.

A recent study by Helgason et al. (2016) applied 5 material mapping methods and 10 Modulus/Density relationships on a femoral neck to simulate impact. In the individual papers, agreement was good between FE and experimental work. When applied by Helgason et al. with different specimens under different experimental conditions, there was less agreement. This revealed the large difference arising from different mapping techniques and density relationships.

Fatigue of bone has been simulated using a variety of FE techniques, from cycle block set estimated damage accumulation (Hambli et al., 2016) to full element by element damage modelling (Harrison et al., 2013).

The basics of modelling fatigue in bone are laid out by Mostakhdemin, Amiri and Syahrom (2016). Discussing stress, strain and crack based failure models and their individual advantages and disadvantages.

Stress based models are thought to be good when stresses are below the elastic limit but have been displaced by strain failure models for reasons of computational efficiency (Keaveny and Hayes, 1993)

The strain based model selected in the paper by Mostakhdemin et al. requires physical testing and applying the derived fatigue constants in the FE models. This leads to a model which depends heavily on the sample set and testing methodology, creating the same issues as noted by Helgason et al. when applying this model elsewhere.

Modelling trabecular bone failure is not without its problems; the calculations needed to estimate crack initiation are complex, resource intensive, difficult to apply in 3D space and under fatigue loading (Weißgraeber, Leguillon and Becker, 2016).

## 1.8 Conclusion

While more data has been collected on exposure to WBV and legislation limiting exposure to vibration exists, we are no closer to obtaining evidence that WBV causes LBP. The averaging methods developed in the 70s are still in use today even though they have been shown to be inadequate at describing severity of vibration exposure and at predicting the incidence of LBP.

From the lack of a cause/effect relationship of WBV and LBP it might be inferred that none exists, though studies have shown that risk factors for LBP correlate with WBV exposure. The examination of the health effects deriving from WBV is multifactorial and heavily related to the environment in which exposure occurs.

There is a difference between what tests can be made with living and cadaveric specimen. For a living human subject assessing comfort from a vibration signal on a seat pad is acceptable but exposing the same subject to internal damage is ethically unacceptable; all relevant testing must then be carried out on cadaveric samples from either human or animals.

Although these tests can be more rigorous and are based on quantitative analysis, it removes the sample from its natural conditions. This is problematic as LBP is a condition that develops over a lifetime; within the human body bones are given chance to recover; intervertebral discs decompress, muscles relax and bone repairs itself.

Of the vertebral tissue, vertebrae, facet joints and intervertebral discs bear the brunt of the loading distribution. Of these the vertebrae are considered the most fragile, with the cancellous bone capable of being more easily damaged then the cortical (Hansson, Keller and Spengler, 1987). Many previous studies have performed fatigue testing on cancellous bone and it is accepted in the literature that WBV can lead to mechanical fatigue of the musculoskeletal system, primarily in the lower back (Ayari et al., 2009; Sandover, 1983).

When exposing bone to vibration it may be useful to quantify the testing signal in regards to ISO 2631-1 especially as this is the basis for legislation in the UK,

leading to an improved understanding of how the standardised way we examine WBV and damage interact.

A problem that plagues the pursuit to connect WBV and LBP is that many vibrational studies tend to be purely mathematical, examining vibration statistics for different conditions with the assumption that reduction of exposure will reduce the incidence of LBP. Many studies are also occupational; examining the risk factors of certain tasks and operations rather than the likelihood that exposure to WBV is causing damage; there has been no clearly defined link between WBV and LBP (Stayner, 2001). A lot of work has been conducted into examining the possible health effects from WBV, from epidemiological tests of high risk populations to tests on humans and animals to examine biodynamic responses and damage.

Although IVDs and endplates have been shown to be the most commonly damaged part of the spine under WBV, accidents at sea (Branch, 2009) as well as in-vitro tests (Yingling, Callaghan and McGill, 1997) have shown that as loading rates approach dynamic loading, failure within the vertebral body is more common.

Research into modelling fatigue damage within trabeculae is limited. Each individual has unique bone formations and there is a need for the accurate prediction of trabecular fatigue failure that is sample specific yet can be automated and derived from basic principles.

A more robust Finite element model for trabecular fatigue damage is needed before linking with WBV and sea craft. This model should be able to accurately model the mechanical properties of bone as well as simulate trabecular micro-damage caused by fatigue which is thought to contribute towards LBP.

# 2 MATERIALS AND METHODS

## 2.1 Introduction

This thesis will focus on four main areas:

- Fatigue testing of porcine trabecular cores
- Signal Analysis in regards to the legislations and standards used in the UK
- Finite element validation of the density/modulus relations as described by Adams
- Sample specific FEA to examine models of fatigue
- Application of these FE models on human trabecular bone

Fatigue testing of the spine is well documented in the literature (Section 1.6), as is the use of vibration statistics (Section 1.5), though the two are rarely compared. Through examining this relationship a greater understanding of how the two may be interconnected is sought.

The finite element technique developed by Adams (2017) was previously conducted on tension for four samples. The methods used in this thesis are compressive and fatigue testing; this difference will be investigated with a mechanical validation of the finite element models before further analysis.

Simulation of fatigue using FE techniques is resource intensive with many different methods available in the literature (Mostakhdemin, Amiri and Syahrom, 2016). A selection of finite element methods which model trabecular failure is detailed in the relevant chapter (2.4.1) and the best performing method will be taken forward into testing on human trabecular tissue.

## 2.2 Porcine Fatigue Testing

### 2.2.1 Ethical Approval

All tests conducted on porcine tissue for this thesis have been ethically cleared for experimentation through the Cranfield University Research Ethics System with reference number: CURES/686/2015.

### 2.2.2 Sample Preparation

Two porcine spines were obtained from the human food chain through a local butcher. The pigs were slaughtered between the ages of 20-24 weeks.After purchase spines were sectioned using a band saw to cut through each IVD. Five thoracic vertebrae from each spine were cored using a 9mm diameter diamond tipped coring tool in the Inferior-Superior (IS) direction while hydrated. This produced 10 spinal cores for fatigue testing.

The resulting 9mm diameter cores were cut to lengths of 15mm to keep the diameter to length ratio between 1-2 as recommended by DIN 50106 (2016). This was done with a 300µm thick diamond blade in a diamond blade cutter (Struers Accutom 2, Ballerup, Denmark) under constant water irrigation. The ends were polished flat on a grinder and polishing machine (Metaserv Rotary Pregrinder, Metallurgical Services, Surrey, UK).

The samples were cleaned in a water jet, expulsing the fat and marrow from the open cell trabecular regions. Samples were then measured using electronic callipers and weighed in both water and air. Apparent density was calculated using the Archimedes method and bone volume to total volume fraction (BV/TV, also known as “volume fraction”) was calculated using Equation (2-1) below.

$$\frac{BV}{TV} = \frac{\rho_{app}}{\rho_{mat}} \quad \textbf{(2-1)}$$

Where,

$\rho_{app}$ = Apparent density

$\rho_{mat}$ = Material density

Cyanoacrylate adhesive was used to attach 5mm PVC end caps to the free faces of the samples to avoid end effect artefacts which cause inaccurate readings of stiffness and bone mechanical properties (Keaveny et al., 1997). The resulting specimens were approximately 25mm long.

After sample preparation samples were scanned in air in a micro-CT (Nikon XTEK XT G 225, Tokyo, Japan) at 80kV and 65µA with ABS sample holders. The scans were reconstructed using CT Pro 3D (Nikon, Tokyo, Japan), an example of which is shown in Figure 2-1.

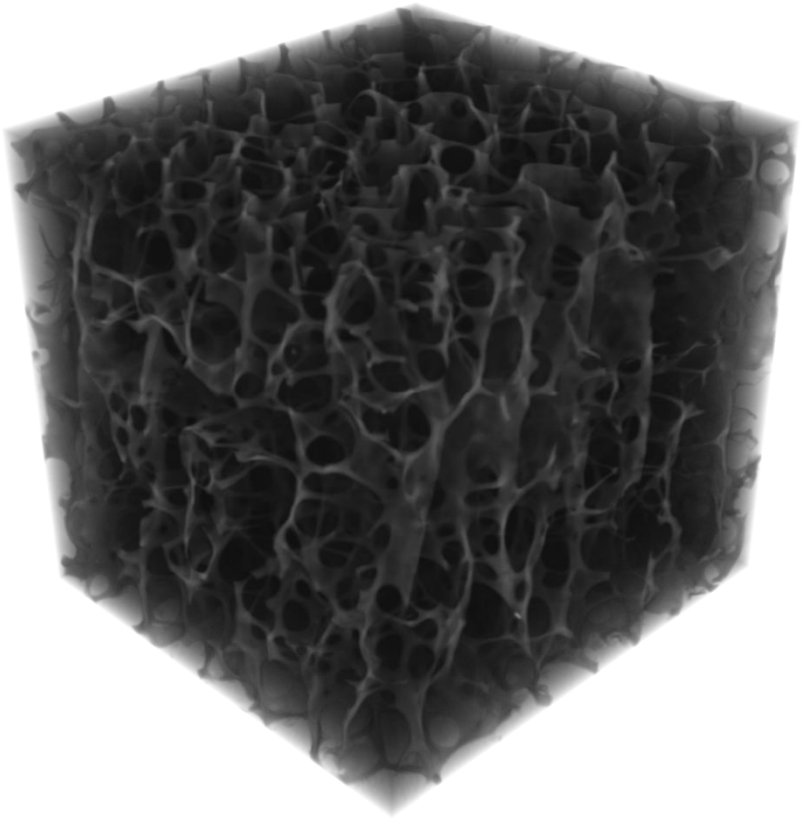

**Figure 2-1: Example reconstruction of a region of trabecular bone**

The CT image voxel size was ~13µm allowing for measurements of sample morphology (Yan et al., 2011). Additionally a scan of a QRM-MicroCT-HA bone density standard (QRM GMBH, Möhrendorf, Germany) was conducted at the same settings to allow for density calibration.

All samples were then frozen and kept at -20°C prior to fatigue testing, which does not affect the compressive mechanical properties of mineralised tissues such as bone (Pelker et al., 1983).

### 2.2.3 Mechanical Fatigue Testing

All cores were fatigue tested in a servo-hydraulic testing machine (Dartec Series HC25, Dartec Ltd. Stourbridge, UK) with cylindrical cups to secure the end caps. Samples were tested under force control monitored using a 5kN load cell (Sensotec, RDP Electronics Ltd., Wolverhampton, UK). A 6mm gauge length contact extensometer (Model 3442, Epsilon Technology Corp., Jackson, USA) was attached using knife edge grips held with dental elastics. The dental elastics were strong enough to hold the sample in place but not to cause deformation in the bone. The testing machine was controlled by 'Workshop 96' (Dartec Ltd. Stourbridge, UK) via a 9610 controller.

Before testing, samples were removed from the freezer and rehydrated in a saline water bath at 37°C for 30 minutes. The samples were kept constantly hydrated during testing with a directed saline water jet kept at 37°C. The test set up is shown in Figure 2-2.

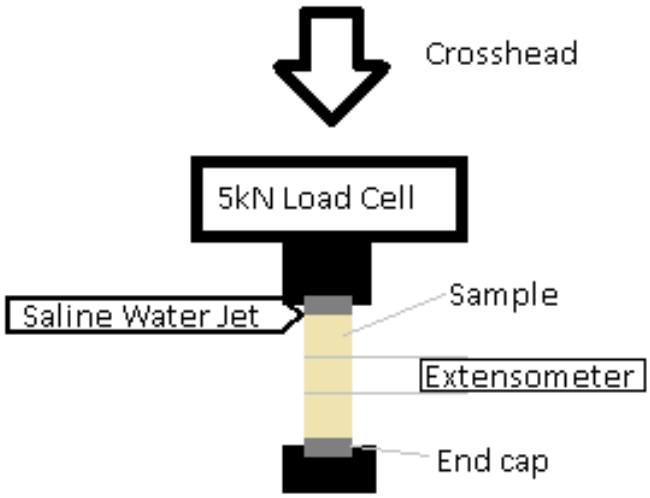


**Figure 2-2: Test set up for porcine core fatigue testing**

Samples were subjected to 20 compressive preconditioning cycles of 10-50N at a frequency of 2Hz. A linear fit of the Force/Extension graph of cycles 12-16 was used to calculate the initial sample stiffness. The extensometer was filtered at 5Hz to remove temporal artefacts over this examination window. The stiffness was then converted into initial apparent modulus using the cylindrical area and gauge length of the sample using equation (2-2).

$$E_0 = \frac{kL_0}{A} \quad \textbf{(2-2)}$$

Where

$E_0 = \text{Initial Young's modulus}$

$k = \text{Specimen Stiffness } (\text{kN/mm})$

$L_0 = \text{Initial gauge length } (\text{mm})$

$A = \text{Area of cylindrical section } (\text{mm}^2)$

Using cyclic loading in this manner has been shown to be a non-destructive method to obtain the elastic modulus (Kasra and Grynpas, 1998).

Porcine cylindrical samples were tested at 2Hz from 10N to a selected normalised compressive stress value: $\sigma_n$ between 0.0113 and 0.0022. Tests were stopped when a prescribed failure strain of $\varepsilon_f$ = 0.4% over the extensometer gauge length was reached or 1.5 million cycles elapsed.

Throughout testing, at approximately 1 second intervals, data was logged from the Dartec. This was the cyclic maximum and minimum values for the force, extensometer displacement and crosshead displacement; as well as the cycle number the measurement was made at.

Four load cycles were recorded in detail at increasing intervals throughout the experiment, starting at every $y^3$ cycle, where $y$ is the capture number. All data capture was performed on the testing machine at a sampling frequency of 500Hz. Once specimen failure was reached the number of cycles to failure ($N_f$) was recorded.

### 2.2.4 Signal Analysis

Using the full test logged data it is possible to estimate the acceleration through equation (2-3).

$$a_{pk} = 2\pi^2 f^2 x \quad \textbf{(2-3)}$$

Where

$a_{pk} =$ the peak acceleration $(\mathrm{m/s^2})$

$f =$ the frequency $(\mathrm{Hz})$

$x =$ peak to peak displacement $(\mathrm{m})$

Idealised sine waves were created from 0 seconds until time to failure with a sampling frequency of 500 Hz. ISO 2631 is used for the human response to vibration over the whole spine; it stands to reason that the accelerations modelled above will be transmitted into the vertebrae and the internal trabecular structure. Therefore when analysing the signals, acceleration was weighted as per ISO 2631-1. Figure 2-3 and Figure 2-4 shows a recorded sine wave and a detailed view of the same sine wave respectively.

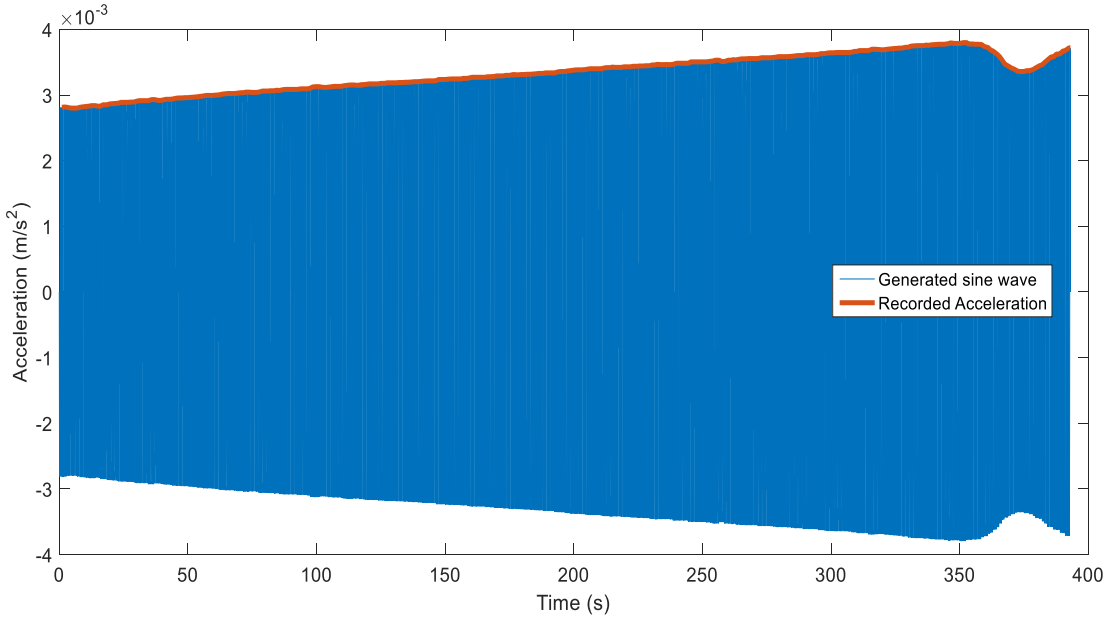


**Figure 2-3: Example sine wave generation based on data logged at 1 second intervals (f = 2Hz)**

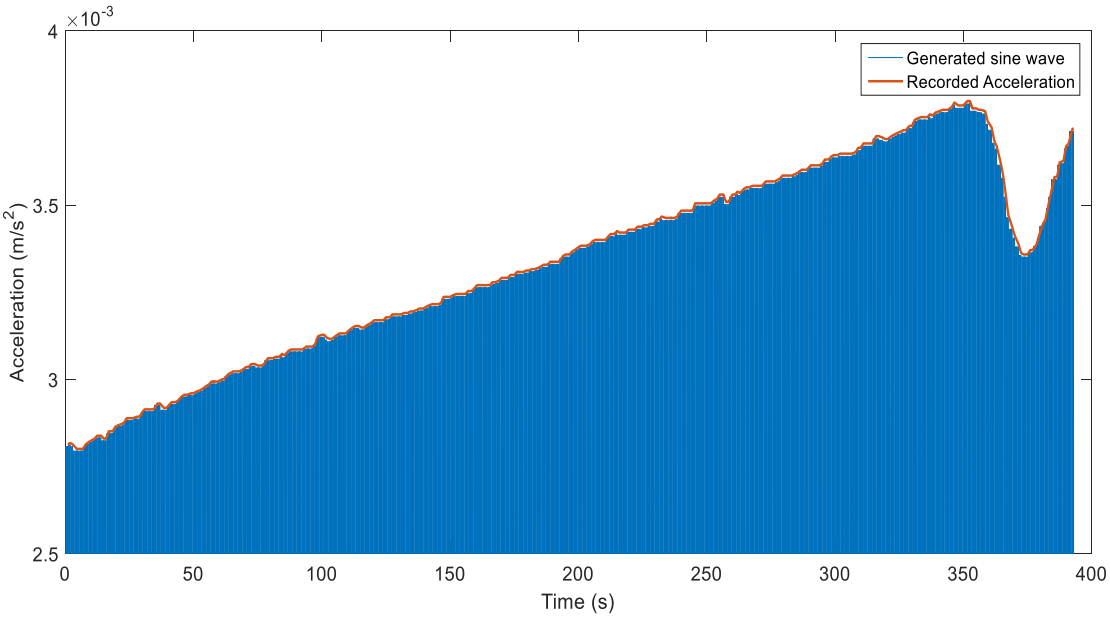


**Figure 2-4: Detailed view of generated sine wave shown in Figure 2-1**

From this sine wave RMS, VDV and $VDV_{exp}$ were calculated (section 1.3.2). For the analysis T was set to the duration of test and $T_{exp}$ was set to a 10 minute reference period (600 seconds). From this time to the exposure limit was calculated from equation (2-4)

$$T_{VDV} = \left(\frac{21}{VDV_{exp}}\right)^4 T_{exp} \quad \textbf{(2-4)}$$

Where

$T_{VDV}$ = Time to VDV exposure limit of 21 $m/s^{1.75}$ (s) (Regulations, 2005)

$T_{exp}$ = 600 (s)

All sine wave generation and analysis was performed using a commercial software package (MATLAB R2017, The MathWorks Inc., Natick, MA, 2017).

The cyclic data recorded at $y^3$ cycles (where y is the current record number) was used to determine the initial Young's modulus of the samples, $E_{0,}$ and the change of plastic strain per cycle, $\Delta\varepsilon_{pl}$. For the high-cycle tests, where the number of cycles to failure is over 10,000 cycles, the data was taken as an average over the first three sets of recorded cycles, while for the low-cycle tests

it was taken over the first recorded set of cycles. An example of this is shown in Figure 2-5.

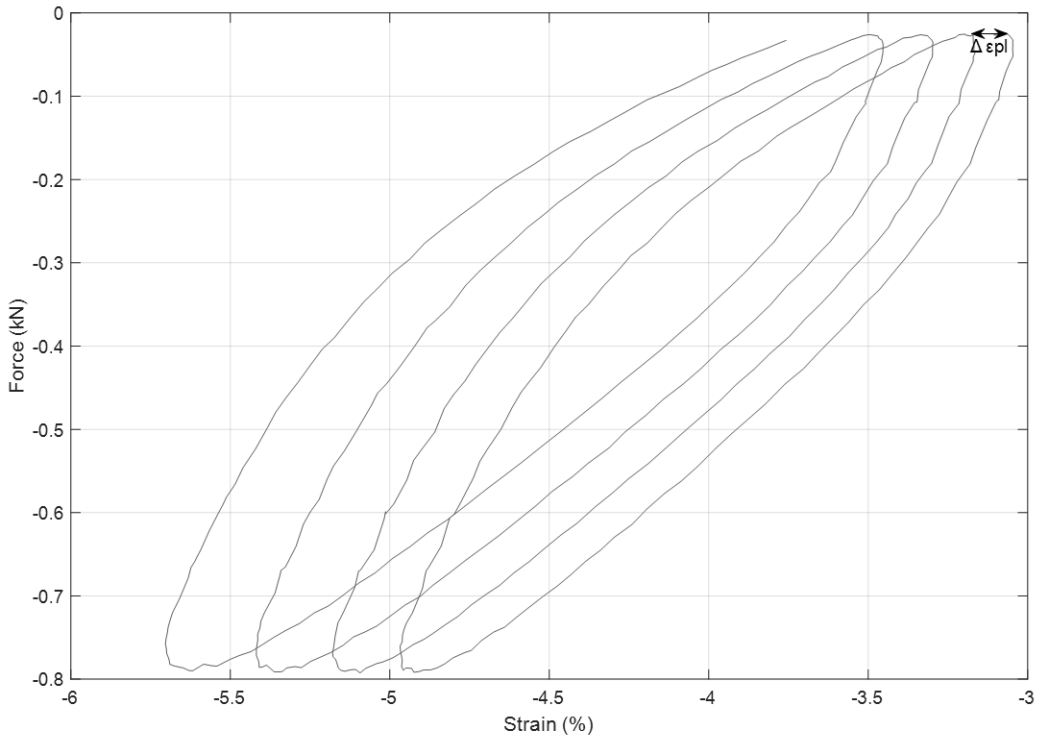


**Figure 2-5: Example Cyclic loading data for four cycles recorded at high resolution (section 2.2.3) with plastic strain for one cycle shown.**

Trabecular bone can be characterised as behaving under the Coffin-Manson law under low-cycle fatigue (Murakami, 1988) as shown in equation (2-5):

$$\Delta\varepsilon_{pl} = X{N_f}^{Y} \quad \textbf{(2-5)}$$

Where X and Y = experimentally derived constants and $N_f$ = Number of cycles to failure

Under high-cycle fatigue the Basquin law can be applied (Basquin, 1910) as shown in Equation (2-6):

$$\Delta\sigma = I{N_f}^{J} \quad \textbf{(2-6)}$$

Where I and J = experimentally derived constants

For calculating the combined Coffin-Manson-Basquin Law, the number of cycles to a specified strain ($N_{\varepsilon\ max}$ = -1.3%) was used instead of number of cycles to failure as in a previous study (Moore and Gibson, 2003b) as it: “represented a strain level where failure was imminent, and where data for a large number of samples were available”.

## 2.3 Apparent modulus of human trabecular cubes

### 2.3.1 Ethical Approval

All tests conducted on porcine tissue for this thesis have been ethically cleared for experimentation through the Cranfield University Research Ethics System with reference number: CURES/2493/2017. Further approval for the human vertebral specimens was obtained from the NHS with REC number: 10/H0107/14 and IRAS Number: 42670

### 2.3.2 Sample Preparation

This study utilised a selection of human vertebral cancellous cubes from existing listings, obtained from a previous study conducted by Pisula (Pisula, 2002). The sample preparation is available in more detail in the written thesis, but will be briefly discussed here. The samples were originally sectioned but had remained untested.

The samples were excised from 10 vertebral bodies from levels T10 to L5 of a 65 year old Caucasian female with no recorded history of pathological bone conditions obtained from the National Disease Research Interchange (NDRI, PA). Vertebrae were first aligned in the inferior-superior orientation and then rotated clockwise around the mediolateral (ML) axis to a specified angle (shown in Table 2-1). They were then sectioned into cubes approximately 10x10x10mm.

Although cubic sections do not conform to known testing standards they were used to investigate the influence of loading axis on the mechanical properties. The primary orientation as cut was used to define the orientations: Inferior-Superior, Mediolateral, Anterior-Posterior (AP). This is illustrated in Figure 2-6.

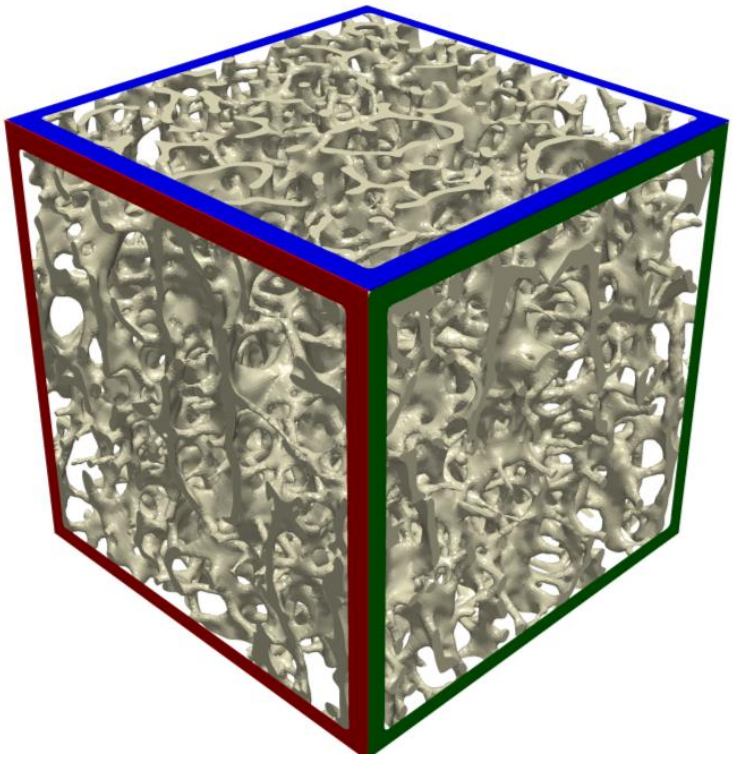

**Figure 2-6: Example orientation loading (Blue = IS, Red = ML, Green = AP)**

The lower lumbar vertebrae (L4 and L5) were large enough to allow for two samples to be taken from the left and right. Table 2-1 shows the sample location and respective orientation. After sectioning the samples were then kept frozen at -20°C until Micro-CT scanning, measurement of density using the Archimedes principal and subsequent mechanical testing. Micro-CT scanning was conducted in the same machine and under the same settings as the porcine tissue (section 2.2.2). Due to the human vertebral cubes being of different dimensions to the porcine cores, the resulting voxel size for the cubes was 16µm. Two sets of samples were produced: one at the original 32-bit greyscale depth ($2^{32}$ intensity units, also known as “floating point precision”) and one resampled to 8-bit ($2^{8}$ intensity units). This resampling was done using CT Pro 3D during the export process following Micro-CT scanning.

| Sample Location | Primary orientation relative to ML-axis |
|---|---|
| **T10** | 0° |
| **T11** | 90° |
| **T12** | 90° |
| **L1** | 20° |
| **L2** | 20° |
| **L3** | 70° |
| **L4 (Left)** | 45° |
| **L4 (Right)** | 45° |
| **L5 (Left)** | 70° |
| **L5 (Right)** | 70° |

**Table 2-1: Cube sample location and orientation**

Morphometric analysis was performed using ImageJ (Schneider, Rasband and Eliceiri, 2012) with the BoneJ plugin (Doube et al., 2010) on the full range 32-bit images. A 7x7x7mm region of interest was selected from the middle of the cube to measure: Degree of Anisotropy (DA), Connectivity, Connectivity Density (Conn. D), Mean Trabecular thickness (TbTh), Material Volume (BV), Total Volume (TV). Volume fraction was determined by dividing the BV by the TV (BV/TV). The samples were aligned in the main trabecular direction during determination of DA. The resulting angle of this transformation in the ML-axis to the neutral axis was measured.

### 2.3.3 Mechanical Testing

Mechanical testing was conducted using the same equipment as in section 2.2.3. The only difference being the production of rectangular endcaps instead of cylindrical endcaps, due to the differences in sample geometry.

The testing procedure was also similar, except the samples were only subjected to the 3 cyclic preconditioning measurements; the stiffness and Young's modulus was calculated from this data.

### 2.3.4 Finite Element Methods

The two sets of micro-CT images obtained prior to mechanical testing were segmented using Simpleware ScanIP (M-2017.06-SP2, Synopsys Inc., Mountain View, CA, USA). Samples were resized to 32μm, which was a quarter of the mean trabecular thickness and needed to reduce numerical errors (Guldberg, Hollister and Charras, 1998).

The trabecular region was identified using standard upper-lower peak thresholding techniques (Adams, 2017), where the peaks relating to air and bone are quantified, the average peak value found and everything above this level is classified as bone. Voxel with a greyscale lower than this level was designated as air to generate a continuum to aid convergence on FE on low bone volume fraction human specimens. The images were cropped to 6mm in their direction of loading in order to model the area over which the extensometer was placed.

The meshes were created using quadratic 8-node hexahedral elements using the voxel based FE-grid routine of Simpleware Scan-IP. All elements were of equal size using a 1:1 mapping with the scanned voxel size (32 μm). Quadratic nodes were used as the greater number of integration points allows for more complex element behaviour and thus more accurate results.

Adams (2017) described a method for generating a material model obtained from matched nanoindentation and micro-CT from a large data set from many species. In brief:

1. A linear relationship between GS and ρ is made through the scanning of the bone density phantom with known densities
2. These densities are mapped to the corresponding GS values within the mesh

3. Using the density/Young`s modulus relationship defined by Adams (2017)' the elements are assigned a Young's modulus

The linear relationship between GS and density is sample specific due to differences in scanning settings and conditions. This relationship of assigning Young's modulus as defined by Adams is not GS dependant and therefore remains the same. There were two sets of DICOM images reconstructed: one was the original 32-bit while one was compressed to 8-bit. The materials were assigned to 256 GS levels corresponding to the upper and lower thresholding limits. The material models used are detailed in Table 2-2.

| Material | GS-Density relationship (g/cm^3) | Young's modulus (GPa) | Poisson's Ratio |
|---|---|---|---|
| Bone (8-bit) | 4.286E-03(*GS*) + 0.970 | $1.027e^{1.481\rho}$ | 0.3 |
| Bone (32-bit) | 2.671E-03 (*GS*) + 1.011 | $1.027e^{1.481\rho}$ | 0.3 |
| Air | N/A | 0.001 | 0.3 |

**Table 2-2: Human Finite Element Material Properties for 32 and 8-bit image stacks**

The top face of each specimen was coupled, meaning that the displacements of the top face were linked, to replicate the testing conditions of a fixed platen and a compressive load of 1kN was applied. The bottom face was fixed in all directions. The boundary conditions are shown Figure 2-7.

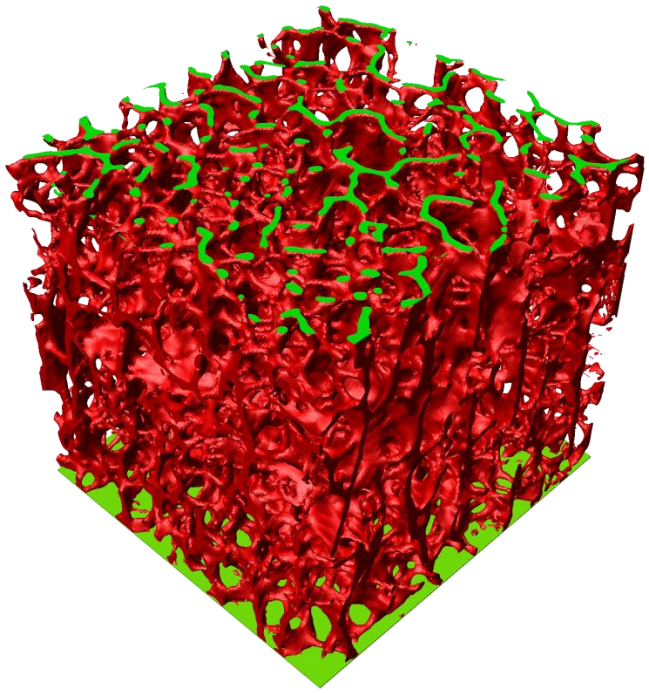

**Figure 2-7: Finite-Element boundary conditions**

The displacement of the coupled face was obtained after loading; this was divided by the applied force to obtain stiffness and which was used to calculate Apparent Young's modulus for comparison against the mechanical testing.

Analysis was conducted using ANSYS APDL (v15.0, ANSYS Inc., Canonsburg, PA, USA) using the Preconditioned Conjugate Gradient (PCG) Solver with a convergence tolerance of $1x10^{-6}$. No convergence study was undertaken, although this is a weakness of the study, the convergence tolerance was set to be very restrictive limiting FEA inaccuracy at the expense of computational time.

## 2.4 Finite Element Fatigue Life Estimation of a Porcine Core

Although previously noted in section 2.2.2, 10 samples were collected for fatigue testing. Due to a cascading hardware failure of the reconstruction machine, only one scan for the porcine cores was available for the finite element analysis (FEA). This sample was sample 8.

### 2.4.1 Finite Element Methods of Fatigue

A 32-bit image stack of a porcine trabecular core was prepared for FEA using the same methods and material mapping techniques as in section 2.3.4. Due to variation in scan settings, the phantom was rescanned and a different GS-Density measurement calculated, the material assignment is show in Table 2-3.

| Material | GS-Density relationship (g/cm^3) | Young's modulus (GPa) | Poisson's Ratio |
|---|---|---|---|
| Bone | 2.671E-03 (*GS*) + 1.011 | $1.027e^{1.481\rho}$ | 0.3 |
| Air | N/A | 0.001 | 0.3 |

**Table 2-3: Porcine Finite Element Material Properties**

Element failure was assessed using three methods:

1. Stress based trabecular failure model derived from experimental testing on human trabecular bone beams (Choi and Goldstein, 1992)

$$\sigma_{Yield}{}^{VM} = 168 - 12.5(\log N_c) \quad \textbf{(2-7)}$$

Where,

$\sigma_{Yield}{}^{VM} = \text{Von-Mises Stress Failure (MPa)}$

$N_C = \text{Current FE cycle number}$

2. Tissue modulus related strain function as described by Chevalier et al. (Chevalier et al., 2007)

$$\sigma_{Yield}{}^{VM} = \sqrt{\frac{3}{2}(E_{mat} \times \varepsilon^T)} \quad \textbf{(2-8)}$$

Where

$E_{mat} = \text{Material Young's modulus (MPa)}$

$\varepsilon^T = \text{Tissue yield strain } (0.41\% \text{ as in Chevalier et al. 2007})$

3. Tissue yield strain criterion (Morgan and Keaveny, 2001)

$$\varepsilon^T = 0.77\% \quad \textbf{(2-9)}$$

The boundary condition on the bottom face was as previous; the force applied to the top face was varied to determine how the applied stress affects the fatigue life of the cylindrical samples.

Three fatigue simulations for each method were conducted at 600, 800 and 1000N. Fatigue was simulated iteratively, assuming linear elastic behaviour, with element failure checking occurring at every load step (Kosmopoulos and Keller, 2003).

The failure was calculated considering the average stress/strain of the element. Failed elements had their modulus reduced by 95% (Reilly and Burstein, 1975) but were kept in place to avoid re-meshing while still simulating failure. This reduced the computational cost of direct fatigue FE simulation. This simulation loop continued until the total strain of the 6mm mesh was 4%, the same as the experimental testing.

Displacement, Cycles to failure, number of failed elements, total failed element percentage as well as the location of failed elements were all recorded at each load step. As the sample tested was cylindrical these locations were translated onto a cylindrical polar coordinate system and the distance from the central point for each element was calculated.

The normalised stress was calculated from the finite element analysis to account for variation in Young's modulus in comparison to the values obtained via experimentation. All the elements were meshed as voxels using a 1x1x1 grid at scanning resolution (32µm) therefore all the elements are of equal

volume. This allows for the calculation of total damage fraction of the sample as shown in Equation (2-10)

$$\frac{DV}{BV} = \frac{N_{EF}}{N_E} \times 100 \quad \textbf{(2-10)}$$

Where,

$DV/BV = \text{Damage fraction } (\%),$

$N_{EF} = \text{Number of Failed elements},$

$N_E = \text{Total number of elements}$

Modulus degradation was also calculated for each load step by calculating the load step Apparent Young`s Modulus. This allowed examination of the development and effects of damage accumulation within the sample.

## 2.5 Finite Element Fatigue Life Estimation on Human Vertebral Samples

The samples obtained from section 2.3 were evaluated using the fatigue method shown in Equation (2-7) (section 2.4) in the IS direction as it was the best predictor of fatigue failure of bone.

Force was applied as normalised stress over the range of $\sigma/E_0 = 0.011$ to $\sigma/E_0 = 0.005$ with 0.001 intervals. The initial modulus was obtained from earlier finite element calculations (section 2.3.4 for method and section 3.2 for results) and then the applied force was back calculated from this. The change of the boundary condition is due to much lower Young's moduli of the human samples in comparison to the porcine cylinders; testing under the same forces would yield much larger normalised stress values for the simulations.

In order to set reasonable failure limits for human trabecular bone a modulus degradation of 10% was chosen (Bowman et al., 1998; Haddock et al., 2004).

Fatigue analysis was run until the fatigue modulus was reached or for 150 cycles, whichever came first.

# 3 RESULTS

## 3.1 Porcine Fatigue Testing

As previously mentioned in the introduction to section 2.4, due to a cascading data failure CT data for all but one sample was unavailable. This meant that the only morphometric data available to characterise all the samples were those obtained from physical measurement (Apparent Density, Material density, BV/TV). This data is collated in Table 3-1 along with Initial Young's modulus and their means and standard deviations (SD).

| # | $Diameter$ $(mm)$ | $Length$ $(mm)$ | $\rho_{app}$ $(g/cm^3)$ | $\rho_{mat}$ $(g/cm^3)$ | $BV/TV$ | $E_0$ $(MPa)$ |
|---|---|---|---|---|---|---|
| *1* | 8.96 | 24.82 | 0.887 | 2.166 | 0.4094 | 1111 |
| *2* | 8.96 | 24.39 | 0.890 | 2.176 | 0.4090 | 1175 |
| *3* | 8.99 | 24.80 | 0.901 | 2.217 | 0.4062 | 1025 |
| *4* | 8.99 | 24.61 | 0.883 | 2.157 | 0.4094 | 928 |
| *5* | 9.01 | 24.67 | 0.929 | 2.258 | 0.4115 | 1064 |
| *6* | 8.96 | 24.69 | 0.867 | 2.156 | 0.4022 | 1108 |
| *7* | 9.01 | 24.46 | 0.890 | 2.152 | 0.4134 | 1187 |
| *8* | 9.04 | 24.94 | 0.932 | 2.254 | 0.4137 | 1694 |
| *9* | 9.03 | 24.89 | 0.898 | 2.157 | 0.4162 | 1747 |
| *10* | 9.05 | 24.86 | 0.931 | 2.292 | 0.4061 | 953 |
| *Mean (SD)* | 9.02 (0.031) | 24.71 (0.174) | 0.901 (0.0214) | 2.200 (0.0497) | 0.4097 (0.0040) | 1199 (273) |

**Table 3-1: Morphometric data for porcine samples**

Table 3-1 shows that the samples created were of almost uniform diameter and length with little deviation from the mean. There is a large variation in the volume fraction in comparison to slight variation for apparent density. This is reflected in the variation between volume fraction and initial Young's modulus of the specimens shown in Figure 3-1.

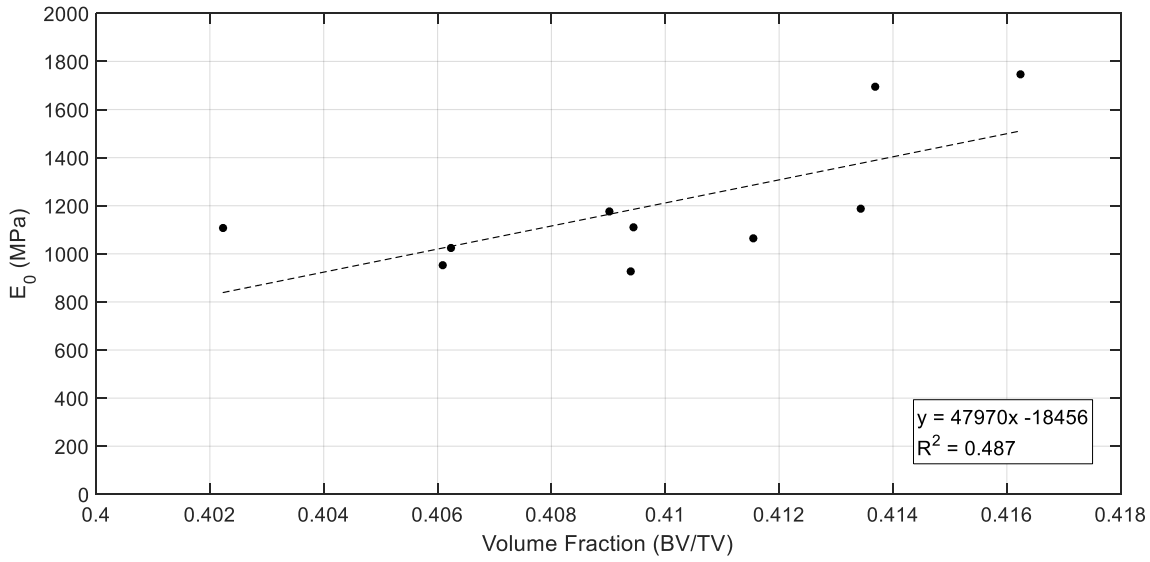


**Figure 3-1: Volume Fraction against Initial Young's modulus (for 10 porcine trabecular cores). There is an upward trend with a weak correlation between volume fraction and initial Young's modulus**

Two samples had a much higher initial Young's modulus, #8-9, this is expected as they also had the highest volume fractions. The rest of the samples have very similar initial Young's modulus with a mean and SD of 1069 ± 89 MPa.

Table 3-2 below shows the normalised stresses, cycles and time to failure and the associated vibration statistics of all tested samples. Sample #5 was the only sample not to fail within the allotted number of cycles. This sample was therefore excluded from subsequent analysis.

| # | $\sigma/E_0$ | $N_f$ | $T_f$ (s) | RMS ($mm/s^2$) | VDV ($mm/s^{1.75}$) | $VDV_{exp}$ ($mm/s^{1.75}$) | $T_{exp}$ (s) |
|---|---|---|---|---|---|---|---|
| 1 | 0.0113 | 30 | 15 | 4.155 | 6.535 | 16.434 | 1600 |
| 2 | 0.0054 | 3,456 | 1728 | 1.845 | 13.788 | 10.584 | 9299 |
| 3 | 0.0054 | 7,800 | 3900 | 1.060 | 9.629 | 6.030 | 88240 |
| 4 | 0.0068 | 786 | 393 | 2.368 | 11.751 | 13.062 | 4008 |
| 5 | 0.0022 | 1,500,000* | * | * | * | * | * |
| 6 | 0.0106 | 49 | 24.5 | 4.528 | 7.175 | 15.961 | 1798 |
| 7 | 0.0060 | 23,760 | 11880 | 0.838 | 11.756 | 5.573 | 120946 |
| 8 | 0.0056 | 192 | 96 | 1.078 | 5.443 | 8.606 | 21269 |
| 9 | 0.0038 | 43,577 | 21788.5 | 0.835 | 12.915 | 5.261 | 152311 |
| 10 | 0.0051 | 386,705 | 193352.5 | 1.050 | 27.836 | 6.570 | 62634 |

**Table 3-2: Testing and Vibration Statistics for Porcine Trabecular Cores (* indicates test run-out)**

The data in this table is examined in more detail in Figure 3-2 to Figure 3-5.

$T_f$ is directly linked to $N_f$ as testing was conducted using a stable frequency of 2 Hz therefore all the $T_f$ values are half that of the number of cycles to failure.

All of the samples tested failed before reaching the time to exposure limit ($T_{exp}$) with the exception of sample #10, which failed ~36 hours after $T_{exp}$ was reached.

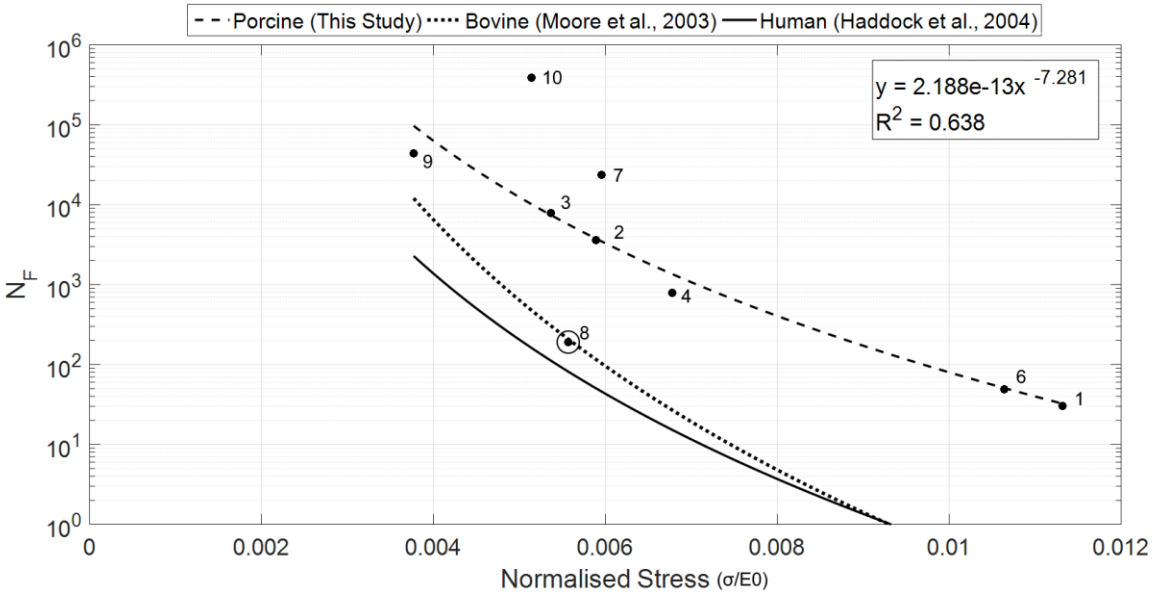


**Figure 3-2: Number of cycles to failure vs Normalised Stress. Stress is normalised by initial Young's modulus to remove scatter due to sample variation. Grouping is apparent at $\sigma/E_0$ = ~0.55. Bovine and Human data fits are also shown. Outlier sample #8 is highlighted with a circle**

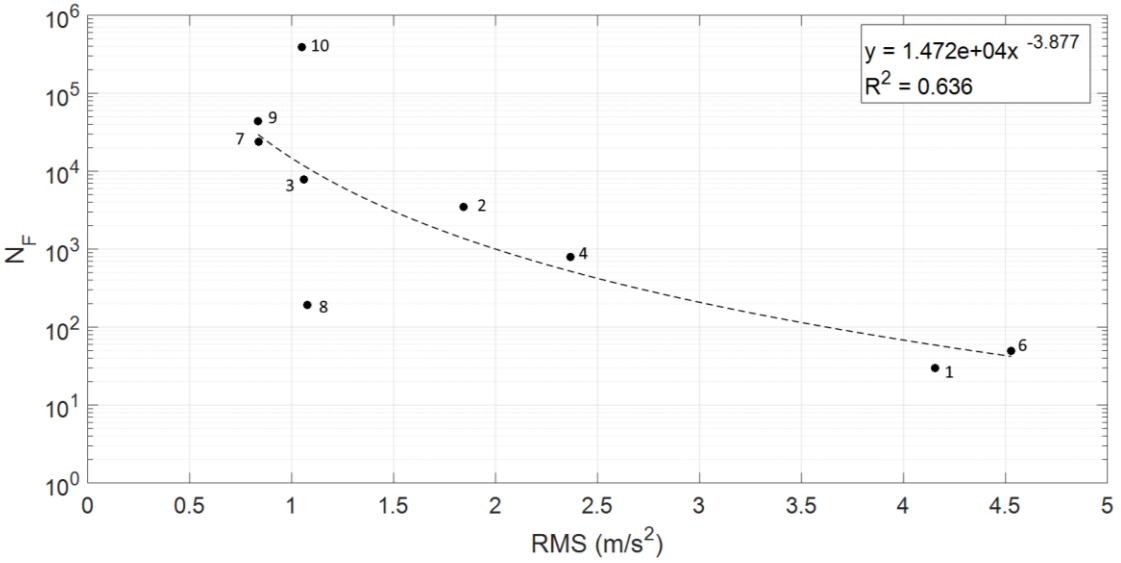


**Figure 3-3: Number of cycles vs RMS to failure for 10 porcine cores. RMS is a rudimentary normalised measure of vibration. There is grouping at RMS = ~1.1 $m/s^2$**

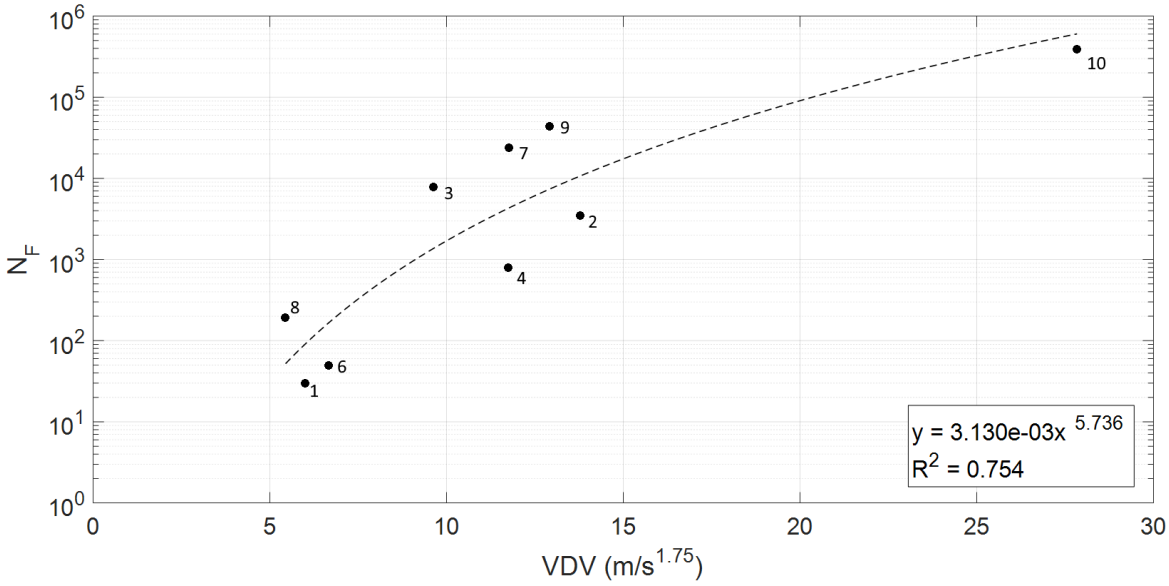


**Figure 3-4: Number of cycles to failure vs VDV for 10 porcine cores. VDV is 4$^{th}$ order acceleration averaging. In this context it is the cumulative acceleration over the entire test period; samples that lasted longer experienced an overall higher VDV**

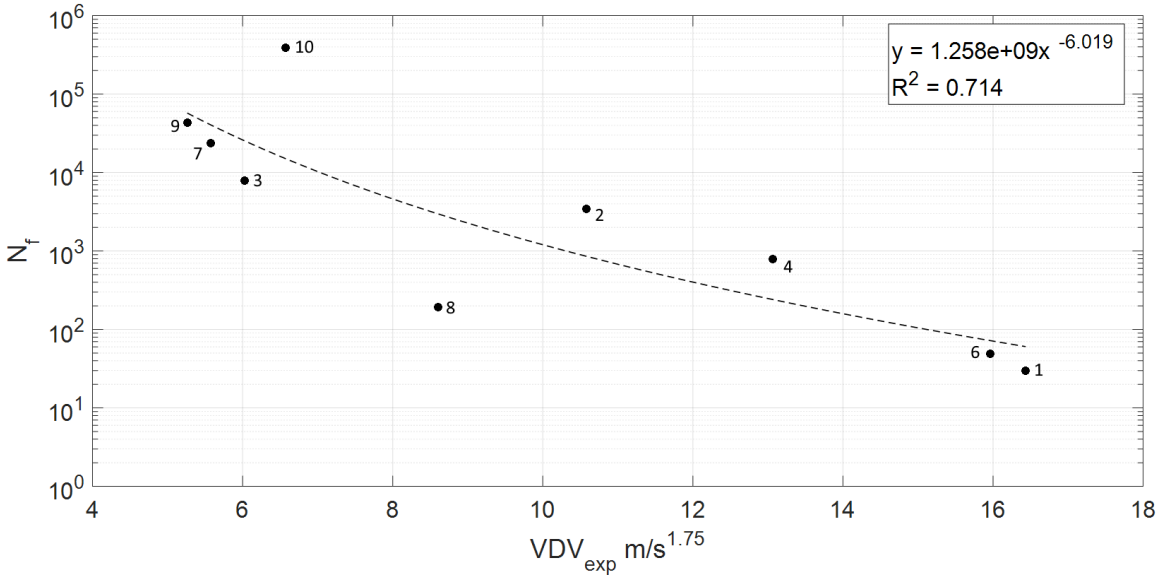


**Figure 3-5: Number of cycles to failure vs VDV$_{exp}$ for 10 porcine cores. VDV$_{exp}$ is a predictive measure of vibration exposure normalising the VDV with respect to a chosen time period (10 minutes in this case)**

Figure 3-2 shows that the relationship between normalised stress and number of cycles to failure follows a power law with an exponent of -7.281 ($R^2$ = 0.638). There is considerable scatter within the samples even though most were tested at similar normalised stress values. For comparison, regressions obtained from fatigue testing of human and bovine trabecular bone are included.

When the RMS is plotted against number of cycles to failure (Figure 3-3) the same downward trend is visible, with a power law relationship with a lower exponent (-3.877, $R^2$ = 0.636)

In general; as the vibration statistic increases the number of cycles to failure decreases. The only statistic which does not follow this convention is VDV, which shows an upward trend with the highest coefficient of determination of all measured vibration statistics ($R^2$=0.754).

When VDV is normalised against 10 minutes (Figure 3-5) the upward trend is replaced by a descending one following a power law relation with an exponent of -6.019 ($R^2$=0.714)

Although sample #5 did not reach total failure (ε = 4%) within the 1.5 million cycles, it did go beyond ε = 1.3% thus allowing for its inclusion in calculating the combined Coffin-Manson-Basquin Law (Figure 3-6). A combined Basquin-Coffin-Mason plot shows the relationship between the strain based deformation at low cycle fatigue with the stress based deformation of high cycle fatigue.

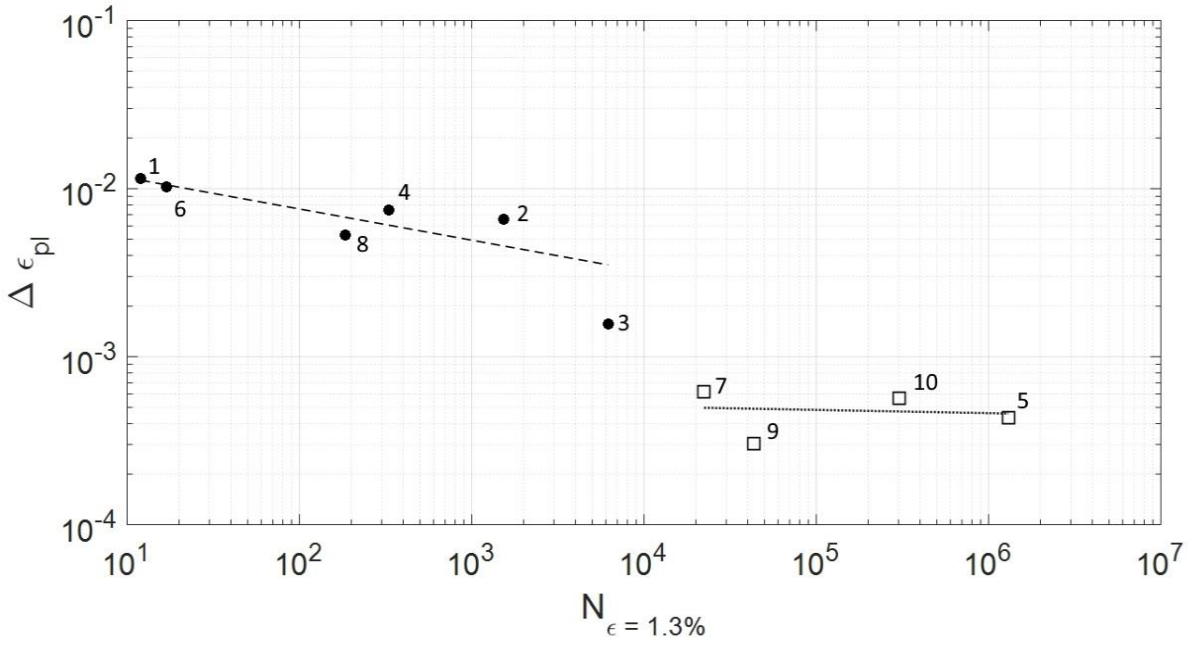


**Figure 3-6: Combined Basquin-Coffin-Mason Plot (Filled square = Low cycle, Open square = High cycle).**

In Figure 3-6 there is an uncharacteristic overlap with high cycle fatigue if the power law regression of low cycle fatigue is extended, possibly due to a lack of data points. Due to this overlap there is no clear transition point from low to high cycle fatigue, however there is a sharp drop off around 6171 cycles to ε = 1.3% which could be a possible transition point.

## 3.2 Apparent Modulus of Human Trabecular Cubes

Ten human vertebral cubes were scanned as described in section 2.2.2 and subsequently tested to obtain Young's modulus for the validation of material model. Table 3-3 below shows the material density and morphological properties of these samples taken from the full 32-bit image depth, with the overall means and standard deviations where appropriate.

| *Location* | *Angle (°)* | *Density ($g/cm^3$)* | *DA* | *Conn.* | *Conn.D ($mm^{-3}$)* | *BV/TV* | *TbTh mean (mm)* | *TbTh (SD) (mm)* |
|---|---|---|---|---|---|---|---|---|
| T10 | 0 | 1.764 | 2.584 | 2096 | 4.184 | 0.0899 | 0.128 | 0.034 |
| T11 | 90 | 1.749 | 3.122 | 2090 | 4.381 | 0.0896 | 0.130 | 0.034 |
| T12 | 90 | 1.787 | 3.502 | 1884 | 3.975 | 0.0876 | 0.132 | 0.033 |
| L1 | 20 | 1.799 | 3.099 | 1637 | 3.699 | 0.0816 | 0.135 | 0.039 |
| L2 | 20 | 1.778 | 2.485 | 1735 | 3.894 | 0.0920 | 0.145 | 0.034 |
| L3 | 70 | 1.854 | 2.080 | 1233 | 3.905 | 0.0905 | 0.143 | 0.042 |
| L4L | 45 | 1.859 | 2.355 | 1084 | 3.503 | 0.0818 | 0.133 | 0.038 |
| L4R | 45 | 1.596 | 2.168 | 1610 | 3.96 | 0.1067 | 0.144 | 0.041 |
| L5L | 70 | 1.819 | 1.735 | 2190 | 4.286 | 0.0902 | 0.131 | 0.033 |
| L5R | 70 | 1.843 | 2.334 | 1937 | 4.249 | 0.0994 | 0.142 | 0.039 |
| Mean (SD) | - | 1.785 (0.072) | 2.546 (0.515) | 1750 (350) | 4.003 (0.261) | 0.0910 (0.007) | 0.136 (0.006) | - |

**Table 3-3: Human vertebral cube morphometric analysis, material density obtained from Archimedes principal, other properties from ImageJ. Degree of Ansiotropy (DA) is a dimensionless variable, where 1 = Isotropic and increases with anisotropy. Connectivity (Conn.) is the approximate number of trabeculae within the section whereas connectivity density (Conn. D) normalises this against the total volume. BV/TV also known as "Volume fraction", is the volume fraction of bone within the sample. TbTh (mean and SD) are the trabecular thickness mean and standard deviations respectively.**

The morphometric analysis of the samples (Table 3-3) shows a low value for connectivity for samples L3 and L4L in comparison to other samples. The mean

trabecular thickness was consistent within the sample set with little intra-sample and inter-sample variability. DA varies considerably with respect to the level the cores are taken at, with the thoracic vertebrae being more anisotropic than the low lumbar vertebrae.

| *Location* | *Reported angle (°)* | *Angular Deviation (°)* |
|---|---|---|
| T10 | 0 | 2 |
| T11 | 90 | 2.1 |
| T12 | 90 | 3.6 |
| L1 | 20 | 2.9 |
| L2 | 20 | 5.1 |
| L3 | 70 | 1.2 |
| L4L | 45 | 4.3 |
| L4R | 45 | 5.3 |
| L5L | 70 | 1.8 |
| L5R | 70 | 1.8 |

**Table 3-4: Angular deviation from ML-Axis between reported values and those measured through MIL registration in ImageJ.**

Table 3-4 shows the absolute angular deviation from the ML-axis line, defining the differences between the physiological and the measured angle. The overall deviation is low with a mean and SD of 2.99 ± 1.42°, showing that the samples were generally cut with good accuracy at the specified angle.

Conversion to 8-bit depth was computed over the entire image greyscale range, an example of this is given in Figure 3-7.

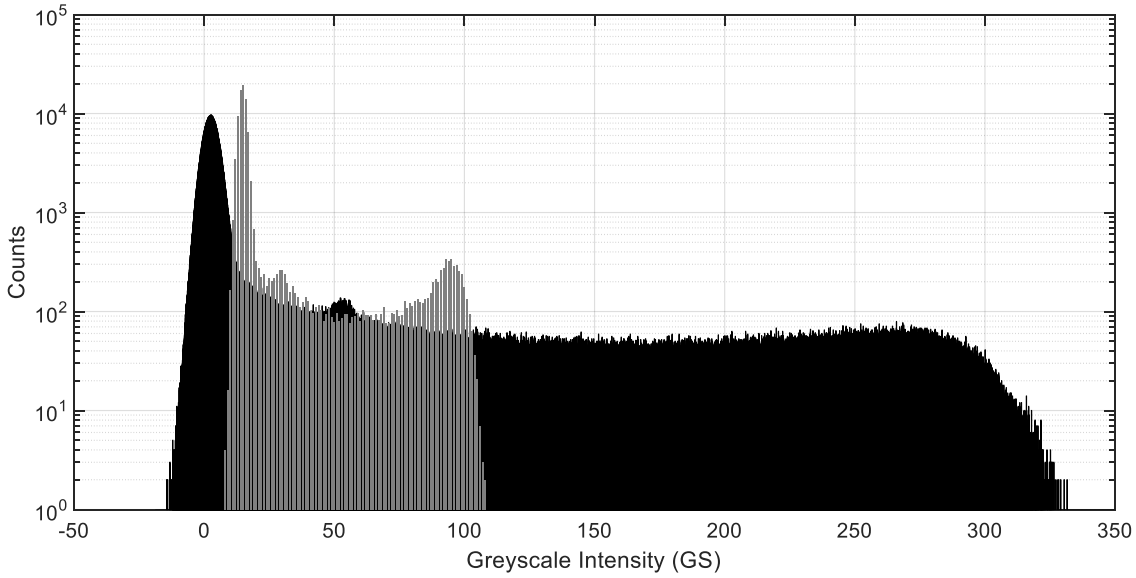


**Figure 3-7: Example greyscale Intensity Histogram for sample L1, 8-bit (grey) and 32-bit (black). X-axis is truncated from 600 to 350, the maximum GS intensity of the 32-bit histogram.**

Figure 3-7 shows the effects of binning from a 32-bit depth image to an 8-bit, there is compression in greyscale intensity and an overall increase at the peaks of air, marrow and bone. The peaks are in order of GS intensity which is related to density, as air has the lowest density, that peak shows first, followed by marrow and bone. At the 8-bit image depth the greyscale resolution is an integer whereas the 32-bit resolution is much finer at 4 decimal places, (as reported by Scan-IP) as presented by the comparative width of the histogram bars. The effect of image depth on sample thresholding is investigated in Table 3-5.

| *Threshold (GS)* | *T10* | *T11* | *T12* | *L1* | *L2* | *L3* | *L4L* | *L4R* | *L5L* | *L5R* |
|---|---|---|---|---|---|---|---|---|---|---|
| 8-bit | 59 | 78 | 74 | 57 | 56 | 97 | 38 | 56 | 42 | 27 |
| 32-bit | 134 | 131 | 137 | 134 | 128 | 135 | 134 | 133 | 131 | 132 |

**Table 3-5: Threshold Greyscale values for vertebral location and image depth**

Table 3-5 shows a strong effect of image depth on the threshold value (calculated as half the difference between the upper and lower peaks), the 32-bit thresholds have a mean and standard deviation of 133 ± 2.4 (GS) in comparison to 58 ± 19.5 (GS) for an image depth of 8-bit. A full table for the apparent moduli obtained from mechanical testing and FEA are shown in Table 3-6.

| | | *Experimental average from 2-3 tests* $E_{app}$ *(MPa)* | | | *8-bit FEA* $E_{app}$ *(MPa)* | | | *32-bit FEA* $E_{app}$ *(MPa)* | | |
|---|---|---|---|---|---|---|---|---|---|---|
| *Location* | *Angle* | IS | AP | ML | IS | AP | ML | IS | AP | ML |
| T10 | 0 | 363 | 67 | 81 | 436 | 112 | 136 | 314 | 49 | 61 |
| T11 | 90 | 86 | 415 | 97 | 78 | 383 | 90 | 88 | 382 | 99 |
| T12 | 90 | 72 | 359 | 60 | 97 | 344 | 54 | 71 | 307 | 36 |
| L1 | 20 | 254 | 177 | 42 | 145 | 64 | 35 | 253 | 118 | 65 |
| L2 | 20 | 158 | 145 | 49 | 192 | 133 | 91 | 146 | 132 | 47 |
| L3 | 70 | 230 | 137 | 35 | 319 | 125 | 93 | 233 | 76 | 57 |
| L4L | 45 | 144 | 106 | 21 | 58 | 54 | 38 | 86 | 83 | 54 |
| L4R | 45 | 74 | 236 | 89 | 126 | 199 | 168 | 94 | 155 | 125 |
| L5L | 70 | 75 | 90 | 152 | 78 | 72 | 162 | 74 | 84 | 186 |
| L5R | 70 | 131 | 281 | 116 | 70 | 173 | 57 | 77 | 217 | 64 |

**Table 3-6: Apparent Modulus for each human trabecular sample for each experimental technique**

The apparent modulus of the finite element models at different bit depths were compared against the experimental results as a validation of the material models (Figure 3-8 and Figure 3-9).

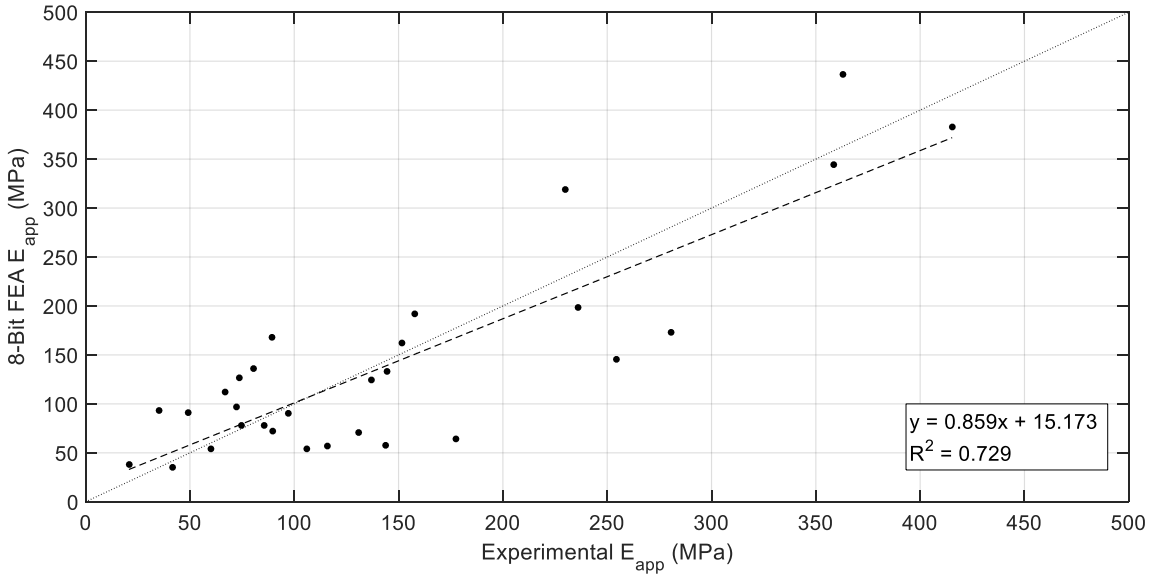


**Figure 3-8: 8-bit Finite Element Analysis Apparent Modulus vs Experimental, shown with an ideal 1:1 ratio (dotted line) and a fitted linear regression (dashed line) comparing the experimental and finite element results**

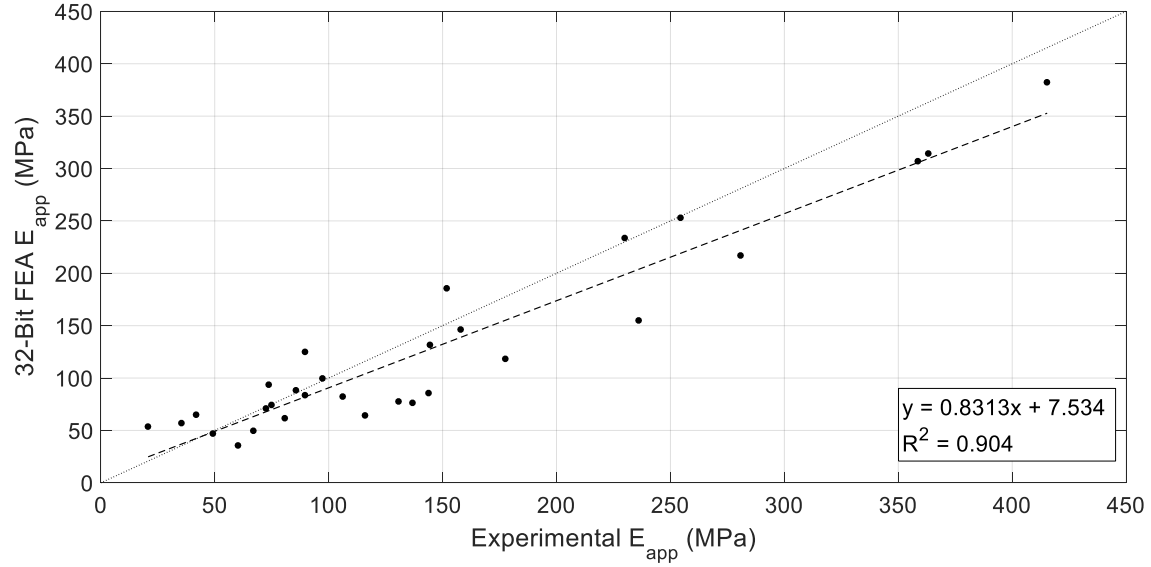


**Figure 3-9: 32-bit Finite Element Analysis Apparent Modulus values vs Experimental, shown with an ideal 1:1 ratio (dotted line) and a fitted linear regression (dashed line) comparing the experimental and finite element results**

Figure 3-8 shows a large amount of scatter which is evident in the coefficient of determination ($R^2$=0.721). There is no clear pattern to the model stability, with a

large amount of models being both over and underestimated between the experimentally derived modulus of 50-150 MPa.

Figure 3-9 shows good agreement ($R^2$=0.901) between the experimental and finite element models for 32-bit segmentation. In general the 32-bit FE models tend to underestimate the apparent young's moduli, this error increases with the experimental apparent modulus.

Although 8-bit model appears to show a slightly better fit than the 32-bit model while comparing the linear fit, there is more scatter in the points. This can be seen in the percentage error between the experimental and the FEA (Figure 3-10).

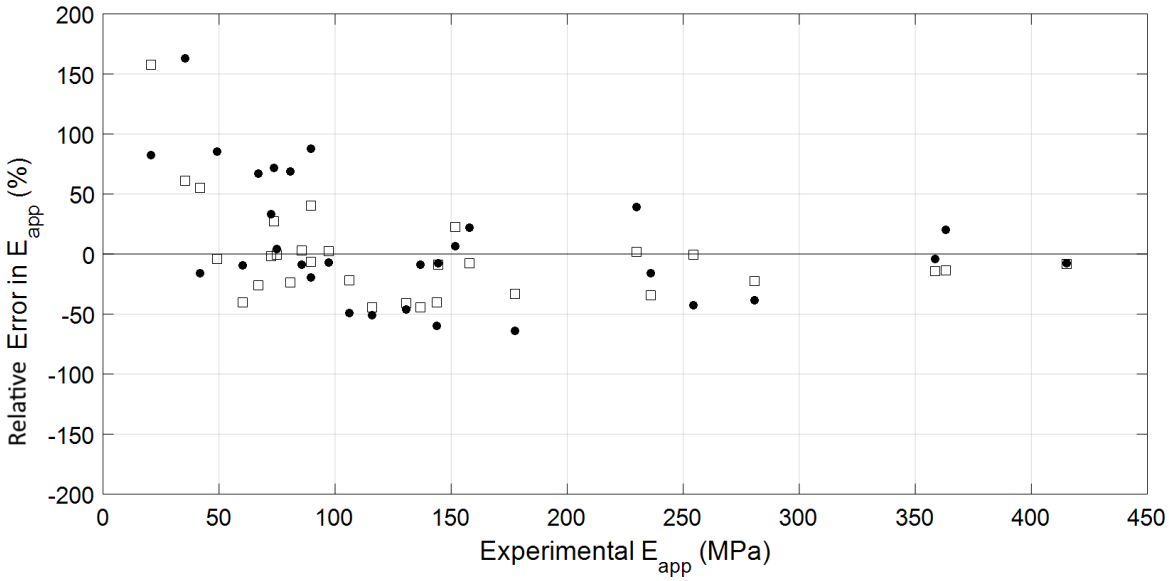


**Figure 3-10: Relative error of FEA $E_{app}$ against experimental $E_{app}$. Solid circles represent the 8-bit models while the open squares represent the 32bit. A solid line at a difference of 0 is shown to clarify the over/underestimation of apparent Young's modulus**

Figure 3-10 shows the percentage error of the two sets of finite element models relative to the experimental Young's modulus. Models generated using an 8-bit image depth exhibit a greater scatter in comparison to the 32-bit with a mean and SD of 9.8 ± 52.5% and -2.3 ± 40.2% respectively. Both sets of models

overestimate the stiffness when the apparent modulus is low, however the 32-bit depth models shows this tendency for fewer samples than the 8-bit.

The samples were obtained with a variation of angle in the medial-lateral axis the relationships between this angle and obtained apparent modulus for each bit depth and loading direction (Inferior-Superior, Medial-Lateral and Anterior-Posterior) is shown in Figure 3-11 to Figure 3-13.

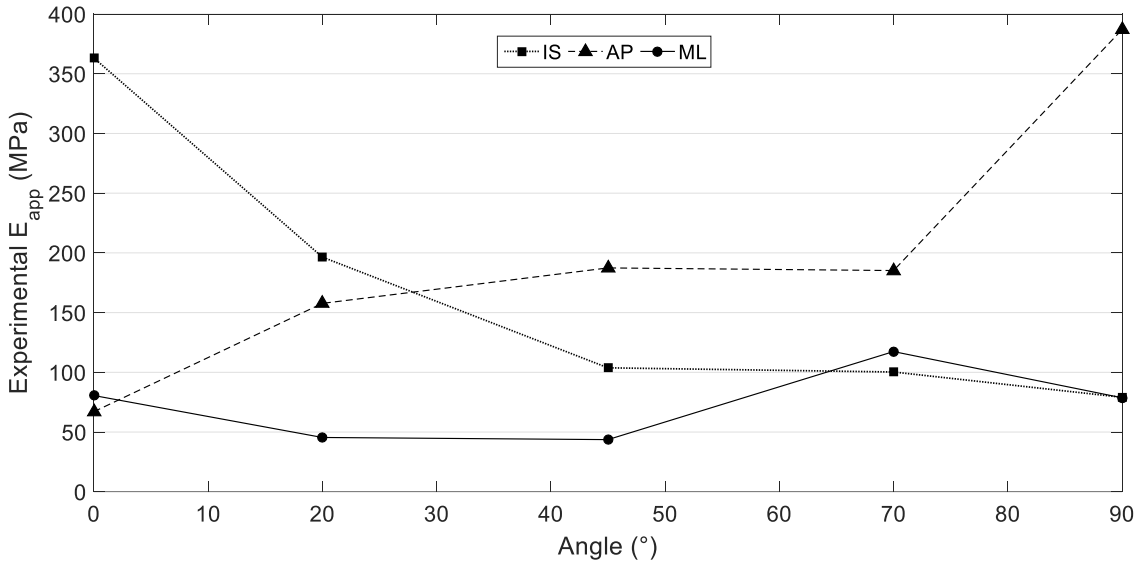


**Figure 3-11: Variation of Experimental $E_{app}$ mean with ML axis angle. Mean results taken from experimental testing were grouped by angle in the ML axis**

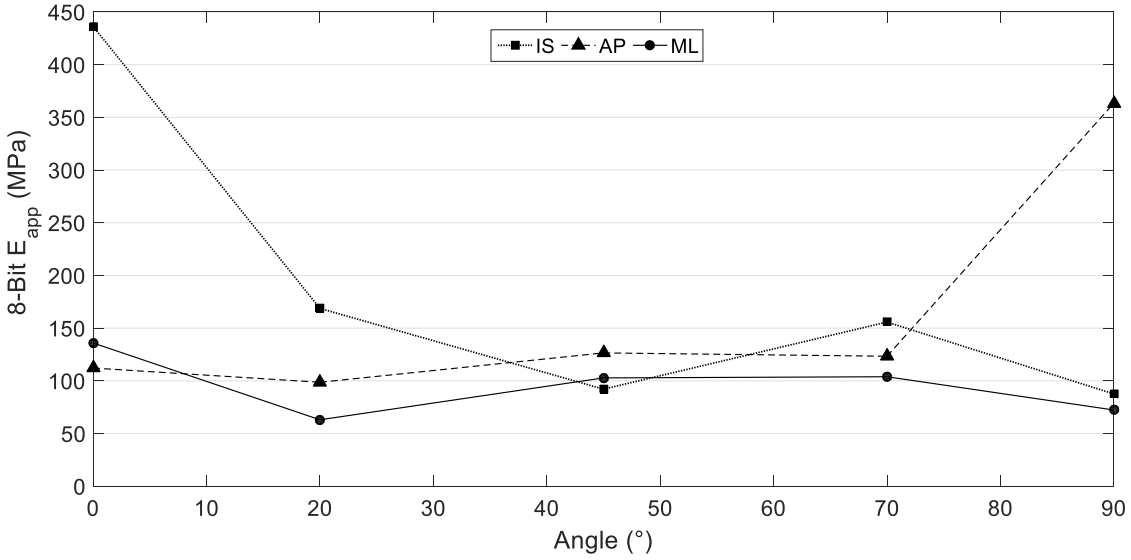


**Figure 3-12: Variation of 8-bit $E_{app}$ mean with ML axis angle. Mean results taken from finite element analysis of 8-bit down sampled images were grouped by angle in the ML axis**

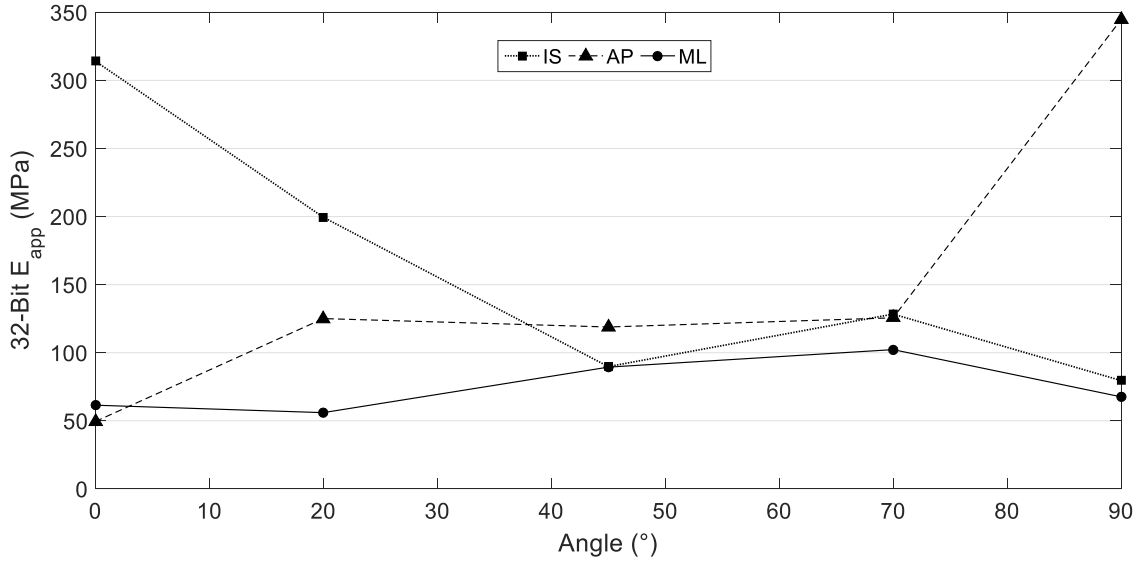


**Figure 3-13: Variation of 32-bit $E_{app}$ mean with ML axis angle. Mean results taken from finite element analysis of 32-bit original images were grouped by angle in the ML axis**

The experimental and finite element methods show similar trends (Figure 3-11 to Figure 3-13) with $E_{app}$ in the IS direction highest at 0° and lowest at 90°. This

is reversed in the AP direction where $E_{app}$ is lowest at 0° and highest at 90°. This corresponds to the main trabecular alignment of the bone, with respect to the ML axis.

There is lower variation in the ML $E_{app}$ for the experimental results which is also seen in the finite element simulations. Both 8-bit and 32-bit simulations overestimate the force in the IS direction at 70°. Figure 3-12 shows a severe underestimation of $E_{app}$ for both IS and AP loading.

Overall, the 32-bit model provides a better representation of the experimental testing. The FE models reduce the clear separation between the loading directions; each loading direction is examined in greater detail using the scatter plots below (Figure 3-14 to Figure 3-16).

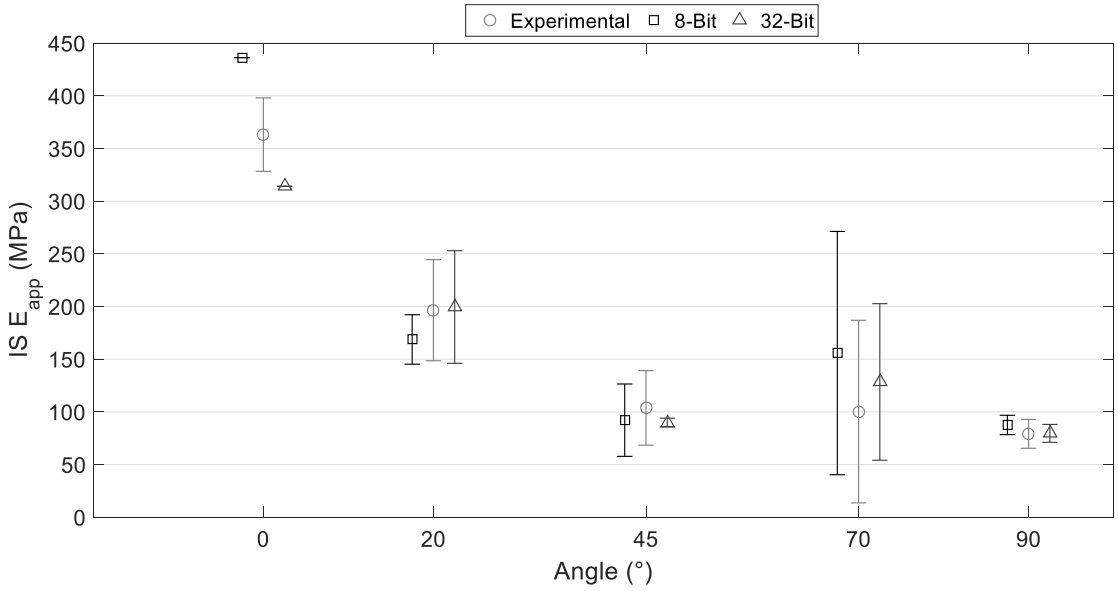


**Figure 3-14: IS $E_{app}$ in relation to ML Angle variation. Loading in the IS direction with means and standard deviations from the experimental results (Circle, central), the 8-bit (Square, left) and 32-bit (Triangle, right) finite element analysis. Samples are offset around the ML angle for clarity.**

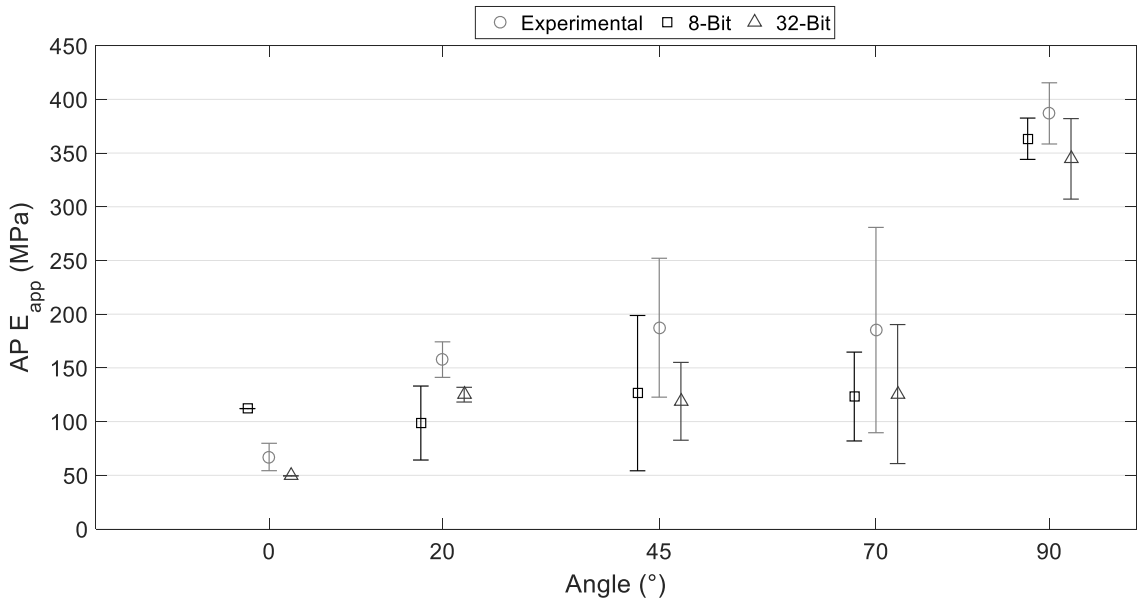


**Figure 3-15: AP $E_{app}$ in relation to ML Angle variation. Loading in the AP direction with means and standard deviations from the experimental results (Circle, central), the 8-bit (Square, left) and 32-bit (Triangle, right) finite element analysis.**

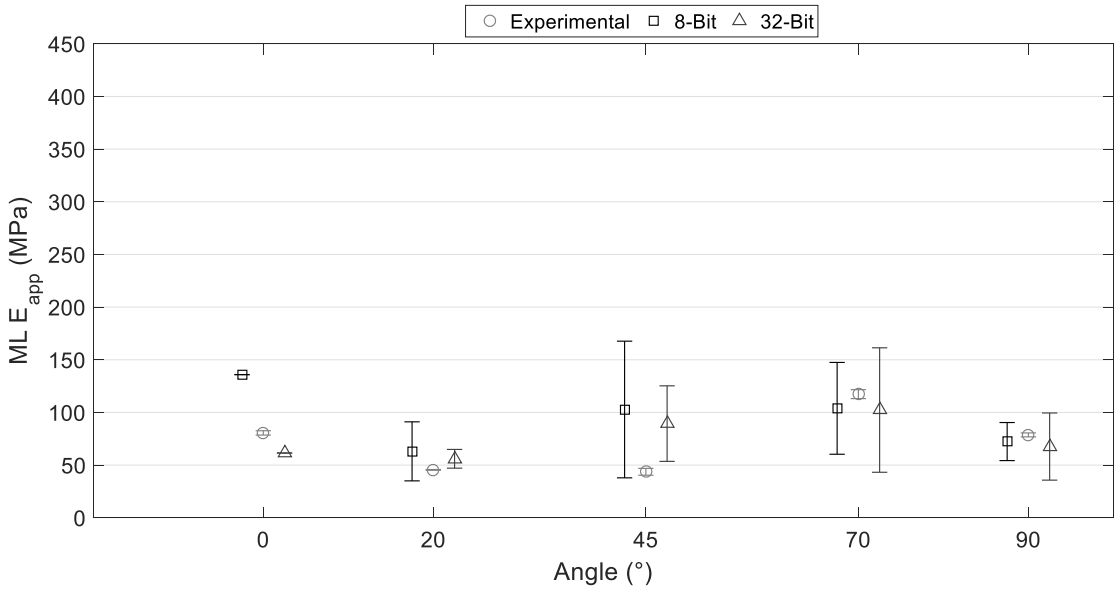


**Figure 3-16: ML $E_{app}$ in relation to ML Angle variation. Loading in the ML direction with means and standard deviations from the experimental results (Circle, central), the 8-bit (Square, left) and 32-bit (Triangle, right) finite element analysis.**

Figure 3-14 to Figure 3-16 shows that both sets of finite element models display good agreement with the experimental in terms of angular orientation. With

similar standard deviations in the IS direction, for the FEA in comparison to the experimental.

As there was only one sample at 0°, Figure 3-14 to Figure 3-16 shows no standard deviation for the FEA, whereas the experimental mean Young's modulus was obtained through multiple cyclic loading tests (detailed in section 2.3.3) leading to the standard deviation seen here. The opposite is seen at 70° where there were three samples: the experimentally obtained results show a high standard deviation in both the IS and AP directions (Figure 3-14 and Figure 3-15) which is also seen in the FEA results.

FEA models show disparity is examining the forces in the ML direction (Figure 3-16) both sets of finite element results show a large amount of deviation, and a tendency to overestimate the apparent modulus in comparison to the experimental results.

## 3.3 Finite Element Fatigue on a Porcine Core

An initial test was used to confirm the accuracy of the initial Young's modulus of the sample. This initial modulus is included with the morphometric data in Table 3-7.

| # | ***Angular Deviation (°)*** | ***DA*** | ***Conn.*** | ***Conn.D ($mm^{-3}$)*** | ***BV/TV*** | ***TbTh mean (mm)*** | ***TbTh (SD) (mm)*** | ***$E_{0\ Exp}$ (MPa)*** |
|---|---|---|---|---|---|---|---|---|
| 8 | 5.4 | 3.117 | 1818 | 2.433 | 0.414 | 0.138 | 0.063 | 1972 |

**Table 3-7: Porcine Core Sample 8 Morphometry**

Angular deviation was calculated for the sample as in section 2.3.2 for the human vertebral cubes, it was found to be reasonable at 5.4°. The FEA produced a value of $E_0$ = 1972 MPa.

With the applied forces of 1kN, 800N and 600N, normalised stresses equated to 0.0079, 0.0063 and 0.0048. Table 3-8 shows the number of cycles to failure ($N_F$) for these normalised stresses for each method tested. The methods are

based on the literature as follows: Method 1 (Choi and Goldstein, 1992), Method 2 (Chevalier et al., 2007) and Method 3 (Morgan and Keaveny, 2001). The methods are detailed in section 2.4.1.

| *Normalised Stress* | *$N_F$ Method 1* | *$N_F$ Method 2* | *$N_F$ Method 3* |
|---|---|---|---|
| 0.0079 | 10 | 3 | 3 |
| 0.0063 | 29 | 4 | 3 |
| 0.0048 | 185 | 11 | 7 |

**Table 3-8: Number of Cycles to failure for Porcine Core Sample 8 from FEA for Methods under a given normalised stress**

This data is shown graphically in Figure 3-17 with the fatigue regressions from section 3.1 and the point for the specific sample modelled (#8).

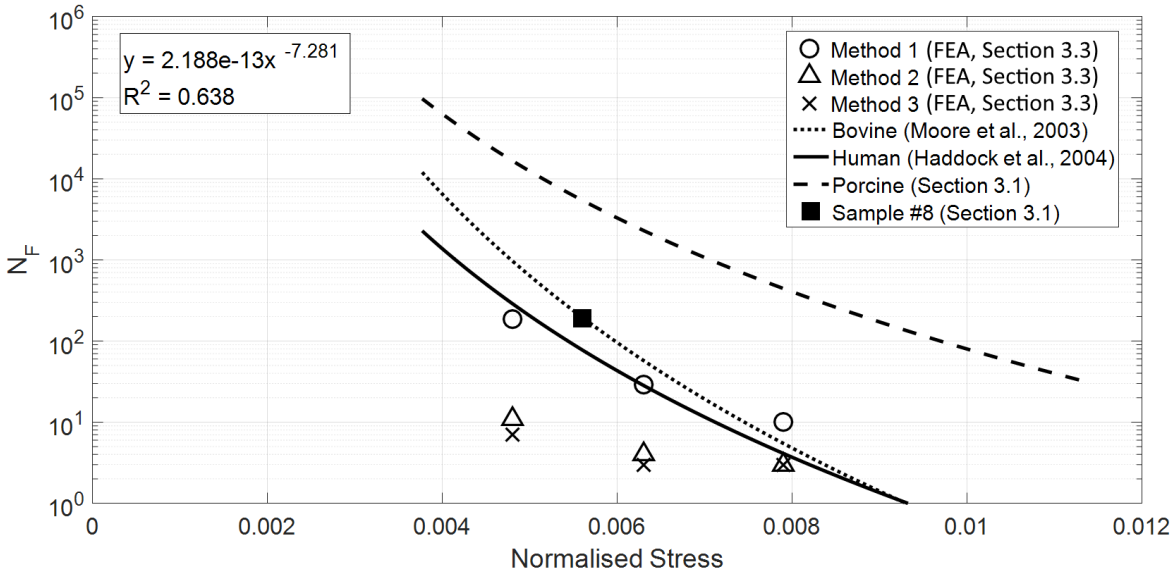


**Figure 3-17: Normalised Stress vs Number of Cycles to 4% Failure strain (FEA and EXP) for Porcine Core Sample 8. The regression equation displayed is for the porcine fatigue study (3.1).**

From this figure, it is clear that all the fatigue methods applied in this study underestimate the fatigue life of porcine trabecular bone in regards to the experimental power law shown in section 3.1. Method 1 shows reasonable

agreement with both the human fatigue life power law (-6) and the number of cycles of the experimental. Example cyclic failure obtained from FEA is shown in Figure 3-18

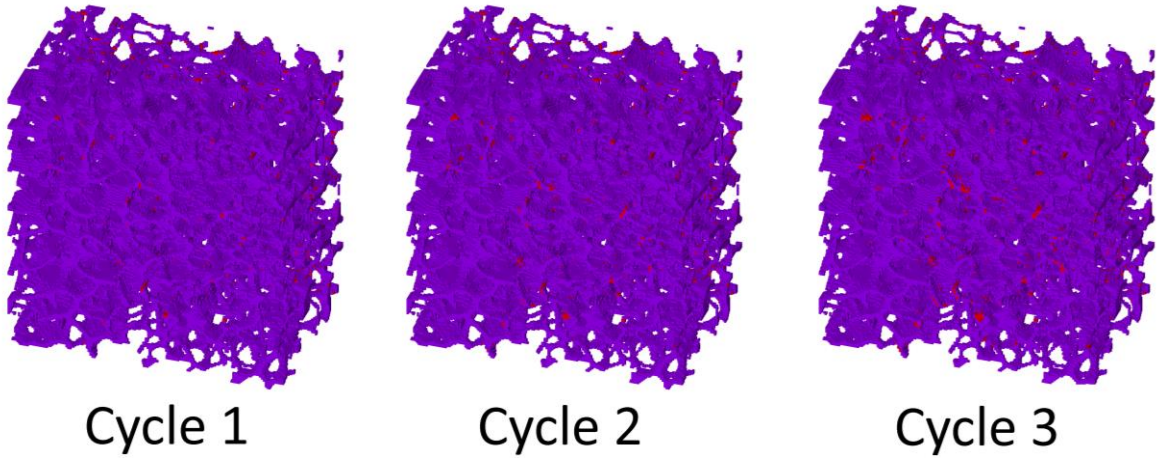


**Figure 3-18: Example of FEA cyclic failure where the red elements have failed**

Power law regressions of the failure were taken and presented in Table 3-9

| | Method 1 | Method 2 | Method 3 |
|---|---|---|---|
| $N_f$ Power regression | 3.8E-12 $(\sigma/E_0)^{-5.89}$ | 7.4E-6 $(\sigma/E_{0)}^{-2.64}$ | 5.53E-4 $(\sigma/E_{0)}^{-1.75}$ |

**Table 3-9: Power law regressions for Porcine Fatigue FEA for Porcine Core Sample 8**

Methods 2 and 3 are very similar, with low exponents which are far away from the porcine experimental data ($\sigma/E_0^{-7.281}$). Method 1 has the highest exponent for all of the fatigue models due to the consistently higher number of cycles to failure and is much closer to the experimental.

Sample #8 had been tested previously (section 3.1), therefore it was possible to examine the modulus degradation over the life time fraction of the sample and compare it with the methods examined here. This is shown in Figure 3-19. The fatigue data at 600N was chosen to examine this in detail due to it being the same force the sample was tested to and because there was more data available to analyse at this load for each method.

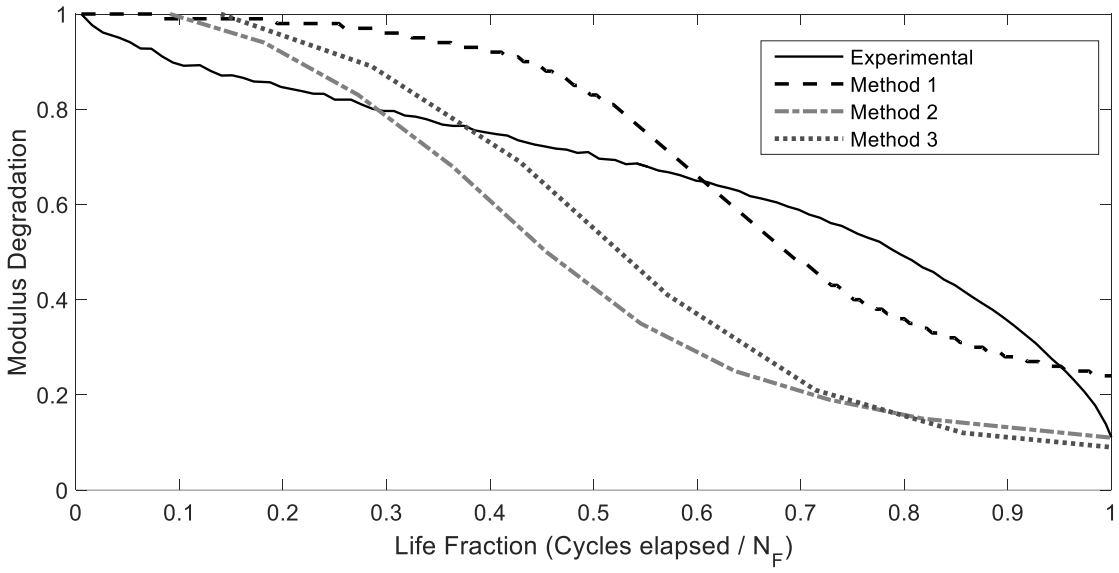


**Figure 3-19: Modulus Degradation vs Life Fraction at 600N until 4% failure strain for Porcine Core Sample 8. Life fraction is defined as the current cycle number over the total number of cycles to failure. Modulus degradation is the fraction of $E / E_0$ where E is calculated from the current cycle displacement.**

The experimental test shows that initially the Young's modulus degrades quickly, stabilises and then begins to accelerate close to end of its life. All of the FEA methods examining fatigue behave in the opposite way, the initial modulus degradation is slow, then accelerates until it stabilises towards the end of its fatigue life. There appears to be a critical modulus degradation point at roughly 0.8 after which point the modulus begins to decay rapidly.

Method 2 shows the most accurate modulus degradation at failure in comparison to the experimental at 600N ($E_{deg}$ = ~0.11), although its cycles to failure drastically different to the experimental with $N_F$ = 11 (FEA) in comparison to $N_F$ = 192 (Experimental). A comparison of modulus degradation without normalising to life fraction is shown in Figure 3-20.

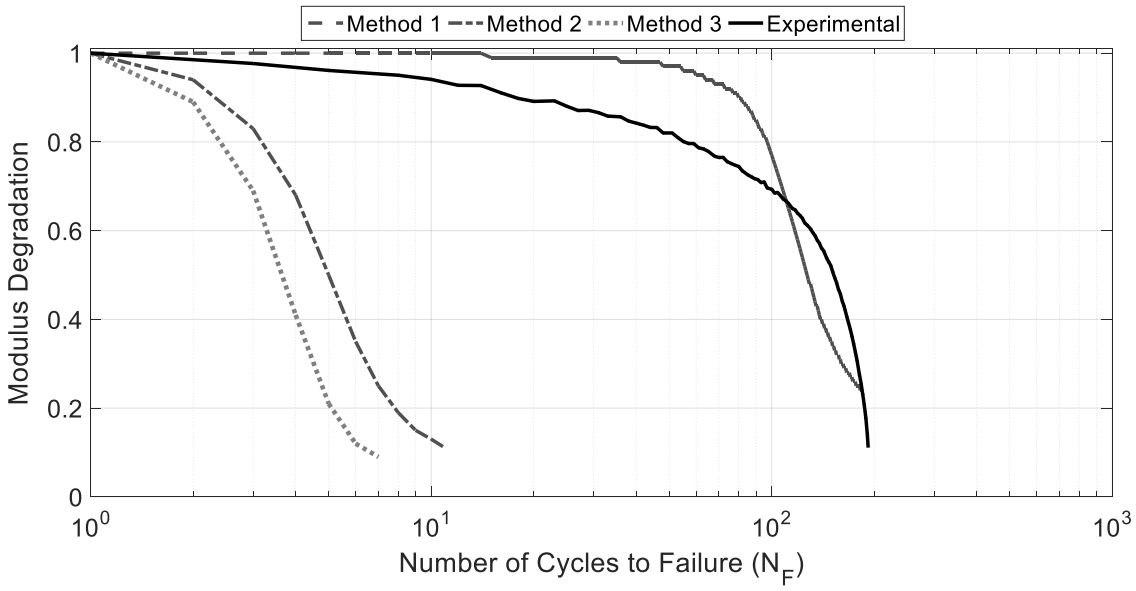


**Figure 3-20: Modulus Degradation vs Number of Cycles to Failure for Porcine Core Sample 8. A comparison of the different methods at 600N which is the same force for the sample tested**

In Figure 3-20, method 1 is seen as the best fit to the experimental in terms of numbers of cycle to failure. The modulus decay rate, however, is much sharper when the finite element model begins to fail and the amount of damage within the sample is less.

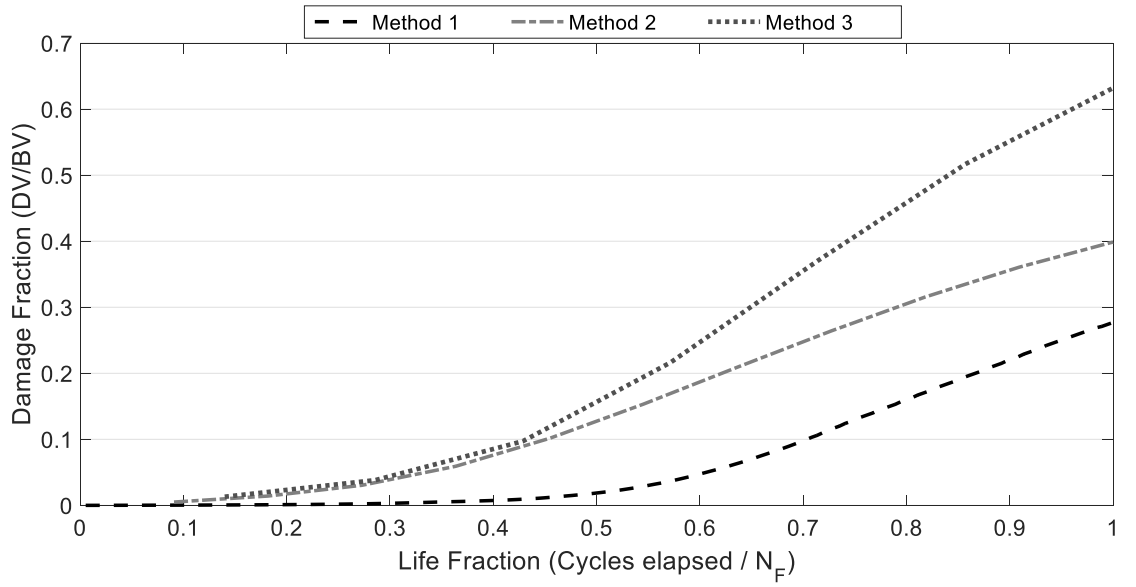


**Figure 3-21: Damage Fraction vs Life Fraction for FEA at 600N until 4% strain for Porcine Core Sample 8**

All the methods have varying amounts of damage recorded at failure. Method 3 reports the highest damage fraction (0.63), followed by method 2 (0.40) and then by method 1 (0.277). Method 1 and 2 have an inflection point at roughly the same life fraction (0.3), this occurs much later for method 1 (0.55) showing that time taken for damage to reach a critical point, varies for each FEA method. After this critical value, the rate of damage accumulation within the sample is increased. Figure 3-22 examines this without normalising to life fraction.

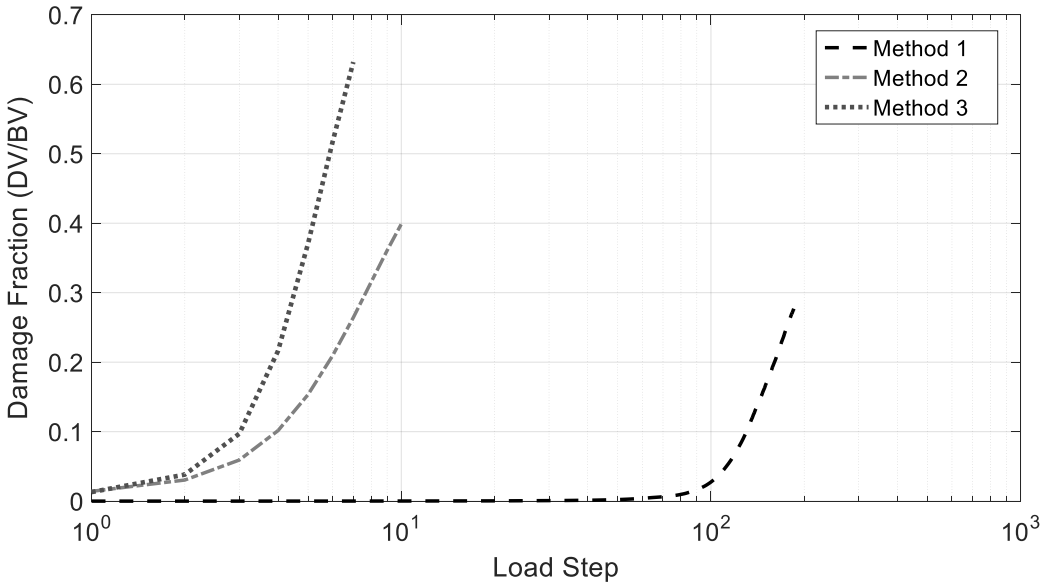


**Figure 3-22: Damage Fraction at load step for each FEA fatigue method at 600N for Porcine Core Sample 8**

When the data is not normalised, it shows that damage accumulation occurs suddenly for method 1 whereas the onset is quicker for methods 2 and 3.

The relationship between damage fraction and modulus reduction is shown in Figure 3-23 for the FEA results. All fatigue methods display an initial loss of Young's' modulus at low damage fractions which decelerates with increasing damage.

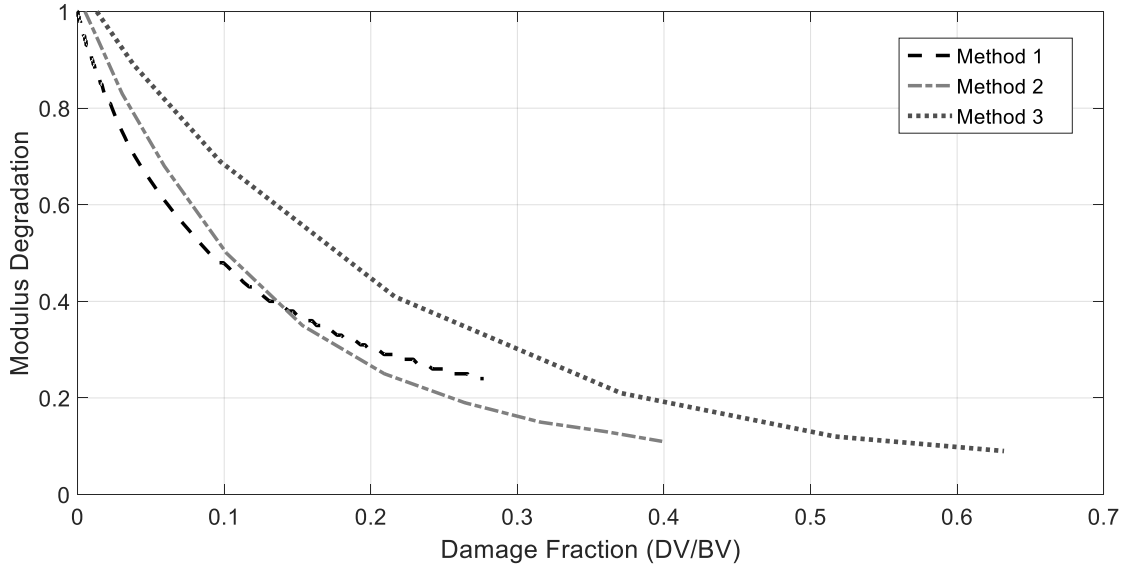


**Figure 3-23: Modulus Degradation vs Damage Fraction for all three FEA fatigue methods for Porcine Core Sample 8 until failure strain of 4% at 600N**

Figure 3-24 to Figure 3-26 shows how the damage varies with distance from the centre of the cylinder for each fatigue method.

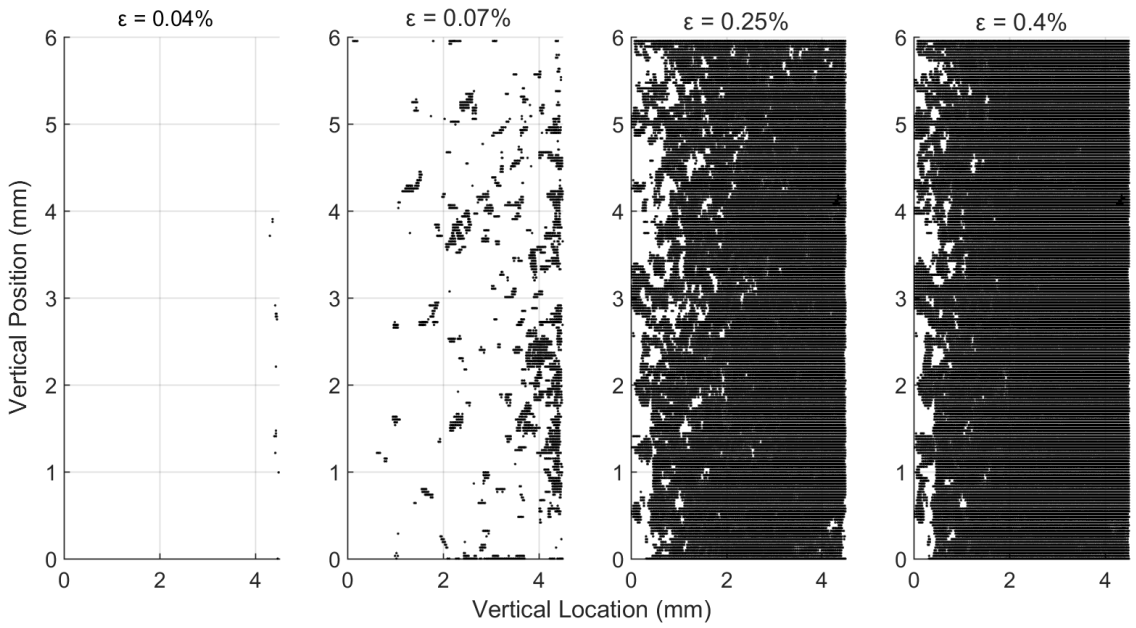


**Figure 3-24: Nodal failure location for FEA of Porcine fatigue (Method 1) at various strains**

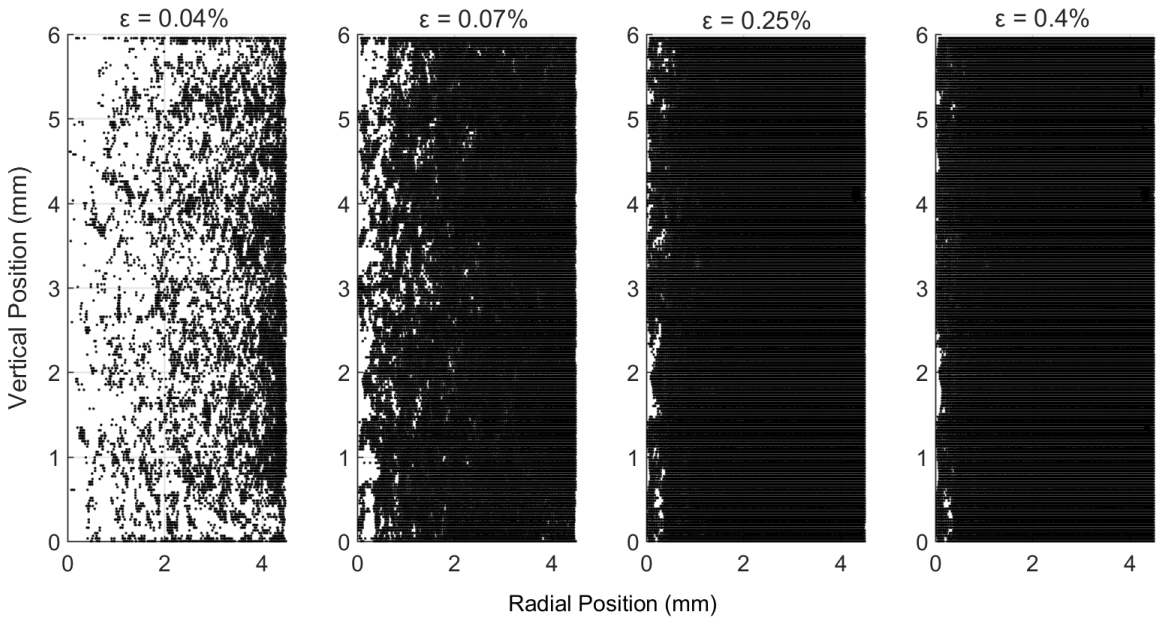


**Figure 3-25: Nodal failure location for FEA of Porcine fatigue (Method 2) at various strains**

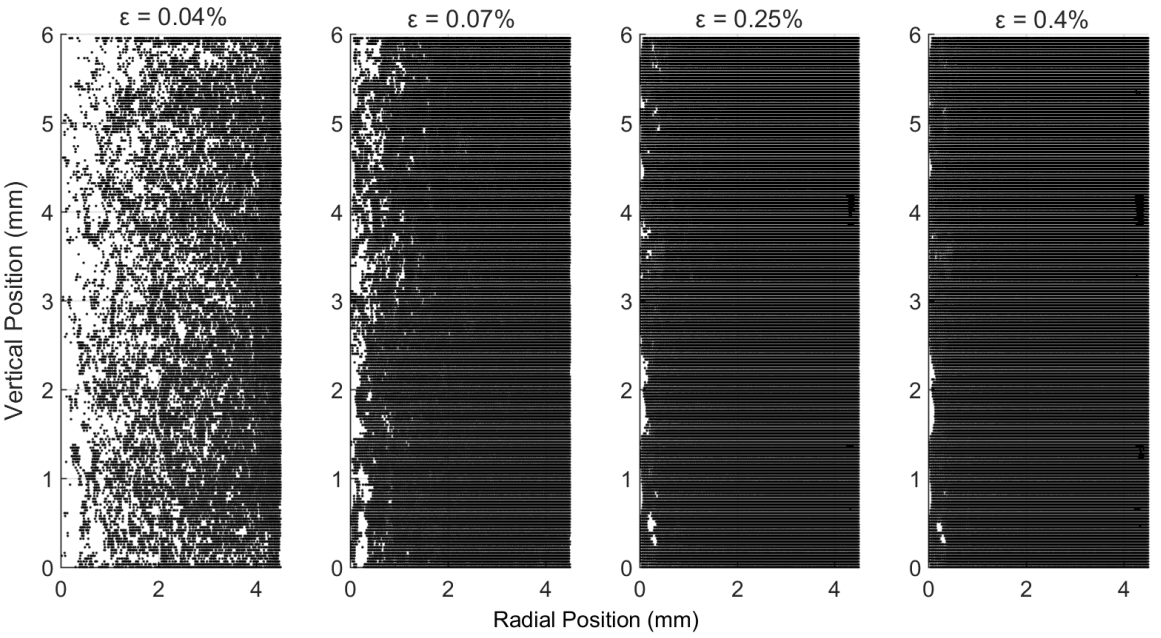


**Figure 3-26: Nodal failure location for FEA of Porcine fatigue (Method 3) at various strains**

From Figure 3-24 to Figure 3-26 it is clear that the damage starts towards the outer radial surface and then radiates inwards, this is less apparent for methods 2 and 3 because of the much higher number of failed elements for these

methods. Figure 3-24 to Figure 3-26 also shows that for methods 2 and 3 the vertical damage location is mostly spread evenly throughout the sample at all strain steps. Method 1 shows a much more varied damage distribution: damage starts in the upper two thirds of the sample which appears to spread downwards and then equalise with the top section.

## 3.4 Finite Element Fatigue on Human Vertebral Samples

The samples tested were only tested in one direction IS, stress was applied to the top surface that corresponds with the normalised stress values. The applied stress values are shown in Table 3-10. During analysis it was also found that two of the samples were tested along the wrong loading direction (T10 and T11), through examination of the input files the corrected angle is given in Table 3-10.

| # | *Angle (°)* | *$E_0$ (MPa)* | *Stress for given $\sigma/E_0$ (MPa)* | | | | | | |
|---|---|---|---|---|---|---|---|---|---|
| | | | **0.011** | **0.01** | **0.009** | **0.008** | **0.007** | **0.006** | **0.005** |
| T10 | 0 | 314 | 3.46 | 3.14 | 2.83 | 2.51 | 2.20 | 1.88 | 1.57 |
| T11 | 0 | 382 | 4.20 | 3.82 | 3.44 | 3.06 | 2.67 | 2.29 | 1.91 |
| T12 | 0 | 307 | 3.38 | 3.07 | 2.76 | 2.46 | 2.15 | 1.84 | 1.54 |
| L1 | 20 | 283 | 3.12 | 2.83 | 2.55 | 2.27 | 1.98 | 1.70 | 1.42 |
| L2 | 20 | 146 | 1.61 | 1.46 | 1.31 | 1.17 | 1.02 | 0.88 | 0.73 |
| L3 | 70 | 233 | 2.57 | 2.33 | 2.10 | 1.87 | 1.63 | 1.40 | 1.17 |
| L4L | 45 | 86 | 0.94 | 0.86 | 0.77 | 0.69 | 0.60 | 0.51 | 0.43 |
| L4R | 45 | 155 | 1.71 | 1.55 | 1.40 | 1.24 | 1.09 | 0.93 | 0.78 |
| L5L | 70 | 185 | 2.04 | 1.86 | 1.67 | 1.49 | 1.30 | 1.11 | 0.93 |
| L5R | 70 | 217 | 2.39 | 2.17 | 1.95 | 1.74 | 1.52 | 1.30 | 1.09 |

**Table 3-10: Applied stress for each vertebral sample**

The applied stress applied to each sample varies heavily (Table 3-10) due to differences in the apparent modulus as determined from an earlier FEA study

(Table 3-6). As normalised stress has constant levels, the stronger samples (T10, T11 and T12) are subjected to higher stresses the opposite is true for the weaker samples (L4L, L2, L4R).

After finite element analysis was concluded, the number of iterations to failure using fatigue method 1 was recorded. These are shown in Table 3-11.

| ***Sample*** | ***Angle (°)*** | ***Number of Cycles to failure for $\sigma/E_0$*** | | | | | | |
|---|---|---|---|---|---|---|---|---|
| | | **0.011** | **0.01** | **0.009** | **0.008** | **0.007** | **0.006** | **0.005** |
| T10 | 0 | 2 | 2 | 3 | 3 | 5 | 13 | 62 |
| T11 | 0 | 2 | 2 | 3 | 4 | 5 | 12 | 45 |
| T12 | 0 | 2 | 2 | 2 | 3 | 5 | 9 | 37 |
| L1 | 20 | 3 | 3 | 4 | 6 | 13 | 50 | 62 |
| L2 | 20 | 2 | 3 | 3 | 4 | 8 | 22 | 101 |
| L3 | 70 | 2 | 2 | 3 | 4 | 6 | 15 | 53 |
| L4L | 45 | 5 | 9 | 20 | 56 | 142 | * | * |
| L4R | 45 | 3 | 4 | 6 | 14 | 46 | 128 | * |
| L5L | 70 | 2 | 3 | 3 | 4 | 8 | 33 | 122 |
| L5R | 70 | 2 | 2 | 3 | 4 | 8 | 25 | 119 |
| Mean | | 2.5 | 3.2 | 5 | 10.2 | 24.6 | 34.1 | 75.1 |
| (SD) | | (0.92) | (2.04) | (5.10) | (15.57) | (40.87) | (35.32) | (31.60) |

**Table 3-11: Predicted number of cycles to failure for each sample with a given normalised modulus. * indicates that the maximum iterations of 150 load steps were reached before the modulus degradation of 10%**

The data presented in the table shows the relationship between normalised stress and number of cycles. Three of the finite element tests did not reach a 10% modulus reduction with 150 load steps: L4L at $\sigma/E_0$ = 0.006 and 0.005; L4R at $\sigma/E_0$ = 0.05. These lost results reduce the standard deviation of the population, as the number of cycles only increases as normalised stress decreases.

Grouping the population allows the calculation of a power law regression based purely on normalised stress and mean cycles to failure. This is taken over the normalised stress values where cycles to failure exists for the entire population ($\sigma/E_0$ = 0.011 - 0.007). This gives the regression:

$$N_F = 1.814E^{-10} \times \left(\frac{\sigma}{E_0}\right)^{-5.139} \quad \textbf{(3-1)}$$

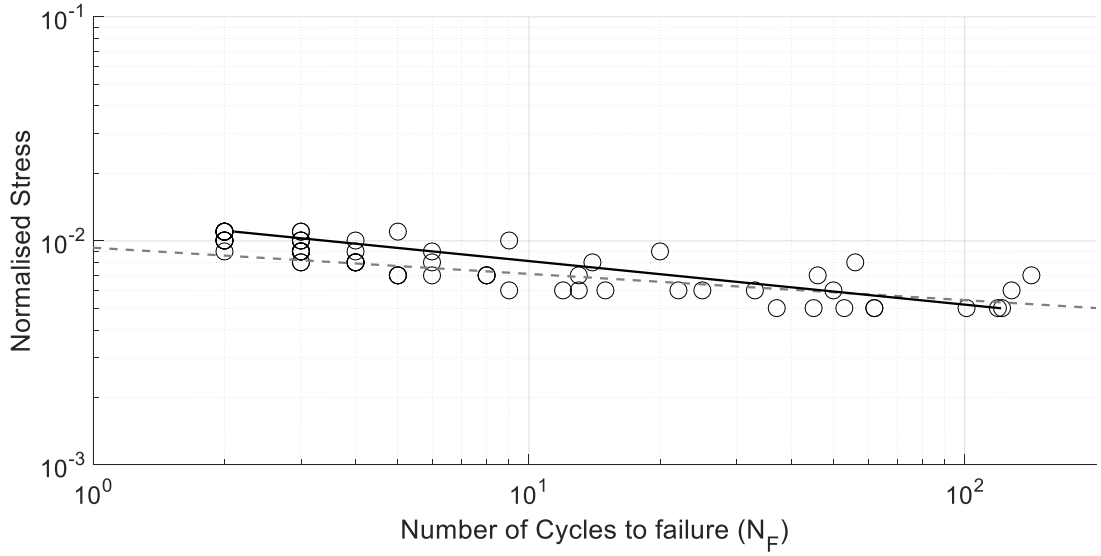


**Figure 3-27: Number of cycles to failure (Fatigue method 1) vs Normalised Stress for Porcine Sample 8. Regression calculated in equation (3-1) shown as solid line. Regression by Haddock et al. (2004) from mechanical testing of human vertebral specimens shown in dashed grey line**

Over the normalised stresses simulated in this study the bone shows good agreement with Haddock et al. (Figure 3-27), there is a tendency for the number of cycles to be under represented overall.

Table 3-12 shows the regressions when the models are grouped together by angle. They are shown in comparison to Dendorfer et al. (2008) who performed fatigue tests of human vertebral bone with varying angles.

| *Study* | $\sigma/E_0 = a \times N_F^b$ | | |
|---|---|---|---|
| | Angle | A | b |
| Human FEA (This study) | 0 | 0.0113 | -0.232 |
| | 20 | 0.0121 | -0.204 |
| | 45 | 0.136 | -0.157 |
| | 70 | 0.0113 | -0.19 |
| Human Vertebral (experimental) (Dendorfer et al., 2008) | 0 | 0.0098 | -0.109 |
| | 22 | 0.0091 | -0.111 |
| | 45 | 0.0096 | -0.121 |
| | 90 | 0.0087 | -0.119 |

**Table 3-12: Lifetime regressions grouped by specimen angle**

The regressions measured from the simulations are higher than in the literature. This equated to a lower fatigue life of the specimens as seen above in Table 3-11.

Normalised stress reduces the scatter in fatigue plots, from Figure 3-27 it is not clear what effect angle has on the predicted fatigue failure. The average number of cycles to failure against average stress for each group, a non-normalised variable is presented in Figure 3-28.

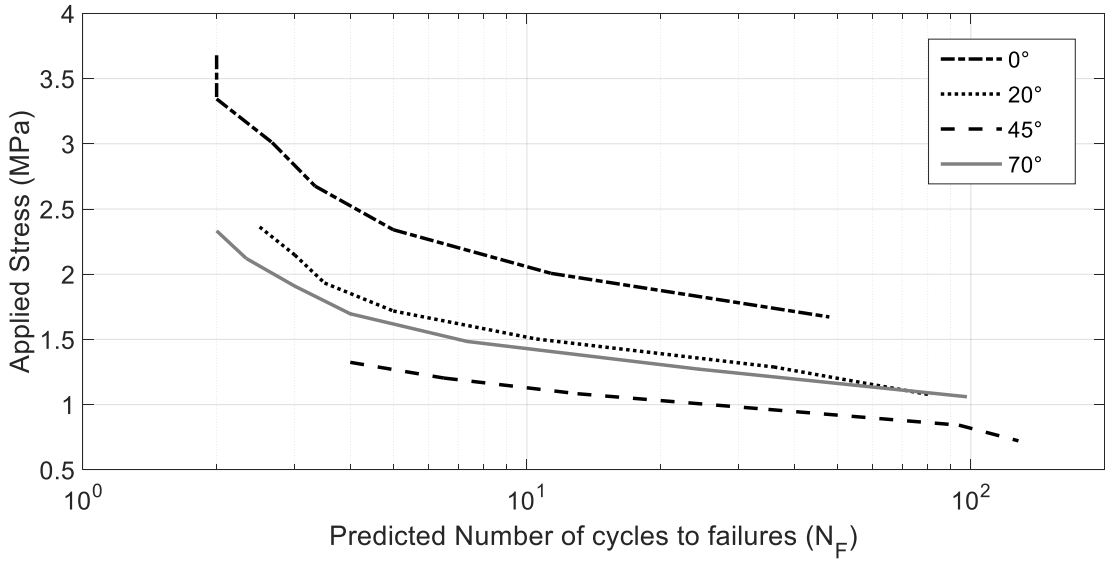


**Figure 3-28: Applied Stress vs Number of cycles to failure prediction grouped by angle of testing. The different angles are represented by different lines on the graphs**

There is a clear difference between the predicted cycles to failure for the different stress levels. At 0° the stresses are much higher than at 45° for the normalised values under examination. 20° and 70° behave very similarly to one another due to the axis being complimentary to one another. This graph shows that as the orientation of a sample approaches shear loading (45°) the stress must drop significantly for it to maintain its high number of cycles to failure. The samples at the physiological angle of 0° have the longest predicted life in regards to the stress applied.

T10 was examined in more detail. Figure 3-29 studies the difference that normalised stress has on the modulus degradation of the sample over the normalised life fraction.

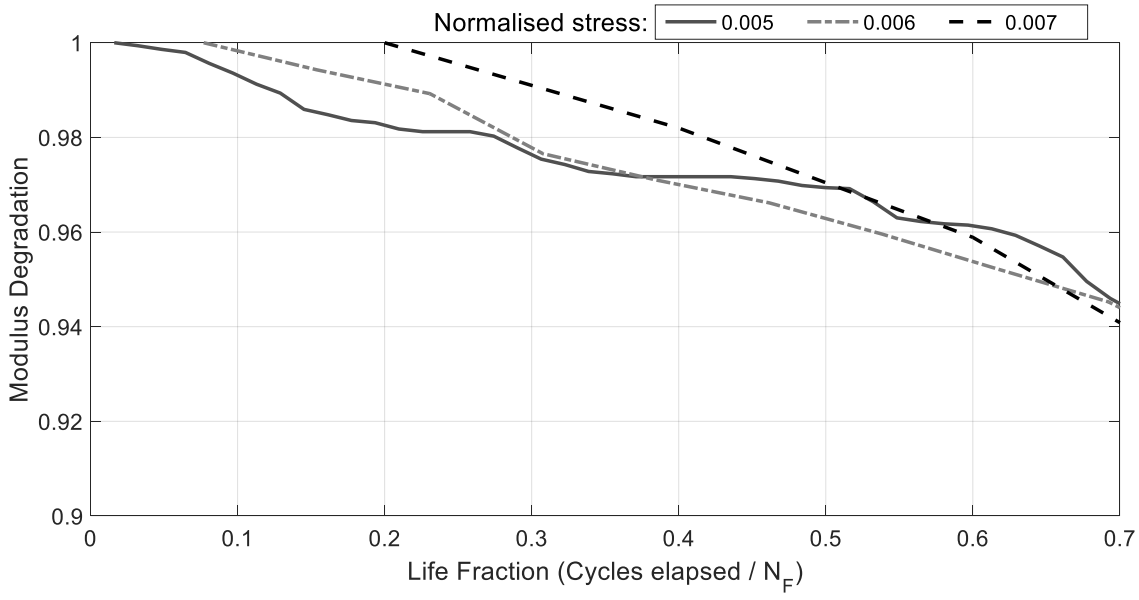


**Figure 3-29: T10 Modulus degradation vs Life fraction for varying normalised stress values. $\sigma/E_0 = 0.007$ (Dashed line), $\sigma/E_0 = 0.006$ (Dot Dashed line) and $\sigma/E_0 = 0.005$ (Solid line).**

Figure 3-29 shows that the model behaves with increasing non-linearity as the normalised stress decreases. At $\sigma/E_0 = 0.005$ the effect of trabecular failure can be noticed from the periods of linearity followed by instability. Figure 3-30 shows the above without normalised the life fraction of the sample.

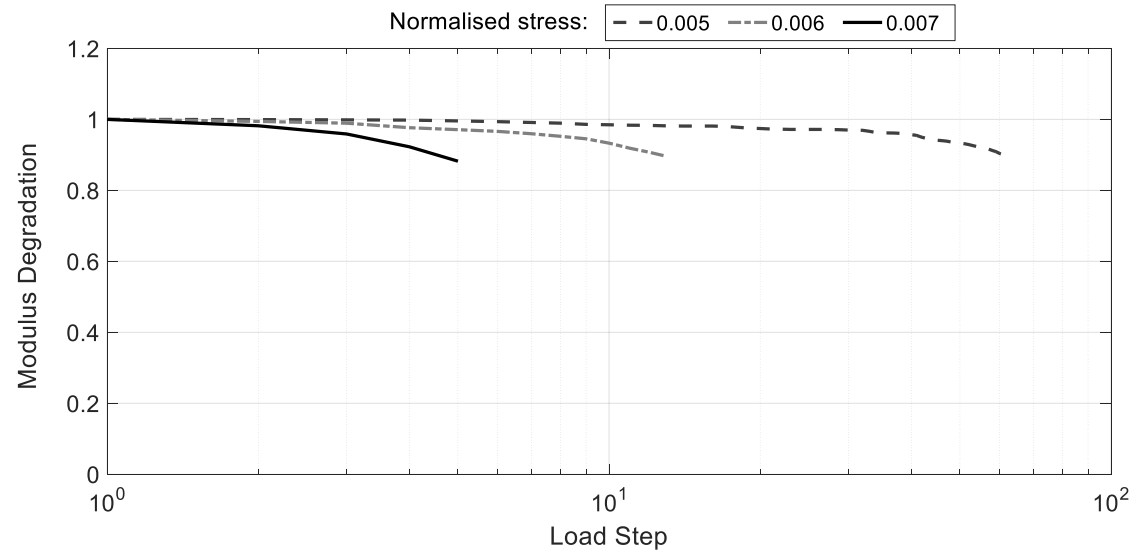


**Figure 3-30: T10 Modulus Degradation with respect to Load Step for various normalised stresses. $\sigma/E_0 = 0.007$ (Dashed line), $\sigma/E_0 = 0.006$ (Dot Dashed line) and $\sigma/E_0 = 0.005$ (Solid line).**

Figure 3-30 shows a linear stable section followed by an acceleration of modulus degradation. The simulated number of cycles to failure decreases with normalised stress which is characterised in Table 3-12.

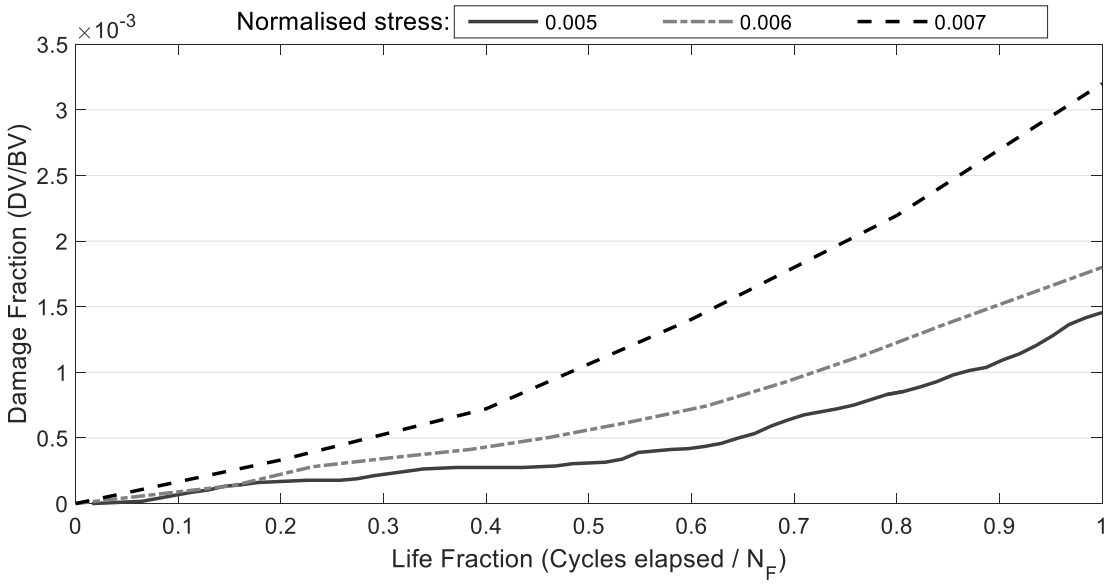


**Figure 3-31: T10 Relationship between Damage Fraction and Life Fraction for sample T10 at various normalised stresses. $\sigma/E_0$ = 0.007 (Dashed line), $\sigma/E_0$ = 0.006 (Dot Dashed line) and $\sigma/E_0$ = 0.005 (Solid line).**

Figure 3-31 describes the relationship between damage fraction and life fraction at various normalised stresses. It shows that as the normalised stress increases so does the damage fraction at failure as well as the rate of damage accumulation within the sample. All the behaviours mentioned in Figure 3-29 to Figure 3-31 were seen for all samples tested and is consistent with the stress based failure method used.

The total damage fraction at failure for all samples are scrutinised in Table 3-13.

| *Sample* | *Angle (°)* | *Damage Fraction for given $\sigma/E_0$ (%)* | | | | | | |
|---|---|---|---|---|---|---|---|---|
| | | **0.011** | **0.01** | **0.009** | **0.008** | **0.007** | **0.006** | **0.005** |
| T10 | 0 | 2.96% | 1.59% | 1.54% | 0.54% | 0.32% | 0.18% | 0.15% |
| T11 | 0 | 2.55% | 1.30% | 1.25% | 0.80% | 0.31% | 0.26% | 0.27% |
| T12 | 0 | 2.03% | 1.09% | 0.50% | 0.38% | 0.25% | 0.11% | 0.08% |
| L1 | 20 | 1.13% | 0.55% | 0.33% | 0.21% | 0.14% | 0.10% | 0.01% |
| L2 | 20 | 0.63% | 0.63% | 0.32% | 0.19% | 0.13% | 0.10% | 0.10% |
| L3 | 70 | 0.87% | 0.49% | 0.42% | 0.24% | 0.13% | * | * |
| L4L | 45 | 0.08% | 0.06% | 0.05% | 0.05% | 0.02% | 0.02% | * |
| L4R | 45 | 0.34% | 0.22% | 0.15% | 0.12% | 0.09% | 0.02% | 0.02% |
| L5L | 70 | 0.23% | 0.24% | 0.11% | 0.07% | 0.05% | 0.03% | 0.02% |
| L5R | 70 | 0.85% | 0.45% | 0.35% | 0.19% | 0.13% | 0.10% | 0.05% |

**Table 3-13: Damage Fraction at failure. Damage fractions are shown as percentages for clarity, * indicates that the maximum iterations of 150 load steps were reached before the modulus degradation of 10%**

Table 3-13 shows the overall damage fraction when predicted fatigue failure occurs. Samples with bone oriented in the direction of loading accrue more damage before the failure criterion is reached. This decreases with misalignment until 45° where comparatively small amounts of damage cause failure.

The relationship between modulus degradation and damage fraction is linear for the human vertebral samples. Figure 3-32 gives an example of this.

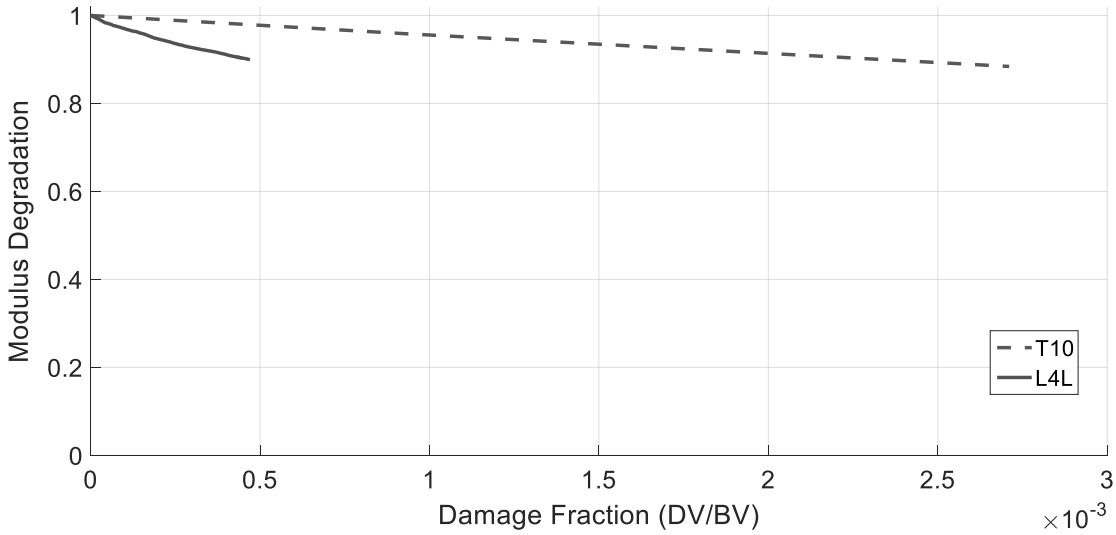


**Figure 3-32: Modulus Degradation vs Damage Fraction at $\sigma/E_0$ = 0.008. Two samples are plotted here for illustration purposes, T10 and L4L**

In Figure 3-32 the differences between the linear gradients is visible, with bone having a greater modulus loss with damage at 45° than at 0°.

Table 3-14 shows the Linear regressions for modulus reduction to damage fraction across the entire population at $\sigma/E_0 = 0.008$.

| Sample | Angle (°) | $E_{deg} = 1 + a \times (DV/BV)$ | | |
|---|---|---|---|---|
| | | a | $R^2$ | Average |
| T10 | 0 | -43 | 0.999 | |
| T11 | 0 | -43 | 0.999 | -52.7 |
| T12 | 0 | -72 | 0.999 | |
| L1 | 20 | -66 | 0.996 | -74.5 |
| L2 | 20 | -83 | 0.999 | |
| L4L | 45 | -202 | 0.995 | -146 |
| L4R | 45 | -90 | 0.988 | |
| L3 | 70 | -92 | 0.991 | |
| L5L | 70 | -217 | 0.996 | -125.8 |
| L5R | 70 | -68 | 0.999 | |

**Table 3-14: Linear regressions for Modulus Degradation vs Damage Fraction (at $\sigma/E_0 = 0.008$). Samples are grouped by angle to obtain the average regression per orientation group**

The coefficient of determinations present for all the regressions in Table 3-14 show a strong linear behaviour in trabecular bone, there are dissimilarities in the gradient which appear to be dependent on the angle. The samples tested at angles closer to the physiological accumulated more damage before failure. The gradients for all the normalised stresses are given in Table 3-15 below.

| *Sample* | *Angle (°)* | *Gradient a ($E_{deg}$ = 1 + a x (DV/BV)) for given $\sigma/E_0$* | | | | | | |
|---|---|---|---|---|---|---|---|---|
| | | **0.011** | **0.01** | **0.009** | **0.008** | **0.007** | **0.006** | **0.005** |
| T10 | 0 | -23 | -28 | -33 | -43 | -54 | -66 | -69 |
| T11 | 0 | -23 | -28 | -35 | -43 | -55 | -63 | -68 |
| T12 | 0 | -38 | -48 | -60 | -72 | -91 | -126 | -146 |
| L1 | 20 | -36 | -43 | -54 | -66 | -77 | -79 | -99 |
| L2 | 20 | -52 | -53 | -70 | -83 | -98 | -111 | -120 |
| L4L | 45 | -177 | -193 | -207 | -202 | -237 | * | * |
| L4R | 45 | -64 | -71 | -82 | -90 | -94 | -138 | * |
| L3 | 70 | -52 | -62 | -73 | -92 | -112 | -130 | -63 |
| L5L | 70 | -140 | -146 | -186 | -217 | -260 | -286 | -316 |
| L5R | 70 | -41 | -47 | -57 | -68 | -82 | -90 | -92 |

**Table 3-15: Linear regressions for Modulus Degradation vs Damage Fraction. Samples are grouped by angle. * indicates that the maximum iterations of 150 load steps were reached before the modulus degradation of 10%**

Table 3-15 demonstrates that the pattern for $\sigma/E_0 = 0.008$ is apparent across all normalised stress levels. There is a decrease in the regression gradient as the normalised stress increases.

# 4 DISCUSSION

## 4.1 Porcine Fatigue Testing

In this study (Sections 2.2 and 3.1), porcine trabecular cores were subjected to cyclic compressive loading at 2 Hz with a prescribed normalised stress to a failure strain of 4% over the extensometer gauge length. Comparisons between the subjected vibrational measures were made as well as an examination of the regression models used to predict fatigue failure. Usage of ISO 2631-1 is contentious with laboratory fatigue testing of trabecular bone as there are whole sections of the body not accounted for. There are concerns about the low sample size and lack of morphological data for further analysis.

### 4.1.1 Mechanical Analysis

The length and diameter for the samples were very uniform (Table 3-1), although it is difficult to examine the surface finish of the trabecular cores without further morphological analysis, it is possible that the machining could have a detrimental effect on the fatigue properties of cancellous bone (Choi and Goldstein, 1992). All samples were taken from the same position on the vertebrae and machining was conducted using the same techniques and equipment, so any defects should be consistent between samples.

Sample #5 did not fail within the maximum cycle number allotted to the testing, this sample was tested at $\sigma_n = 0.0022$ which is less than the hypothesised endurance limit for bovine trabecular bone of $\sigma_n = 0.0035$ (Cheng, 1992). Although Cheng performed fatigue testing on bovine bone; if it is the morphology that has the strongest influence on the mechanical properties of bone (Morgan, Bayraktar and Keaveny, 2003) it can be theorised that this endurance limit also exists for porcine trabecular cores.

Sample #10 has one of the lowest volume fractions (BV/TV = 0.265) and one of the lowest initial Young's modulus ($E_0$ = 953) but the longest fatigue life of all samples which failed (386705 Cycles). Sample #10 appears to be an outlier but due to the sample size and high natural variance of trabecular bone that cannot be said with confidence.

A possible reason for this difference could be a chemical difference in the sample; collagen has been shown to play a significant role in bone toughness (Wang et al., 2001) but not stiffness. Sample #10 may have a much higher collagen content therefore allowing it to survive a significantly longer period of time yet still exhibit a similar initial Young's modulus. Examination of this sample was further hindered by the cascading data failure of the CT reconstruction machine, which meant that possible differences in morphology could not be further examined. Deviation from the main axis of loading during sample preparation or testing has been shown to affect fatigue life (Dendorfer et al., 2008). As the CT scans were lost, this effect is unaccounted for in this investigation.

Treating the damage caused from vibration as a form of fatigue has been examined extensively in the literature (Ayari et al., 2009; Sandover, 1983). Under fatigue loading high exponents are typically seen between the normalised stress and cycles to failure such as $(\sigma/E_0)^{-8.54}$ (Haddock et al., 2004) and $(\sigma/E_0)^{-10.4}$ (Moore and Gibson, 2003b) as shown in Figure 3-2. In this study the exponent was calculated to be $(\sigma/E_0)^{-7.281}$, this is lower than the values reported in the literature.

Fatigue testing of porcine trabecular cores has not been previously presented. Although porcine bone has proven to be a suitable analogue for human bone under compressive loading (Yingling, Callaghan and McGill, 1999), this study shows that the fatigue properties vary considerably in comparison to both human and bovine.

### 4.1.2 Vibration Analysis

When calculating acceleration the assumption was made that the signal does not change significantly between logged data points. Before acceleration was calculated the displacement data was checked for errors; save some expected variation in applied forces, no samples tested logged unexpected displacements or loads.

An assumption that is made when examining this data is that the methods and limits used in ISO 2631-1 (ISO, 1997) are applicable. Frequency weighting was applied to all the samples as per ISO 2631-1. Although the methodology used is different to real world WBV, the weighting affects the samples equally and so the effect on influencing the final vibration statistic is universal. This allows for comparative measures to be between RMS, VDV and $VDV_{exp}$.

Table 3-2 shows that the time to the VDV action limit is generally much greater than the number of cycles to failure (which was often catastrophic for low-cycle fatigue), which is unexpected as humans have been exposed to higher levels of vibration without failure (Garme, Burstrom and Kuttenkeuler, 2011).

ISO 2631-1 examines the whole human body human under vibration whereas testing was conducted in laboratory conditions on porcine trabecular cores. The vibration interaction position for users of marine craft is typically the seat or the vehicle deck, there exist several transfer functions in the literature to equate this vibration to spinal loads and force (Coe, Xing and Shenoi, 2010; Fritz, Fischer and Bröde, 2005; ISO, 2004; Kitazaki and Griffin, 1997; Mansfield and Griffin, 2000; Olausson and Garme, 2015; Seidel, Blüthner and Hinz, 2001). Application of an inverse transfer function to back calculate real world exposure is infeasible in the study due to the differences in marine craft and seating vibration characteristics. A further complication is the interaction between the different elements of the spine; it is one thing to calculate the spinal forces at different vertebral locations but to calculate the force applied to the trabecular section tested was outside of the scope of this study. Consequently the regressions put forth in section 3.1 should not be used as definite relationships between vibration and spinal damage but examined comparatively and as a critical look at the different statistics.

Only some of the vibration statistics, discussed in section 1.3.2, were examined: DRI, and the $6^{th}$ order RNN as set forth in ISO 2631-5 (ISO, 2004), were not examined due to their inherent problems. Therefore only the average and cumulative statistics (RMS and VDV) of ISO 2631-1 were used.

RMS as a possible predictor is no better than normalised stress; with a coefficient of correlation $R^2$ = 0.636 for RMS and an $R^2$ = 0.638 for normalised stress respectively. This is reflective of its inability to accurately characterise vibration which has been widely noted in the literature (Boileau, Turcot and Scory, 1989).

VDV is a cumulative measure of vibration; as acceleration increases with damage (and loss of stiffness) so does the total vibration exposure (Figure 3-4). An increase of VDV correlating with an improved fatigue life, and thus less spinal damage from vibration, is counterintuitive in regards to the limits set out in legislation (European Parliament, 2002; Regulations, 2005; VDI, 2002). VDV is typically measured against a fixed time or over a fixed operation (McIlraith, Paddan and Serrao, 2014) generating a VDV which can be compared meaningfully. In this thesis VDV was measured over the total experimental time of the tests; so the trend that it increases with number of cycles to failure is expected. VDV has the highest coefficient of determination of any of the vibration statistics ($R^2$=0.754) but due to the manner in which it was calculated, it cannot serve as a predictor for fatigue failure.

To rectify this $VDV_{exp}$ was used, this normalises VDV with respect to a 10 minute period allowing for meaningful comparison between results. Excluding VDV, $VDV_{exp}$ (Figure 3-5) has the highest coefficient of determination ($R^2$ = 0.714) of all vibration statistics. Such $4^{th}$ order techniques are known to be more sensitive to changes in vibration (Stayner, 2001).

There is a large grouping of normalised stresses ($\sigma/E_0$ = ~0.0055) against cycles to failure (Figure 3-2) which is also evident in RMS (RMS = ~1.1). This grouping is not visible when examining $4^{th}$ order measurements (VDV and $VDV_{exp}$).

RMS and $VDV_{exp}$ are both based on a derived acceleration based on the peak to peak displacements. These measures are consequently normalised measures based upon the plastic deformation of the sample to failure, as the $4^{th}$ order averaging is more sensitive to changes it is more accurate. This work is in

agreement with work by Cotton et al. (2005) who have shown that the most reliable measurement for cycles to failure is the damage rate.

Of all the calculated applicable statistics $VDV_{exp}$ has the best correlation for fatigue life. ISO 2631-1 suggests that VDV only be calculated when the crest factor is larger than 6, however, testing was conducted at a fixed frequency of 2Hz and the worst case acceleration was for sample #1 at ~7 m/s giving a crest factor of 1. $VDV_{exp}$ offered a marked improvement in predicting fatigue failure over any of the other regression models and also explains the variation of fatigue life when samples have been tested under similar normalised stresses.

## 4.2 Finite Element Assumptions

Several assumptions were made during finite element analysis in the following chapters:

1. Bone that is not visibly damage through micro-CT scans is assumed to be undamaged in regards to its mechanical properties
2. The complex trabecular structure of bone can be accurately modelled using 8-node quadrilateral hexahedral elements
3. The application of boundary conditions on a subsection of bone is valid
4. At the tissue level bone properties are linear and isotropic

Prior damage of bone whether due to handling, machining or storage is usually detected in Micro-CT in conjunction with staining techniques (Leng et al., 2008; Nagaraja, Couse and Guldberg, 2005). Some bone damage will be apparent in the form of bone disconnection which may be quantified in the morphometric results of the samples such as connectivity.

Accurately representing bone morphology is very important for finite element models (Ulrich et al., 1998). 8-node quadrilateral hexahedral nodes are commonly used in the literature as a way to reduce computational costs. For all FEA the mesh voxel size was set to a quarter of mean trabecular thickness to truthfully characterised the morphology (Guldberg, Hollister and Charras, 1998).

The boundary conditions applied onto the models are based on subsections of trabecular tissue which is susceptible to errors from localised morphological variation when applying FE methods (Bayraktar et al., 2004). For the FEA studies the apparent modulus was calculated over the gauge length of the extensometer, which was the area modelled to calculate the apparent modulus in finite element tests. Although the samples were reduced in height, all other dimensions of the sample remained the same reducing the error using a subsection. The porcine core has the largest possible error from this, due to the greater sample height in comparison to the gauge length, making segmentation in regards to the extensometer vital.

Another assumption with the FE models presented here is that the boundary conditions are coupled at the gauge length. During testing the platen was at a different location than the section observed through mechanical testing which would lead to a non-uniform application of loading at the gauge length. This has a knock-on effect for the FEA as this measured central section is where the boundary conditions were applied. This is due to trabecular architecture which is non-uniform by nature making loading non-uniform throughout the sample too. It was outside the scope of this study to examine the internal forces of the samples therefore this assumption is a necessary idealisation.

Bone is known to be anisotropic at the macro scale (Whitehouse, 1974), showing distinct variations with loading directions which is supported from the results of mechanical testing (section 3.2). At the tissue level it has been demonstrated that this anisotropy is a function of trabecular architecture (Oftadeh et al., 2015), therefore the assumption of isotropy at the tissue level is valid.

Although bone has been shown to have non-linear properties at the tissue level (Bayraktar et al., 2004) the finite element methods presented here use the same philosophy as Kosmopoulos and Keller (2003). They modelled trabecular bone with linear isotropic materials which was solved iteratively with good agreement to experimental testing. Applying this philosophy in these studies

allowed the modelling of fatigue failure while eliminating the increased computational cost associated with material plasticity.

## 4.3 Apparent Modulus of Human Trabecular Cubes

### 4.3.1 Mechanical Analysis

In sections 2.3 and 3.2, a human lumbar-thoracic spine from a 65 year old Caucasian female was dissected into 10 cuboid samples from levels T10 to L5, mechanical tests were performed to obtain the apparent Young's modulus and used to validate FEA using a novel greyscale material mapping technique as described in section 2.3.4.

Examining the morphology of the vertebral samples shown in Table 3-3, the DA (2.55 ± 0.515) is high in comparison to values obtained from Dendorfer, Maier and Hammer (2008), (DA = 1.65 ± 0.29) who obtained morphometric data from a pooled set of human cancellous samples. Human vertebral bone has been shown to be highly anisotropic (Keaveny and Hayes, 1993) and increase with aging with a related drop in volume fraction (Mosekilde and Mosekilde, 1986). The age of the cadaver from which the sample was obtained was 65 years old, past the age of 60 where bone remodelling is thought to occur again (Frost, 1964), this also provides an explanation for the low volume fractions in the samples tested.

The DA for sample L5L was considerably less than the mean and was much lower than any samples with a similar connectivity. This seems anomalous but, as the purpose of this study was comparative, the sample was analysed further.

Figure 3-11, which examines experimental $E_{app}$ in relation to reported ML angle, does not follow the expected behaviour. For 45°, both samples should theoretically behave similarly in both the AP and IS directions. Table 3-6 shows that this is not the case for the experimental $E_{app}$ for L4L and L4R, which had different mechanical responses in both the IS and AP directions and in particular L4R which showed the greatest variation at this angle ($E_{app}$ = 74 and $E_{app}$ = 236 MPa for IS and AP directions respectively). Table 3-4 shows that these samples had deviated greatly from the reported angle (L4L = 4.3° and L4R = 5.3°). It can be assumed that at 45°, angular deviation would have the most pronounced effect as this would result in bone becoming more orientated

in respect to a particular loading direction. Connectivity is roughly a measure of the number of trabecular in the structure, which is much higher for L4R at 1609 in comparison to 1084 for L4L. This means that there are more unconnected structures within L4R which could lead to a weaker structure. Together the differences of connection and alignment could account for the differences in mechanical behaviour.

There is also a high inter-sample variation in apparent modulus between L4L and L4R even though they were taken from the same vertebral level (Table 3-6). There are significant morphological differences between these two samples, the most apparent being the differences in volume fraction. For L4L and L4R the BV/TV is 0.0818 and 0.1067 respectively, these two values constitute two extremes across the whole cohort and are contained at the same vertebral level. This underscores the difference which can occur between two samples of trabecular bone and highlights the limitation of the small sample size present in this study.

The mechanical results, shown in Figure 3-11, indicate that orientation of trabecular bone has an evident effect on the apparent modulus, where bone becomes weaker as it deviates from its true alignment. This in agreement with Öhman et al. (2007) who studied the effects of misalignment on Young's modulus and ultimate compressive stress. This study examines greater angles than Öhman et al., and on bone with a higher degree of anisotropy, building a more detailed picture of the relationship between mechanical properties and orientation.

### 4.3.2 Finite Element Analysis

Both the 8-bit and 32-bit models of L4L underestimate $E_{app}$ (Table 3-6) in the IS and AP loading directions. Even though this sample exhibited a low BV/TV from morphometric analysis (0.0818), at which errors in thresholding are amplified (Hara et al., 2002), another sample with a similarly low volume fraction did not register this variation (L1, BV/TV = 0.0816). This could be attributed to intra-specimen variability when determining apparent modulus from a subsection of bone (Chevalier et al., 2007).

Figure 3-14 to Figure 3-16 shows large variation at 70°, again in the IS and AP directions for the FEA as well as the experimental. Table 3-3 shows that while 0° had 1 sample; 20°, 45° and 90° had two; 70° was comprised of three samples. This leads to a greater spread in the standard deviations due to inter-specimen variation.

The material model which this study uses (Adams, 2017) was validated under different conditions to those described by Adams. Rather than simulating tensions tests, compression was used in this analysis. Adams also tested to the ultimate tensile stress for five notched femoral trabecular discs. They found that the finite element models had good agreement with stiffness on three of the five samples at peak load.

The models generated by Adams were also idealised, the disc was modelled with symmetry across the notch, possibly leading to the discrepancy in experimental vs finite element observations. From the relative error % (Figure 3-10) it has been shown that modelling the relevant section of bone and applying accurate boundary conditions improves the computational accuracy of the model.

The vertebral bone examined in this study had an average material density of 1.8 g/cm$^3$, which falls in the range of the materials tested by Adams (1.6–2.3 g/cm$^3$). This allows the application of the material model without making further assumptions about the mechanical response of bone.

Other models measure the linear tissue modulus response to apparent modulus to back-calculate the effective tissue modulus (Bayraktar et al., 2004). The material model examined in this study does not require this step, allowing for material characterisation with just a CT scan of a sample and a calibration standard. It also treats bone as behaving over a continuum; the mechanical properties of bone vary with density. This has been examined previously by Helgason et al. (2016) who demonstrated that material models based upon the same samples examined for FEA provide good agreement but this is reduced when applied to other samples. This has not been seen in this study where

good agreement was found between the experimental and 32-bit FEA results and the material model was derived from different samples than those tested.

As noted in the results (section 3.2), the FE models reduce the variability from the loading directions as seen in Figure 3-14 to Figure 3-16. Both models systematically underestimate the apparent modulus in the AP and IS direction while generally being a good predictor in the ML direction. Both models show reasonable accuracy in expressing the effect of orientation on apparent modulus. When the experimental results are directly compared to their finite element counterparts (Figure 3-8 and Figure 3-9) this accuracy is diminished, in particular for analysis performed on 8-bit images (8-bit $R^2$ = 0.729, 32-bit $R^2$ = 0.904). Examining the percentage error in $E_{app}$ predictions (Figure 3-10), the errors are greatest when the experimental modulus is lowest and vice versa. This is anticipated as when the Young's modulus is lower even small deviations result in a much larger percentage change than at higher values.

Overall, the 8-bit models are a worse predictor for apparent modulus, the reasoning for this comes from the "partial volume effect" an artefact from averaging methods in imaging processing which removes fidelity from the data. Table 3-5 examines the threshold value of the two image depths showing a lower mean and a larger standard deviation for the 8-bit images, 32bit = 133 ± 2.4 (GS) in contrast to 8bit = 58 ± 19.5 (GS). Resampling to 8-bit was conducted over the entire GS range of the image therefore there was aggressive binning of the greyscale values, leading to the peak shift and compression as seen in Figure 3-7.

Ulrich et al. (1998) demonstrated that morphology is very important for the development of precise FE models. The partial volume effect leads to under thresholding and lower connectivity within trabeculae, reducing the accuracy of the resulting simulations. This effect is even more pronounced on samples with a low volume fraction (Hara et al., 2002) (BV/TV = 0.15) where a difference in thresholding of 0.5% resulted in a difference of apparent modulus by 9%.

As the material properties of bone were modelled as a continuum, the resampling to 8-bit also reduced the number of material models. The 8-bit

models were limited by the GS resolution of 1, whereas the 32-bit models were free to divide the 256 material levels as appropriate due to a much higher GS resolution as it was not restricted by the bounds of GS bit depth.

The partial volume effect also occurs when rescaling the image, as was done here from 16μm to 32μm. Both sets of samples were reduced using the same method, and the resulting meshes conformed to the trabecular thickness to number of voxel ratio of 4 (Guldberg, Hollister and Charras, 1998). This error is not consistent between the 8-bit and 32-bit images though, as averaging an already averaged image leads to a compound error.

## 4.4 Finite Element Fatigue on a Porcine Core

Although there are several less computationally intensive ways to model the fatigue failure of bone (Hambli et al., 2016; Mostakhdemin, Amiri and Syahrom, 2016), they do not examine the fatigue growth on a cycle to cycle basis. This is why a direct iterative solution was applied in this study.

The apparent modulus calculated in this FE study was $E_0$ = 1972 MPa, which is ~14% higher than the experimental at $E_0$ = 1694 MPa. This is counter to the tendency described in section 4.3.2 for the selected material model to underestimate modulus. The higher volume fraction of porcine bone, in comparison to Human and Bovine, at 0.414 could account for this. This would lead to a more connected trabecular architecture which would be stronger.

The finite element models showed that the number of cycles to fatigue failure was consistently lower than in the experiment (Table 3-8, Figure 3-17). This is consistent with papers in the literature which find that the damage model applied can result in large deviations from experimentally measured values (Guo et al., 1994). This is even the case for method 1 (Figure 3-17) which, although is more accurate than the other models tested, still underrepresents the sample modelled (Porcine Core 8, FEA $N_F$ = 185 cycles, Experimental $N_F$ = 192).

This difference may be down to the difference in Initial Young's modulus. If the FE model had a Young's modulus close to the experimental value, it would be

weaker and less resistant to deformation, this could theoretically decrease the internal stresses resulting in less failure at each load step and thus an increased fatigue life.

Figure 3-19 shows that all FEA of fatigue used in this study do not accurately replicate the initial phase of fatigue failure. This is common with other FEA studies into trabecular fatigue (Harrison et al., 2013; Kosmopoulos, Schizas and Keller, 2008). The initial phase in experimental fatigue of trabecular tissue is driven by non-linear viscoelasticity, which settles and the mechanical fatigue behaviour of bone becomes stable. As this model is only linear elastic this effect is not seen here.

The damage fraction for method 3 is much higher than the other methods (Figure 3-21) as its final displacement was 0.33mm, which equates to a strain of 5.5%. During the previous load step it reached a displacement of 0.234mm which was just below failure, this addition of an extra load cycle increased the damage fraction from 0.51 to 0.63. This is the largest damage fraction measured across all three methods. Although the rate of damage in Figure 3-23 seems higher for Method 1 when normalised over fatigue life; when time is taken into account (Figure 3-22) the onset of damage occurs much later than the other methods tested. FE method 1 in Figure 3-19 agrees will with the bovine trabecular fatigue (Moore and Gibson, 2003b) showing a steep increase in modulus degradation to failure.

It has been previously reported that failure of a few trabeculae has a strong impact on the Young's modulus of the sample (Kosmopoulos, Schizas and Keller, 2008). Figure 3-23, which examines the relationship between damage fraction and modulus reduction corroborates this: It indicates that a small amount of damage results in a greater loss of strength at low damage levels compared to higher ones. Method 1 shows a much steeper loss of modulus in regards to the amount of damage whereas Methods 2 & 3 have a much lower modulus reduction with low amounts of damage. This could be due to the location of failed elements.

Figure 3-24 to Figure 3-26 shows that radially, damage begins to accumulate in the outer regions of the sample first. This is where there are areas of discontinuity due to machining of the sample, which leads to increased stresses and strains at this point (Michel et al., 1993). As the FE model is a direct representation of the sample, this discontinuity is also present here. It is also evident that method 1 shows a different picture of fatigue damage accumulation, than methods 2 and 3. The damage starts at the central portion of the sample and not at the ends. This is unlike experimental testing where damage occurs at the force/sample interfaces (Michel et al., 1993). The boundary conditions used in this study explains this discrepancy: the force boundary condition is coupled, so the friction experienced at the ends due to contact with the platen (Linde, Hvid and Madsen, 1992) is not modelled here.

Methods 2 and 3 model different failure mechanisms and demonstrate a much more aggressive element failure criterion which selects more elements. For example, at $\varepsilon = 0.007$ the number of failed elements are 10600, 206916 and 339548 for methods 1, 2 and 3 respectively. This leads to a an even distribution of damage along the IS direction of the sample, even at low strain steps

Method 1 (section 3.3) uses a failure mode which is based upon cycle count and not just upon the intrinsic mechanical properties of the material. In this application it can be seen as characterisation of the relationship between damage accumulation in bone and its failure stress (Hernandez et al., 2014).

This is in contrast to Methods 2 and 3 which are only informed by the intrinsic material properties which leads to rapid failure when modelling bone as a continuum (Table 3-8). This is not expected for method 2 which takes the element modulus into account and therefore models the failure as a continuum (Chevalier et al., 2007). In practice the yield stress values were much lower than those predicted by method 1 therefore leading to the premature failure seen here.

Figure 3-17 demonstrates that Method 1 is the most accurate FEA fatigue model tested in this study but it does not conform to the fatigue regression from

experimental testing (section 3.1). There are two possible explanations for this: The fatigue model used or the sample modelled.

Method 1 is based on human tissue fatigue from Choi and Goldstein (1992), and there are significant differences in the fatigue behaviour of human and porcine bone (Figure 3-2).

The porcine core modelled (#8) had a low number of cycles to failure in comparison to the other porcine cores (Table 3-2). It also sits on the predicted bovine fatigue curve (Figure 3-2) (Moore and Gibson, 2003b) rather than the porcine regression. If this sample is innately different, FEA based on this sample would be too.

Method 1 has a fatigue exponent of $\sigma/E_0^{-5.89}$ which is similar to the porcine experimental data ($\sigma/E_0^{-7.281}$). Human trabecular tissue has an exponent of $(\sigma/E_0)^{-8.54}$ (Haddock et al., 2004) which is much higher than Method 1. It is theorised, then, that the FEA presented has a good agreement with predicted porcine fatigue of this particular porcine sample. Further tests would be required to confirm this, however.

Using iterative techniques bone failure under tension to ultimate tensile strength has been validated previously (Adams, 2017). However fatigue of bone and its underlying mechanics is contentious with authors discussing the role that creep plays in fatigue (Bowman et al., 1998; Moore, O'Brien and Gibson, 2004). This makes fatigue difficult to simulate as these assumptions change how fatigue chould be modelled.

In this study, when failure was reached the modulus of the element was reduced by 95%. This leads to bone being modelled as a semi-brittle composite, where only complete failure is modelled. This is in contrast to the literature where it has been observed that the majority of microdamage in trabeculae occurs as cross-hatching (Moore and Gibson, 2002), which is a form a diffuse damage. Fatigue failure of bone may consequently be better described with a gradual reduction in element modulus consistent with diffuse damage.

This has been implemented by Kosmopoulos et al. (Kosmopoulos, Schizas and Keller, 2008). Rather than treating the mechanical properties of bone as a continuum and applying a universal modulus reduction to the failed elements (as in this study), Kosmopoulos et al. used a linear isotropic material over the entire bone volume and applied a variable based modulus reduction. This is problematic. If fatigue of bone cannot by characterised from its intrinsic material properties this limits the use of their finite element method especially when examining other, or combined, methods of failure, especially when the use material mapping is well accepted in the literature (Helgason et al., 2016)

In addition to the assumptions and limitations of the FE models mentioned in section 4.2 modelling fatigue in this study was conducted using models based upon human trabecular bone. It is assumed that at tissue level, porcine bone behaves similarly and that any differences are due to architecture.

The biggest limitation of this study, however, is that there was only one sample available to test the different methods of iterative fatigue. It is not known if the results presented here would be repeated throughout the cohort.

## 4.5 Finite Element Fatigue on Human Vertebral Samples

In section 2.3, apparent modulus for the 10 human vertebral samples showed good agreement with the experimental tests. These 10 samples were analysed using the same iterative FE techniques as in section 2.4.1. They were tested under quasi-static compression at 7 different normalised stresses, from $\sigma/E_0$ = 0.011 to 0.005. All the normalised stress values here are above the theorised fatigue limit for bovine cancellous bone of $\sigma_n = 0.0035$ (Cheng, 1992) The solution was calculated iteratively with failure checking at the end of each load step to degradation in modulus of 10%. They were only tested in one direction, IS, to examine how orientation affects predicted fatigue life.

From previous morphologic analysis of the samples (Table 3-3) there were no significant differences between the samples tested. There were minor differences between the volume fractions of the specimens and a weak trend of decreasing degree of anisotropy with vertebral level (the effects of which on

modelling have been previously discussed in section 4.3.2). Under fatigue, when using a stress failure method, this discrepancy becomes more pronounced as differences in initial modulus have a cascading effect on the failure. As there was little change in experimental and simulated apparent modulus (Table 3-6) the assumption is made that this not significant in this study.

The amount of damage seen in this study is less than within porcine bone (Figure 3-22) at similar normalised stresses (Table 3-8). This is expected because the apparent Young's modulus for the human samples ($E_0$ = 71 to $E_0$ = 382 MPa, Table 3-10) is much lower than the porcine ($E_0$ = 1694 MPa), resulting in lower stresses which causes fewer elements to fail.

The exponent for predicted cycles to failure with normalised stress for method 1 (Table 3-9) – $(\sigma/E_0)^{-5.89}$ is similar to the experimental Porcine in comparison to the experimental at $(\sigma/E_0)^{-7.284}$. This is low compared to $(\sigma/E_0)^{-8.54}$ (Haddock et al., 2004) obtained in the literature from experimental testing of trabecular samples. An explanation for this is that only low cycle fatigue was examined in this study (Table 3-11). This leads to a much lower cycle range which increases the effect of inter specimen scatter inherent in the samples (Table 3-6). Nevertheless, when examining the number of cycles to failure against normalised stress the samples simulated in this study agree with Haddock et al. (Figure 3-27).

Although the predicted number of cycles (Table 3-11) are lower in comparison to the experimental results produced by others in the literature (Dendorfer et al., 2008; Moore and Gibson, 2003b) this can be explained by the differences in testing methodology:

Moore and Gibson (2003b) tested samples to a specified strain under a set normalised stress ($\sigma/E0$=[0.005,0.008]. One set of samples tested at $\sigma/E0$ = 0.008 took 9 cycles to reach a strain of $\varepsilon$ = -1.9%. In this study T11 took 4 cycles, at the same stress level, to reach $\varepsilon$ = -0.9%. As the modulus reduction accelerates steadily for all samples (as in Figure 3 31) it is theorised that that

the number of cycles would be similar for the T11 if the test conditions were the same.

Dendorfer et al. tested until catastrophic failure which, although difficult to quantify using FEA, would result in much longer fatigue lives than seen here.

Using normalised stress creates fatigue life which does not account for the intrinsic differences in mechanical properties between each sample. This is normally the intended effect but it removes vital data when examining orientation in regards to cycles to failure. However, Dendorfer et al. (Dendorfer et al., 2008) claim to see distinct differences in number of cycles to failure with normalised stress. The authors of this paper did not examine the morphometric properties of their samples and this information could explain differences in fatigue life (Lee, O'Brien and Taylor, 2000).

Other researchers have shown a linear relationship between the mechanical stiffness of bone and its damage fraction (Lambers et al., 2013), predicting a Young's modulus reduction of 31% for a DV/BV of 1.5%. This linearity is in agreement with the methods presented here (Table 3-15) but it is dependent on the sample orientation and applied normalised stress.

This is in contrast to the simulations performed on porcine tissue (Figure 3-23), where all the fatigue failure methods exhibited a non-linear response. The porcine samples were stronger, tested under much higher stresses and for a longer time. It is possible that this non-linear performance would become apparent further on in testing of human samples, but under the conditions of this study it was not evident.

The inverse correlation between the regression gradient and normalised stress is expected (Table 3-15). An increase in the regression gradient means that the modulus degradation reduced; as the models are loaded to different stresses and the failure method is stress based.

This study differs to the literature as it also examines different sample orientations. It is in concordance with Dendorfer et al. (Dendorfer, Maier and Hammer, 2008) who examined this phenomenon experimentally. They found

that deviation from the physiological axis has a pronounced effect on the fatigue life of the samples. When looking at the applied rather than normalised stress the role that trabecular orientation plays is much more visible (Figure 3-28), with the samples loaded under full shear (45°) having a much lower tolerance to stress than those at 0°. The samples were obtained from the spine of an elderly female. They showed large degrees of anisotropy (Table 3-3), which is known to reduce the fatigue life (Dendorfer, Maier and Hammer, 2008).

Small amounts of microdamage have been theorised to have a noticeable effect on the apparent strength of bone (Morgan, Yeh and Keaveny, 2005). This is discernible when examining sample L4L (Table 3-15 ) which reaches a 10% reduction in modulus with very little damage (0.02% at $\sigma/E_0 = 0.006$). this is further highlighted in Table 3-14 where samples were grouped by angle with the highest gradient at 45°

Although the simulations presented here took a long time to complete (approximately 28 days elapsed time), in the real world the number of cycles seen here is considered low-cycle fatigue. Further simulations at lower normalised stresses for longer cycles are required to see if this model predicts trabecular failure at high-cycle fatigue.

Non-linear behaviour in modulus degradation was already visible for T10 at $\sigma/E_0 = 0.005$ (Figure 3-29). The fatigue method used is based on a log relationship between cycle number and stress, therefore an asymptote does exist by which failure would no longer occur. This would be highly dependent on the sample simulated and time consuming to characterise.

This work is currently not validated and it remains to be seen whether this method for predicting trabecular fatigue failure is accurate enough in comparison to a more advanced model (Kosmopoulos, Schizas and Keller, 2008). Stress based models are also heavily dependent on the inherent material properties of the sample (Keaveny and Hayes, 1993), but in this study it showed good agreement with the described experimental behaviour of cancellous bone.

To create accurate finite-element models the model has to be morphologically as well as materially alike to the sample it represents (Wilcox, 2007). Convergence studies examining the effect of thresholding and assigned material values in this model should also be conducted to ensure the assumptions made during model generation are correct.

Using a two-phase semi-brittle fatigue model, the FEA present in this study corresponds to the theory in the literature: at the apparent level fatigue damage manifests as a degradation of material strength (Hambli et al., 2016; Taylor, Cotton and Zioupos, 2002).

This study proposes a stress based fatigue failure criteria based on the work of Choi and Goldstein (1992). Instead of approximating the effects of microdamage over the sample it examines, in detail, damage of the internal trabecular structure caused by fatigue. This resulted in an accurate representation of the porcine core tested.

# 5 CONCLUSION

Qualitative research has shown links between occupational exposure to WBV and LBP. However, the general incidence of LBP and related musculoskeletal disorders within people not exposed to vibration remains very high.

Operators of marine craft are of particularly high risk due to the extreme exposures to vibration (Gollwitzer and Peterson, 1995) with impacts on relatively calm seas at 6g. Low body injuries are often described from these events and a review of US Navy Special Boat Operators (Ensign et al., 2000) identified the lower back as the most common injury site.
The British Navy has received a derogation from the CVWR (Navy Command Secretariat FOI Section, 2016) which is valid until the 6$^{th}$ of July 2020. The official state is that *"No maritime user of these types of craft can currently meet the ELV set out in this legislation"*. This is with the higher limits stipulated in the CVWR as opposed to the standards they are based off.

Seat design has mostly been the focus of mitigating severe vibration into the spine, but there is little evidence to support that improvements in seat design (Lines and Stayner, 1999) would have any effect in reducing incidence of LBP. There is a need for a more ergonomic design of boats, especially in regards to the differences in stature between operators (Dobbins, Rowley and Campbell, 2008). Posture has shown to have a large effect on the fatigue life of the human spine (Gooyers et al., 2012; Huber et al., 2010). If it can be corrected during operation of HSC the incidents of spinal injury is theorised to decrease.

There are still issues in military culture about reporting physical ailments; most personnel see LBP as an occupational risk (Carragee and Cohen, 2009). If this were to change, a more accurate state of LBP within HSC operators might be seen.

The limits set forth in the ISO standards and the regulations (British Standards Institution, 1987; European Parliament, 2002; ISO, 1997, 2004; Maritime and Coastguard Agency, 2007a; Regulations, 2005) are based on qualitative comfort assessment with the idea that uncomfortable vibration causes damage

in the spine. These statistics in general are averaging techniques (RMS, VDV) which seek to quantify exposure level. When examining these statistics as damage predictors, the $4^{th}$ order methods were shown to be more sensitive to minute differences in vibration which improved its capability (section 4.1).

Exploratory studies need to be conducted before increasing the model complexity. Trabecular tissue was examined for these studies into LBP and spinal failure because as the loading rate increases, failure occurs more often within vertebral body. This has been both anecdotally (Branch, 2009) as well as in-vitro (Yingling, Callaghan and McGill, 1997). This study was conducted in-vitro, whereas in-vivo there are significant differences in the behaviour of bone: such as remodelling; regrowth and force interactions within the spine.

Spinal injury is difficult to predict in-vivo due to this. Examination of the spine is typically done after injury has occurred so there is little information on which to build a prediction model from. This is coupled with the fact that currently commercial CT systems for clinical use scan at approximately 500μm (Burghardt, Link and Majumdar, 2011) which is not sufficient enough to currently predict vertebral collapse through direct simulation nor is it detailed enough to determine the exact failure method.

There is little known about the mechanical properties of trabecular bone at the tissue level, mostly due to the complexities of working at such a small scale. A reduction in computational complexity of finite element studies is needed, particularly while performing direct fatigue simulations. The methods put forth in 4.5 does this to an extent. It currently simulates microdamage of trabecular bone rather than directly simulating it on an element by element basis. It also describes most of the bone behaviour over the entire sample. Chief of which being apparent modulus for human samples (section 4.3.2). This is evident in the studies provided in 2.2, 2.3, 2.4 and 2.5, where the predicted fatigue of human trabecular tissue shows good agreement with the experimental results (Haddock et al., 2004).

The vibrations calculated from the porcine study (Section 3.1) must be considered as coming from a much larger vibration source than what is seen in

the real world. The vibrations are high according to RMS and $VDV_{exp}$ considering this is recorded in a trabecular core. The forces at the vertebral endplates would be higher to achieve those internal forces. This is also true when taking into account natural body damping (due to muscle and fat), as well as seat cushion damping.

Although the damage examined is therefore not representative of low vibrational exposure, the methods presented in here (section 2) describe a robust and repeatable method for the calculation of the mechanical properties of bone and sample specific fatigue properties, which can be used to calculate the damage caused by a stimulus such as vibration exposure from a sea craft.

The fatigue FEA on human trabecular cores presented here shows the development of bone damage through direct numerical simulations. The models also show the effect that angular orientation has on not just the apparent modulus but on its predicted fatigue life as well. This is of importance when examining the role that posture plays in spinal damage (Gallagher et al., 2005; Gooyers et al., 2012). Without a further validation study, however, it is difficult to know how accurate these predictions are.

When putting fatigue failure into context of a living human, even the more accurate methods (Kosmopoulos, Schizas and Keller, 2008) fail to take bone remodelling into account, If the mechanostat theorem (Frost, 2004) holds true then the very strains within the bone which lead to failure in simulations could actually help in promoting bone growth and improving fatigue life. Simulation of bone remodelling is not well understood (McNamara and Prendergast, 2007) and combining it with fatigue testing is computationally prohibitive.

A combined model that accurately describes bone is beyond the realm of current technology: None of the techniques encountered which simulate fatigue take into account the visco-elasticity of bone; none of the whole spinal simulations take into account the minute trabecular deformation which ensues. What is needed is a model which is “good enough” in terms of accuracy and computation costs for the damage mode simulated.

Although these models might soon exist, they will undoubtedly be based on laboratory tests; the questions remains about how this translates into the human body and failure within it (Seref-Ferlengez, Kennedy and Schaffler, 2015). No two human vertebrae are the same and the same question still remains: what level of damage is too much?

# 6 FURTHER WORK

There already exists a large body of work examining the cyclic fatigue limits of spinal segments (Brinckmann et al., 1987; Hansson, Keller and Spengler, 1987; Huber et al., 2010; Yalla and Campbell-Kyureghyan, 2010). If the displacement data for these tests remain, the methods detailed in this thesis could be used as a basis for examining fatigue failure in terms of the vibrational statistics in the literature.

A report examining the vibration directive 2002/44/EC highlighted the expense of vibration measurement equipment to the employer (Donati et al., 2008) and a need to bring these costs down. Modernisation of vibration equipment has meant miniaturisation of data logging equipment allowing for tests to be obtained in the field with accuracy and at lower cost to the researcher (Mansfield, Huang and Thirulogasingam, 2016). Studies designed around the use of these accelerometers could lead to data which is exposure specific rather than vehicle specific. This could make a more comprehensive link between an individual's exposure to WBV and damage within the spine.

The tests in the literature and conducted in the studies examined here have been largely performed under a fixed frequency; further research into the effects of frequency on spinal fatigue (and thus, LBP) should be examined. The fatigue method discussed in this thesis should also be validated further to see if its predictions are accurate over a larger sample set.

Other researchers have shown promising results in eliminating the inaccuracy of boundary conditions using digital volume correlation (Chen et al., 2017) and mapping the strain to FE models. This technique has severe restrictions in regards to boundary conditions (only stepped compression was performed) as well as radiation dose (all samples were tested while in a Micro-CT system). With improvements in CT scanning equipment, which theoretically has the capability to reduce radiation dose and increase scanning resolution, these restrictions may be lifted (Kitchen et al., 2017; Nesterets, Gureyev and Dimmock, 2018).

Developments in the field of computed tomography as mentioned above would also allow in-vivo characterisation of trabecular bone, allowing for the prediction of fatigue failure and go towards a more general understanding of spinal mechanics.

There are two directions that FEA of spinal tissue is going: resource intensive specific models and improving the accuracy of spinal prediction in generalised models. The results presented in sections 3.2 to 3.4 focus on high fidelity sample specific FEA however there is room for further improvement.

The usage of finite element modelling in describing fatigue failure is improving. Kosmopoulos et al. (Kosmopoulos, Schizas and Keller, 2008) describe an element by element method to model fatigue failure in trabecular bone which holds promise, but is very resource intensive. Another promising model improving the accuracy of fatigue failure is known as FEEBE (Finite Element, Element-By-Element) (Harrison et al., 2013) which has a similar design philosophy as that of Kosmopoulos but using proprietary code. Although Neural networks are currently in vogue, they should be treated with the utmost of caution. Neural networks, and by extension machine learning, are hampered by a lack of repeatability (Hutson, 2018) which is inherent in the technique and disastrous for any scientific study unless explained in full detail.

Ayari et al. (2009) describes FE models which examine the damage of the spine in terms of vibration, and modal response. There is also the burgeoning field of multiscale modelling which hopes to improve the understanding between the micro and macro-scale FE models (Hambli and Hattab, 2013; Johnson and Troy, 2017) as well as the multi-sim project at the Insigneo “institute for in silico Medicine” group at Sheffield University.

# 7 REFERENCES


Ackerman, W.E. and Ahmad, M. (2000) Lumbar spine pain originating from vertebral osteophytes *Regional Anesthesia and Pain Medicine*. Available at: 10.1016/S1098-7339(00)90025-7 (Accessed: 20 October 2017).

Adams, G.J. (2017) *Quality Factors at the Material and Structural Level that affect the Toughness of Human Cancellous Bone*. Cranfield University.

Adams, M. A and Hutton, W.C. (1980) 'The effect of posture on the role of the apophysial joints in resisting intervertebral compressive forces.', *The Journal of bone and joint surgery. British volume*, 62–B(3), pp. 358–362.

Adams, M. A and Hutton, W.C. (1985) 'The effect of posture on the lumbar spine', *J Bone Joint Surg Br*, 67(4), pp. 625–629.

Adams, M.A. and Hutton, W.C. (1983a) 'The Effect of Posture on the Fluid Content of Lumbar Intervertebral Discs', *Spine*, 8(6) Harper & Row, pp. 665–671.

Adams, M.A. and Hutton, W.C. (1983b) 'The Mechanical Function of the Lumbar Apophyseal Joints.', *Spine*, 8(3)

Adams, M.A., May, S., Freeman, B.J.C., Morrison, H.P. and Dolan, P. (2000) 'Effects of Backward Bending on Lumbar Intervertebral Discs: Relevance to Physical Therapy Treatments for Low Back Pain', *Spine*, 25(4)

Adams, M.A., McNally, D.S., Chinn, H. and Dolan, P. (1994) 'The clinical biomechanics award paper 1993 Posture and the compressive strength of the lumbar spine', *Clinical Biomechanics*, 9(1) Elsevier, pp. 5–14. Available at: 10.1016/0268-0033(94)90052-3 (Accessed: 16 October 2017).

Alem, N. (2005) 'Application of the new ISO 2631-5 to health hazard assessment of repeated shocks in U.S. Army vehicles.', *Industrial health*, 43(3), pp. 403–412.

Alkherayf, F. and Agbi, C. (2009) 'Cigarette smoking and chronic low back pain in the adult population.', *Clinical and investigative medicine. Médecine clinique et experimentale*, 32(5), pp. E360-7. Available at: http://www.ncbi.nlm.nih.gov/pubmed/19796577 (Accessed: 25 August 2017).

Allen, D.P., Taunton, D.J. and Allen, R. (2008) 'A study of shock impacts and vibration dose values onboard high-speed marine craft', *Transactions of the Royal Institution of Naval Architects Part A: International Journal of Maritime Engineering*, 150, pp. 1–10.

Andersen, J.H., Haahr, J.P. and Frost, P. (2011) 'Details on the association between heavy lifting and low back pain.', *The spine journal : official journal of the North American Spine Society*, 11(7) Elsevier Inc., pp. 690-1; author reply 691-2. Available at: 10.1016/j.spinee.2011.04.018 (Accessed: 6 October 2014).

Andersson, G.B. (1999) 'Epidemiological features of chronic low-back pain', *The Lancet*, 354(9178), pp. 581–585.

Ayari, H., Thomas, M., Doré, S., Taiar, R. and Dron, J.P. (2009) 'Predicting the Adverse Health Effects To Long Term Whole-Body Vibration Exposure', *Spine*, (January), pp. 1–19.

Ayotte, D.C., Ito, K., Perren, S.M. and Tepic, S. (2000) 'Direction-dependent constriction flow in a poroelastic solid: the intervertebral disc valve.', *Journal of biomechanical engineering*, 122(6), pp. 587–593.

Ayotte, D.C., Ito, K. and Tepic, S. (2001) 'Direction-dependent resistance to flow in the endplate of the intervertebral disc: An ex vivo study', *Journal of Orthopaedic Research*,

19(6), pp. 1073–1077. Available at: 10.1016/S0736-0266(01)00038-9 (Accessed: 5 July 2017).

Azaroff, L.S., Levenstein, C. and Wegman, D.H. (2002) 'Occupational injury and illness surveillance: Conceptual filters explain underreporting', *American Journal of Public Health*, 92(9), pp. 1421–1429.

Baillargeon, J. (2001) 'Characteristics of the healthy worker effect.', *Occupational medicine (Philadelphia, Pa.)*, 16(2), pp. 359–66. Available at: http://www.ncbi.nlm.nih.gov/pubmed/11319057 (Accessed: 14 November 2014).

Barak, M.M., Lieberman, D.E. and Hublin, J.J. (2011) 'A Wolff in sheep's clothing: Trabecular bone adaptation in response to changes in joint loading orientation', *Bone*, 49(6) Elsevier Inc., pp. 1141–1151.

Basquin, O.H. (1910) 'The Exponential Law of Endurance Tests', *American Society for Testing and Materials Proceedings*, 10, pp. 625–630.

Battié, M.C., Videman, T., Levalahti, E., Gill, K. and Kaprio, J. (2007) 'Heritability of low back pain and the role of disc degeneration.', *Pain*, 131(3), pp. 272–80. Available at: 10.1016/j.pain.2007.01.010 (Accessed: 7 October 2014).

Baumann, A.P., Shi, X., Roeder, R.K. and Niebur, G.L. (2016) 'The sensitivity of nonlinear computational models of trabecular bone to tissue level constitutive model.', *Computer methods in biomechanics and biomedical engineering*, 19(January), pp. 465–73.

Bayraktar, H.H., Morgan, E.F., Niebur, G.L., Morris, G.E., Wong, E.K. and Keaveny, T.M. (2004) 'Comparison of the elastic and yield properties of human femoral trabecular and cortical bone tissue', *Journal of Biomechanics*, 37, pp. 27–35.

Beach, T.A.C., Parkinson, R.J., Stothart, J.P. and Callaghan, J.P. (2005) 'Effects of prolonged sitting on the passive flexion stiffness of the in vivo lumbar spine', *Spine Journal*, 5(2), pp. 145–154.

Beckstein, J.C., Sen, S., Schaer, T.P., Vresilovic, E.J. and Elliott, D.M. (2008) 'Comparison of Animal Discs Used in Disc Research to Human Lumbar Disc', *Spine*, 33(6), pp. E166–E173. Available at: 10.1097/BRS.0b013e318166e001 (Accessed: 6 December 2017).

Boden, S.D., McCowin, P.R., Davis, D.O., Dina, T.S., Mark, A.S. and Wiesel, S. (1990) 'Abnormal magnetic-resonance scans of the cervical spine in asymptomatic subjects. A prospective investigation.', *JBJS*, 72(8)

Boileau, P.-E., Turcot, D. and Scory, H. (1989) 'Evaluation of whole-body vibration exposure using a fourth power method and comparison with ISO 2631', *Journal of Sound and Vibration*, , pp. 143–154.

Boivin, G., Bala, Y., Doublier, A., Farlay, D., Ste-Marie, L.G., Meunier, P.J. and Delmas, P.D. (2008) 'The role of mineralization and organic matrix in the microhardness of bone tissue from controls and osteoporotic patients', *Bone*, 43(3), pp. 532–538.

Bollinger, M.J., Schmidt, S., Pugh, J.A., Parsons, H.M., Copeland, L.A. and Pugh, M.J. (2015) 'Erosion of the healthy soldier effect in veterans of US military service in Iraq and Afghanistan', *Population Health Metrics*, 13(1), p. 8.

Borenstein, D. (2004) 'Does osteoarthritis of the lumbar spine cause chronic low back pain?', *Current pain and headache reports*, 8(6) Current Medicine Group, pp. 512–517. Available at: 10.1007/s11916-004-0075-z (Accessed: 20 October 2017).

Bovenzi, M. and Betta, A. (1994) 'Low-back disorders in agricultural tractor drivers exposed to whole-body vibration and postural stress', *Applied Ergonomics*, 25(4), pp. 231–241.

Bovenzi, M. and Hulshof, C.T. (1999) 'An updated review of epidemiologic studies on the relationship between exposure to whole-body vibration and low back pain (1986-1997)', *Int.Arch.Occup.Environ.Health*, 72(0340–0131 SB–IM), pp. 351–365.

Bowman, S.M., Guo, X.E., Cheng, D.W., Keaveny, T.M., Gibson, L.J., Hayes, W.C. and McMahon, T. a (1998) 'Creep contributes to the fatigue behavior of bovine trabecular bone.', *Journal of biomechanical engineering*, 120(5), pp. 647–654.

Branch, M.A.I. (2009) *Celtic Pioneer Report No 11/2009*.

Brinckmann, P., Johannleweling, N., Hilweg, D. and Biggemann, M. (1987) 'Fatigue fracture of human lumbar vertebrae', *Clinical Biomechanics*, 2(2), pp. 94–96.

Brinjikji, W., Luetmer, P.H., Comstock, B., Bresnahan, B.W., Chen, L.E., Deyo, R.A., Halabi, S., Turner, J.A., Avins, A.L., James, K., Wald, J.T., Kallmes, D.F. and Jarvik, J.G. (2015) 'Systematic literature review of imaging features of spinal degeneration in asymptomatic populations', *American Journal of Neuroradiology*, 36(4), pp. 811–816.

Brinkley, J.W. and Shaffer, J.T. (1971) *Dynamic Simulation Techniques for the Design of Escape Systems: Current Applications and Future Air Force Requirements*. Wright-Patterson Air Force Base, Ohio.

British Standards Institution (1987) *BS 6841 - Guide to Measurement and evaluation of human exposure to whole-body mechanical vibration and repeated shock*.

Buchbinder, R., Blyth, F.M., March, L.M., Brooks, P., Woolf, A.D. and Hoy, D.G. (2013) 'Placing the global burden of low back pain in context.', *Best practice & research. Clinical rheumatology*, 27(5) Elsevier Ltd, pp. 575–89. Available at: 10.1016/j.berh.2013.10.007 (Accessed: 3 August 2014).

Burghardt, A.J., Link, T.M. and Majumdar, S. (2011) 'High-resolution computed tomography for clinical imaging of bone microarchitecture', *Clinical Orthopaedics and Related Research*, 469(8), pp. 2179–2193.

Burke, G.L. (1964) *Backache from Occiput to Coccyx*. W.E.G. MacDonald.

Carragee, E.J. and Cohen, S.P. (2009) 'Lifetime Asymptomatic for Back Pain The Validity of Self-report Measures in Soldiers', *Spine*, 34(9), pp. 978–983. Available at: 10.1097/BRS.0b013e318198d517 (Accessed: 26 September 2017).

Carter, D.R. and Hayes, W.C. (1977) 'The compressive behavior of bone as a two-phase porous structure', *The Journal of bone and joint surgery. American volume*, 59, pp. 954–962.

Chen, Y., Dall'Ara, E., Sales, E., Manda, K., Wallace, R., Pankaj, P. and Viceconti, M. (2017) 'Micro-CT based finite element models of cancellous bone predict accurately displacement once the boundary condition is well replicated: A validation study', *Journal of the Mechanical Behavior of Biomedical Materials*, 65(September 2016) Elsevier, pp. 644–651.

Cheng, D.W.-H. (1992) '*Compressive High Cycle at Low Strain Fatigue Behavior of Bovine Trabecular Bone*'. Massachusetts institute of technology.

Cheng, K.; and Hu (2010) 'Mechanical Properties of Intervertebral Discs from Symptomatic and Asymptomatic Patients', *56th Annual Meeting of the Orthopaedic Research Society*. Available at: http://www.ors.org/Transactions/56/0010.pdf (Accessed: 4 July 2017).

Cheung, B. and Nakashima, A. (2006) '*A review on the effects of frequency of oscillation on motion sickness*', (October). DRDC Toronto TR 2006-229.

Cheung, K.M.C., Karppinen, J., Chan, D., Ho, D.W.H., Song, Y.-Q.Q., Sham, P., Cheah, K.S.E., Leong, J.C.Y. and Luk, K.D.K. (2009) 'Prevalence and pattern of lumbar magnetic resonance imaging changes in a population study of one thousand forty-three individuals', *Spine*

*(Phila Pa 1976)*, 34(9), pp. 934–940.

Chevalier, Y., Pahr, D., Allmer, H., Charlebois, M. and Zysset, P. (2007) 'Validation of a voxel-based FE method for prediction of the uniaxial apparent modulus of human trabecular bone using macroscopic mechanical tests and nanoindentation', *Journal of Biomechanics*, 40(15), pp. 3333–3340.

Choi, K. and Goldstein, S.A. (1992) 'A comparison of the fatigue behavior of human trabecular and cortical bone tissue', *Journal of Biomechanics*, 25(12), pp. 1371–1381.

Coe, T., Xing, J.T. and Shenoi, R. a (2010) 'A human body model for dynamic response analysis of an integrated human-seat-controller-high speed marine craft interaction system', *41st United Kingdom Group Meeting on Human Reponses to Vibration*., pp. 20–22.

Coltman, J.W., Van Ingen, C., Johnson, N.B. and Zimmermann, R.E. (1989) *Aircraft Crash Survival Design Guide Volume II- Aircraft Design Crash Impact Conditions and Human Tolerance*. Pheonix, Arizona.

Comstock, G.W. (1975) 'Effects of selection on mortality', *American Journal of Epidemiology*, 102(3), p. 263.

Corbridge, C. and Griffin, M.J. (1986) 'Vibration and comfort: vertical and lateral motion in the range 0.5 to 5.0 Hz.', *Ergonomics*, 29(2) Taylor & Francis, pp. 249–72. Available at: 10.1080/00140138608968263 (Accessed: 20 November 2014).

Cotton, J.R., Winwood, K., Zioupos, P. and Taylor, M. (2005) 'Damage Rate is a Predictor of Fatigue Life and Creep Strain Rate in Tensile Fatigue of Human Cortical Bone Samples', *Journal of Biomechanical Engineering*, 127(2), p. 213.

Crock, H. V and Goldwasser, M. (1984) 'Anatomic studies of the circulation in the region of the vertebral end-plate in adult Greyhound dogs.', *Spine*, 9(7), pp. 702–706.

Dagenais, S., Roffey, D.M. and Wai, E.K. (2010) 'Reply', *The Spine Journal*, 10(10), pp. 944–945. Available at: 10.1016/j.spinee.2010.08.001 (Accessed: 6 October 2014).

Dagenais, S., Roffey, D.M. and Wai, E.K. (2011) 'Reply', *The Spine Journal*, 11(2), pp. 165–166. Available at: 10.1016/j.spinee.2010.11.018 (Accessed: 3 December 2014).

Dar, G., Masharawi, Y., Peleg, S., Steinberg, N., May, H., Medlej, B., Peled, N. and Hershkovitz, I. (2010) 'Schmorl's nodes distribution in the human spine and its possible etiology', *European Spine Journal*, 19(4) Springer-Verlag, pp. 670–675. Available at: 10.1007/s00586-009-1238-8 (Accessed: 8 September 2017).

Dendorfer, S., Maier, H.J. and Hammer, J. (2008) 'How do anisotropy and age affect fatigue and damage in cancellous bone?', *Stud Health Technol Inform.*, (133), pp. 68–74.

Dendorfer, S., Maier, H.J., Taylor, D. and Hammer, J. (2008) 'Anisotropy of the fatigue behaviour of cancellous bone', *Journal of Biomechanics*, 41, pp. 636–641.

Deyo, R.A. and Bass, J.E. (1989) 'Lifestyle and low-back pain. The influence of smoking and obesity.', *Spine*, 14(5), pp. 501–6. (Accessed: 25 August 2017).

DIN (2016) *DIN 50106: Testing of Metallic Materials*.

Ding, M., Dalstra, M., Danielsen, C.C., Kabel, J., Hvid, I. and Linde, F. (1997) 'Age variations in the properties of human tibial trabecular bone.', *The Journal of bone and joint surgery. British volume*, 79(6), pp. 995–1002. Available at: 10.1080/000164700753749791 (Accessed: 22 September 2017).

Ding, M., Odgaard, A., Linde, F. and Hvid, I. (2002) 'Age-related variations in the microstructure of human tibial cancellous bone', *Journal of Orthopaedic Research*, 20(3), pp. 615–621.

Djurasovic, M., Glassman, S.D., Carreon, L.Y. and Dimar, J.R. (2010) Contemporary Management of Symptomatic Lumbar Spinal Stenosis *Orthopedic Clinics of North America*. Elsevier, Available at: 10.1016/j.ocl.2009.12.003 (Accessed: 18 October 2017).

Dobbins, T., Rowley, I. and Campbell, L. (2008) *High Speed Craft Human Factors Engineering Design Guide*. Chichester.

Donati, P., Schust, M., Szopa, J., Starck, J., Iglesias, E.G., Senovilla, L.P., Fisher, S., Flaspöler, E., Reinert, D. and Op d Beeck, R. (2008) *Workplace exposure to vibration in Europe: an expert review*. European Agency for Safety and Health at Work.

Doube, M., Klosowski, M.M., Arganda-Carreras, I., Cordelières, F.P., Dougherty, R.P., Jackson, J.S., Schmid, B., Hutchinson, J.R. and Shefelbine, S.J. (2010) 'BoneJ: Free and extensible bone image analysis in ImageJ', *Bone*, 47(6), pp. 1076–1079.

Dunlop, R.B., Adams, M.A. and Hutton, W.C. (1984) 'Disc space narrowing and the lumbar facet joints.', *The Journal of bone and joint surgery. British volume*, 66(5), pp. 706–10.

Dupuis, H. and Zerlett, G. (1987) 'Whole-body vibration and disorders of the spine.', *International archives of occupational and environmental health*, 59(4), pp. 323–36. Available at: http://www.ncbi.nlm.nih.gov/pubmed/3497111 (Accessed: 25 March 2015).

Duthey, B. (2013) 'Priority Medicines for Europe and the World " A Public Health Approach to Innovation " Update on 2004 Background Paper Background Paper 6 . 24 Low back pain', *WHO*, (March)

EN/ISO, B. (1997) *ISO 266: Acoustics - Preferred frequencies*. International Organization for Standardization, Geneva, Switzerland.

Ensign, W., Hodgdon, J.A., Prusaczyk, W.K., Ahlers, S., Shapiro, D. and Lipton, M. (2000) *A Survey of Self-reported Injuries among Special Boat Operators*. San Diego.

Ernat, J., Knox, J., Orchowski, J. and Owens, B. (2012) 'Incidence and Risk Factors for Acute Low Back Pain in Active Duty Infantry', *Military Medicine*, 177(11), pp. 1348–1351.

European Parliament (2002) 'Directive 2002/44/EC of the European parliament and of the Council of 25 June 2002 on the minimum health and safety requirements regarding the exposure of workers to the risks arising from physical agents (vibration)', *Official Journal of the European Communities*, L 177(10), pp. 13–19.

European Parliament (2010) 'Directive 2010/63/EU of the European Parliament and of the Council of 22 September 2010 on the protection of animals used for scientific purposes.', *Official Journal of the European Union*, L 276, pp. 33–79.

Ewald, C., Walter, J. and Waschke, A. (2016) 'Degenerative lumbale Spinalkanalstenose', *Chirurgische Praxis*, 81(4), pp. 659–666.

Fairley, T. and Griffin, M. (1989) 'The apparent mass of the seated human body: Vertical vibration', *J Biomech*, 22(2) Elsevier, pp. 81–94. Available at: 10.1016/0021-9290(89)90031-6 (Accessed: 22 November 2017).

Fehlings, M.G., Tetreault, L., Nater, A., Choma, T., Harrop, J., Mroz, T., Santaguida, C. and Smith, J.S. (2015) 'The aging of the global population: The changing epidemiology of disease and spinal disorders', *Neurosurgery*, 77(4), pp. S1–S5.

Fennell, A., Jones, A.P. and Hukins, D.W.L. (1996) 'Migration of the Nucleus Pulposus Within the Intervertebral Disc During Flexion and Extention of the Spine', *Spine*, 21(23), pp. 2753–2757. Available at: http://journals.lww.com/spinejournal/Abstract/1996/12010/Migration_of_the_Nucleus_Pulposus_Within_the.9.aspx (Accessed: 13 October 2017).

Fishbein, W.I. and Salter, L.C. (1950) 'The Relationship between Truck and Traetor Driving and Disorders of the Spine and Supporting Structures-Report of a Survey.', *Industrial Medicine and Surgery*, 19(9) Chicago., pp. 444–445.

Forwood, M.R. and Burr, D.B. (1993) 'Physical activity and bone mass: exercises in futility?', *Bone and mineral*, 21(2), pp. 89–112. Available at: http://www.ncbi.nlm.nih.gov/pubmed/8358253 (Accessed: 12 October 2017).

Fritz, M., Fischer, S. and Bröde, P. (2005) 'Vibration induced low back disorders--comparison of the vibration evaluation according to ISO 2631 with a force-related evaluation.', *Applied ergonomics*, 36(4), pp. 481–8. Available at: 10.1016/j.apergo.2005.01.008 (Accessed: 25 March 2015).

Frost, H.M. (1964) *The laws of bone structure.* Springfield, Ill.: C.C. Thomas.

Frost, H.M. (2001) 'From Wolff's law to the Utah paradigm: Insights about bone physiology and its clinical applications', *Anatomical Record*, 262(4), pp. 398–419.

Frost, H.M. (2004) 'A 2003 update of bone physiology and Wolff's law for clinicians', *Angle Orthodontist*, 74(1), pp. 3–15.

Frymoyer, J.W., Pope, M.H., Clements, J.H., Wilder, D.G., MacPherson, B. and Ashikaga, T. (1983) 'Risk factors in low-back pain. An epidemiological survey.', *Journal of Bone and Joint Surgery - Series A.*, 65(2), pp. 213–218. Available at: https://www.scopus.com/record/display.uri?eid=2-s2.0-0020681117&origin=resultslist&sort=cp-f&src=s&st1=%22back+pain%22+AND+smoking&nlo=&nlr=&nls=&sid=cec552e5b8c0e2cb02403632fc8cab99&sot=b&sdt=b&sl=38&s=TITLE-ABS-KEY%28%22back+pain%22+AND+smoking%29&relpo (Accessed: 25 August 2017).

Fujiwara, A., Lim, T.-H., An, H.S., Tanaka, N., Jeon, C.-H., Andersson, G.B.J. and Haughton, V.M. (2000) 'The Effect of Disc Degeneration and Facet Joint Osteoarthritis on the Segmental Flexibility of the Lumbar Spine', *Spine*, 25(23), pp. 3036–3044.

Gallagher, S., Marras, W.S., Litsky, A.S. and Burr, D. (2005) 'Torso flexion loads and the fatigue failure of human lumbosacral motion segments.', *Spine*, 30, pp. 2265–2273.

Ganguly, P., Moore, T.L.A. and Gibson, L.J. (2004) 'A phenomenological model for predicting fatigue life in bovine trabecular bone', *Journal of Biomechanical Engineering*, 126(3), pp. 330–339.

Garme, K., Burstrom, L. and Kuttenkeuler, J. (2011) 'Measures of vibration exposure for a high-speed craft crew', *Proceedings of the Institution of Mechanical Engineers, Part M: Journal of Engineering for the Maritime Environment*, 225(4), pp. 338–349.

Gauntlett-Gilbert, J. and Wilson, S. (2013) 'Veterans and chronic pain', *British Journal of Pain*, 7(2), pp. 79–84.

Gellhorn, A.C., Katz, J.N. and Suri, P. (2013) 'Osteoarthritis of the spine: the facet joints.', *Nature Publishing Group*, 9(4), pp. 216–224.

Von Gierke, H.E. (1975) 'The ISO Standard Guide for the Evaluation of Human Exposure to Whole-Body Vibration', *Society of Automotive Engineers*

Giers, M.B., Munter, B.T., Eyster, K.J., Ide, G.D., Newcomb, A.G.U.S., Lehrman, J.N., Belykh, E., Byvaltsev, V.A., Kelly, B.P., Preul, M.C. and Theodore, N. (2017) 'Biomechanical and Endplate Effects on Nutrient Transport in the Intervertebral Disc', *World Neurosurgery*, 99 Elsevier Inc, p. e39.

Goff, M.G., Lambers, F.M., Nguyen, T.M., Sung, J., Rimnac, C.M. and Hernandez, C.J. (2015) 'Fatigue-induced microdamage in cancellous bone occurs distant from resorption cavities

and trabecular surfaces', *Bone*, 79 Elsevier Inc., pp. 8–14.

Golding, J.F., Mueller, A.G. and Gresty, M.A. (2001) 'A motion sickness maximum around the 0.2 Hz frequency range of horizontal translational oscillation.', *Aviation, space, and environmental medicine*, 72(3), pp. 188–92. Available at: http://www.ncbi.nlm.nih.gov/pubmed/11277284 (Accessed: 17 November 2014).

Goldstein, S.A., Goulet, R. and McCubbrey, D. (1993) 'Measurement and significance of three-dimensional architecture to the mechanical integrity of trabecular bone', *Calcified Tissue International*, 53(1 Supplement)

Gollwitzer, R.M. and Peterson, R.S. (1995) *Repeated water entry shocks on High-Speed Planing Boats*. Panama City, Florida.

Gooyers, C.E., McMillan, R.D., Howarth, S.J. and Callaghan, J.P. (2012) 'The Impact of Posture and Prolonged Cyclic Compressive Loading on Vertebral Joint Mechanics', *Spine*, 37(17), pp. E1023–E1029.

Griefahn, B. and Bröde, P. (1999) 'The significance of lateral whole-body vibrations related to separately and simultaneously applied vertical motions. A validation study of ISO 2631', *Applied Ergonomics*, 30, pp. 505–513.

Griffin, M.J. (1990) *Handbook of Human Vibration*. Academic Press. Available at: http://books.google.com/books?id=-_JV63L6RMcC&pgis=1 (Accessed: 7 October 2014).

Griffin, M.J. (1976) 'Subjective equivalence of sinusoidal and random whole-body vibration', *The Journal of the Acoustical Society of America*, 60(5) Acoustical Society of America, p. 1140. Available at: 10.1121/1.381215 (Accessed: 20 November 2014).

Griffin, M.J. (1980) 'Discomfort produced by impulsive whole-body vibration', *The Journal of the Acoustical Society of America*, 68(5) Acoustical Society of America, p. 1277. Available at: 10.1121/1.385121 (Accessed: 20 November 2014).

Griffin, M.J. (1998) 'A Comparison of standardised methods for predicting the hazards of whole-body vibration and repeated shocks', *Journal of Sound and Vibration*, 215, pp. 883–914.

Groessl, E.J., Weingart, K.R., Aschbacher, K., Pada, L. and Baxi, S. (2008) 'Yoga for Veterans with Chronic Low-Back Pain', *The Journal of Alternative and Complementary Medicine*, 14(9), pp. 1123–1129.

Guldberg, R.E., Hollister, S.J. and Charras, G.T. (1998) 'The Accuracy of Digital Image-Based Finite Element Models', *Journal of Biomechanical Engineering*, 120(2), p. 289.

Guo, X.E., McMahon, T.A., Keaveny, T.M., Hayes, W.C. and Gibson, L.J. (1994) 'Finite element modeling of damage accumulation in trabecular bone under cyclic loading.', *Journal of biomechanics*, 27(2), pp. 145–55. Available at: http://www.ncbi.nlm.nih.gov/pubmed/8132682 (Accessed: 3 January 2018).

Haddock, S.M., Yeh, O.C., Mummaneni, P. V., Rosenberg, W.S. and Keaveny, T.M. (2004) 'Similarity in the fatigue behavior of trabecular bone across site and species', *Journal of Biomechanics*, 37, pp. 181–187.

Haddock, S.M., Yeh, O.C., Mummaneni, P.M., Rosenberg, W.S. and Keaveny, T.M. (2000) 'Fatigue behavior of human vertebral trabecular bone', *46th Annual Meeting, Orthopaedic Research Society, March 12-15, 2000, Orlando, Florida*

Hamanishi, C., Kawabata, T., Yosii, T. and Tanaka, S. (1994) 'Schmorl's Nodes on Magnetic Resonance Imaging: Their Incidence and Clinical Relevance.', *Spine*, 19(4)

Hambli, R., Frikha, S., Toumi, H. and Tavares, J.M.R.S. (2016) 'Finite element prediction of

fatigue damage growth in cancellous bone', *Computer Methods in Biomechanics and Biomedical Engineering*, 19(5), pp. 563–570.

Hambli, R. and Hattab, N. (2013) 'Application of Neural Network and Finite Element Method for Multiscale Prediction of Bone Fatigue Crack Growth in Cancellous Bone', in Gefen, A. (ed.) *Multiscale Computer Modeling in Biomechanics and Biomedical Engineering*. Berlin: Springer-Verlag, pp. 3–30.

Hansson, T. and Roos, B. (1981) 'Microcalluses of the Trabecular in Lumber Vertebrae and their relation to the bone mineral content', *Spine*, 6(4), pp. 375–380.

Hansson, T.H., Keller, T.S. and Spengler, D.M. (1987) 'Mechanical behavior of the human lumbar spine. II. Fatigue strength during dynamic compressive loading.', *Journal of orthopaedic research : official publication of the Orthopaedic Research Society*, 5(4), pp. 479–487.

Hara, T., Tanck, E., Homminga, J. and Huiskes, R. (2002) 'The influence of microcomputed tomography threshold variations on the assessment of structural and mechanical trabecular bone properties', *Bone*, 31(1) Elsevier Science Inc., pp. 107–109.

Harrison, N.M., McDonnell, P., Mullins, L., Wilson, N., O'Mahoney, D. and McHugh, P.E. (2013) 'Failure modelling of trabecular bone using a non-linear combined damage and fracture voxel finite element approach', *Biomechanics and Modeling in Mechanobiology*, 12(2), pp. 225–241.

Hartvigsen, J., Christensen, K. and Frederiksen, H. (2003) 'Back pain remains a common symptom in old age. A population-based study of 4486 Danish twins aged 70-102', *European Spine Journal*, 12, pp. 528–534.

Helgason, B., Gilchrist, S., Ariza, O., Vogt, P., Enns-Bray, W., Widmer, R.P., Fitze, T., Pálsson, H., Pauchard, Y., Guy, P., Ferguson, S.J. and Cripton, P.A. (2016) 'The influence of the modulus-density relationship and the material mapping method on the simulated mechanical response of the proximal femur in side-ways fall loading configuration', *Medical Engineering and Physics*, 38(7), pp. 679–689.

Helgason, B., Perilli, E., Schileo, E., Taddei, F., Brynjólfsson, S. and Viceconti, M. (2008) 'Mathematical relationships between bone density and mechanical properties: A literature review', *Clinical Biomechanics*, 23(2), pp. 135–146.

Hernandez, C.J., Lambers, F.M., Widjaja, J., Chapa, C. and Rimnac, C.M. (2014) 'Quantitative relationships between microdamage and cancellous bone strength and stiffness', *Bone*, 66 Elsevier Inc., pp. 205–213.

Holm, S., Maroudas, A., Urban, J., Selstam, G. and Nachemson, A. (1981) 'Nutrition of the intervertebral disc: solute transport and metabolism', *Connective tissue research*, 8(2), pp. 101–119.

Hoy, D., Bain, C., Williams, G., March, L., Brooks, P., Blyth, F., Woolf, A., Vos, T. and Buchbinder, R. (2012) A systematic review of the global prevalence of low back pain *Arthritis and Rheumatism*. Available at: 10.1002/art.34347 (Accessed: 18 August 2014).

Hoy, D., Brooks, P., Blyth, F. and Buchbinder, R. (2010) 'The Epidemiology of low back pain', *Best Practice and Research: Clinical Rheumatology*, 24(6) Elsevier Ltd, pp. 769–781.

Huber, G., Skrzypiec, D.M., Klein, A., Püschel, K. and Morlock, M.M. (2010) 'High cycle fatigue behaviour of functional spinal units.', *Ind Health*, 48(5), pp. 550–556.

Hughes, J.M., Charkoudian, N., Barnes, J.N. and Morgan, B.J. (2016) 'Revisiting the debate: Does exercise build strong bones in the mature and senescent skeleton?', *Frontiers in Physiology*, 7(SEP), pp. 1–8.

Hulshof, C. and Veldhuijzen van Zanten, B. (1987) 'Whole-body vibration and low-back pain', *International Archives of Occupational and Environmental Health*, 59(3), pp. 205–220. Available at: 10.1007/BF00377733 (Accessed: 7 October 2014).

Hutson, M. (2018) 'Artificial intelligence faces reproducibility crisis', *Science*, 359(6377), p. 725 LP-726.

Institute for Work & Health (2012) *Factors affecting RTW following acute Low-back pain*. Toronto, Canada.

ISO/BS EN (2017) *ISO 8041-1 : 2017 BSI Standards Publication Human response to vibration — Measuring instrumentation*.

ISO (1997) *ISO 2631-1: Mechanical vibration and shock - evaluation of human exposure to whole-body vibration, part 1: general requirements*.

ISO (1974) *ISO 2631 - Guide for the evaluation of human exposure to whole-body vibration*.

ISO (2004) *ISO 2631-5: Mechanical vibration and shock - Evaluation of human exposure to whole-body vibration - Part 5: Method for evaluation of vibration containing multiple shocks*. International Organization for Standardization, Geneva, Switzerland.

Jaumard, N. V., Welch, W.C. and Winkelstein, B.A. (2011) 'Spinal Facet Joint Biomechanics and Mechanotransduction in Normal, Injury and Degenerative Conditions', *Journal of Biomechanical Engineering*, 133(7), p. 071010.

Jenkins, J. (2014) 'Sickness absence in the labour market February 2014', *Office for National Statistics*, (February), pp. 1–21.

Johnson, J.E. and Troy, K.L. (2017) 'Validation of a new multiscale finite element analysis approach at the distal radius', *Medical Engineering & Physics*, 44 Elsevier Ltd, pp. 16–24.

Jones, B., Manikowski, R., Harris, J., Dziados, J. and Norton, S. (1988) *Incidence of and risk factors for injury and illness among male and female Army basic trainees*. Natick, Massachusetts.

Kalichman, L., Kim, D.H., Li, L., Guermazi, A. and Hunter, D.J. (2010) 'Computed tomography-evaluated features of spinal degeneration: prevalence, intercorrelation, and association with self-reported low back pain', *Spine Journal*, 10(3), pp. 200–208.

Kanda, H., Murayama, Y., Tanaka, M. and Suzuki, K. (1980) 'Ergonomical Methods of Evaluating Repeated Shocks and Vibrations on High Speed Ships (1st Report)', *Japan Institute of Navigation*, 63, pp. 1–10.

Kanda, H., Murayama, Y., Tanaka, M. and Suzuki, K. (1982) 'Ergonomical Methods of Evaluating Repeated Shocks and Vibrations on High Speed Ships (Final Report)', *Japan Institute of Navigation*, 67, pp. 35–44.

Kasra, M. and Grynpas, M.D. (1998) 'Static and dynamic finite element analyses of an idealized structural model of vertebral trabecular bone.', *Journal of biomechanical engineering*, 120(2), pp. 267–72. Available at: http://www.ncbi.nlm.nih.gov/pubmed/10412389 (Accessed: 3 January 2018).

Katz, J.N. (2006) 'Lumbar disc disorders and low-back pain: socioeconomic factors and consequences.', *The Journal of bone and joint surgery. American volume*, 88 Suppl 2, pp. 21–4.

Kearns, S.D. and Vandiver, J.K. (2001) *Analysis and Mitigation of Mehcanical Shock Effects on High Speed Planing boats*.

Keaveny, T.M. and Hayes, W.C. (1993) 'A 20- year perspective on the mechanical properties of trabecular bone', *J Biomech Eng*, 115(November 1993), pp. 534–542.

Keaveny, T.M., Pinilla, T.P., Crawford, R.P., Kopperdahl, D.L. and Lou, A. (1997) 'Systematic and random errors in compression testing of trabecular bone', *Journal of Orthopaedic Research*, 15(1), pp. 101–110.

Keller, T.S. (1994) 'Predicting the compressive mechanical behavior of bone', *Journal of Biomechanics*, 27(9), pp. 1159–1168.

Kelsey, J.L. (1975) 'An epidemiological study of acute herniated lumbar intervertebral discs.', *Rheumatology Rehabilitation*, 14(June 1971), pp. 144–155.

Kettler, A. and Wilke, H.J. (2006) 'Review of existing grading systems for cervical or lumbar disc and facet joint degeneration', *European Spine Journal*, 15(6), pp. 705–718.

Kitazaki, S. and Griffin, M.J. (1997) 'a Modal Analysis of Whole-Body Vertical Vibration, Using a Finite Element Model of the Human Body', *Journal of Sound and Vibration*, 200, pp. 83–103.

Kitchen, M.J., Buckley, G.A., Gureyev, T.E., Wallace, M.J., Andres-Thio, N., Uesugi, K., Yagi, N. and Hooper, S.B. (2017) 'CT dose reduction factors in the thousands using X-ray phase contrast', *Scientific Reports*, 7(1) Springer US, pp. 1–9.

Knox, J., Orchowski, J., Scher, D.L., Owens, B.D., Burks, R. and Belmont, P.J. (2011) 'The Incidence of Low Back Pain in Active Duty United States Military Service Members', *Spine*, 36(18), pp. 1492–1500. Available at: 10.1097/BRS.0b013e3181f40ddd (Accessed: 26 September 2017).

Knutsson, F. (1944) 'The Instability Associated with Disk Degeneration in the Lumbar Spine', *Acta Radiologica*, 25(5–6), pp. 593–609.

Kosmopoulos, V. and Keller, T.S. (2003) 'Finite element modeling of trabecular bone damage', *Computer Methods in Biomechanics and Biomedical Engineering*, 6(3), pp. 209–216.

Kosmopoulos, V., Schizas, C. and Keller, T.S. (2008) 'Modeling the onset and propagation of trabecular bone microdamage during low-cycle fatigue', *Journal of Biomechanics*, 41, pp. 515–522.

Kourtis, D., Magnusson, M.L., Smith, F., Hadjipavlou, A. and Pope, M.H. (2004) 'Spine height and disc height changes as the effect of hyperextension using stadiometry and MRI.', *The Iowa orthopaedic journal*, 24 University of Iowa, pp. 65–71. Available at: http://www.ncbi.nlm.nih.gov/pubmed/15296209 (Accessed: 4 July 2017).

van der Kraan, P.M. and van den Berg, W.B. (2007) Osteophytes: relevance and biology *Osteoarthritis and Cartilage*. W.B. Saunders, Available at: 10.1016/j.joca.2006.11.006 (Accessed: 20 October 2017).

Kuijer, P.P.F.M., Frings-Dresen, M.H.W., Gouttebarge, V., van Dieën, J.H., van der Beek, A.J. and Burdorf, A. (2011) 'Low back pain: we cannot afford ignoring work.', *The spine journal : official journal of the North American Spine Society*, 11(2), p. 164; author reply 165-6. Available at: 10.1016/j.spinee.2010.10.016 (Accessed: 3 December 2014).

Kyere, K.A., Than, K.D., Wang, A.C., Rahman, S.U., Valdivia-Valdivia, J.M., Marca, F. La and Park, P. (2012) 'Schmorl's nodes', *European Spine Journal*, 21(11), pp. 2115–2121.

Lafferty, J.F. (1978) 'Analytical model of the fatigue characteristics of bone', *Aviation, space, and environmental medicine*, 49(1 Pt. 2), pp. 170–174.

Lambers, F.M., Bouman, A.R., Rimnac, C.M. and Hernandez, C.J. (2013) 'Microdamage caused by fatigue loading in human cancellous bone: relationship to reductions in bone biomechanical performance.', *PLoS ONE*, 8(12), p. e83662.

Lambers, F.M., Bouman, A.R., Tkachenko, E. V., Keaveny, T.M. and Hernandez, C.J. (2014) 'The effects of tensile-compressive loading mode and microarchitecture on microdamage in human vertebral cancellous bone', *Journal of Biomechanics*, 47(15) Elsevier, pp. 3605–3612.

Lamer, T.J. (1999) 'Lumbar spine pain originating from vertebral osteophytes', *Regional Anesthesia and Pain Medicine*, 24(4) No longer published by Elsevier, pp. 347–351. Available at: 10.1016/S1098-7339(00)90025-7 (Accessed: 20 October 2017).

Lee, B.B., Cripps, R.A., Fitzharris, M. and Wing, P.C. (2014) 'The global map for traumatic spinal cord injury epidemiology: update 2011, global incidence rate', *Spinal Cord*, 52(2) Nature Publishing Group, pp. 110–116. Available at: 10.1038/sc.2012.158 (Accessed: 25 August 2017).

Lee, C.R., Iatridis, J.C., Poveda, L. and Alini, M. (2006) 'In Vitro Organ Culture of the Bovine Intervertebral Disc', *Spine*, 31(5), pp. 515–522.

Lee, T.C., O'Brien, F.J. and Taylor, D. (2000) 'Nature of fatigue damage in bone', *International Journal of Fatigue*, 22(10), pp. 847–853.

Leng, H., Wang, X., Ross, R.D., Niebur, G.L. and Roeder, R.K. (2008) 'Micro-Computed Tomography of Fatigue Microdamage in Cortical Bone Using a Barium Sulfate Contrast Agent', *J Mech Behav Biomed Mater*, 1(1), pp. 68–75.

LeResche, L. (1999) *Gender Considerations in the Epidemiology of Chronic Pain*., *Epidemiology of Pain* Available at: http://www.pain-initiative-un.org/doc-center/en/docs/GENDER CONSIDERATIONS IN THE EPIDEMIOLOGY OF CHRONIC PAIN.pdf (Accessed: 14 November 2014).

Lewinnek, G.E. and Warfield, C.A. (1986) 'Facet joint degeneration as a cause of low back pain', *Clinical Orthopaedics and Related Research*, 213

Lewis, C.H. and Griffin, M.J. (1998) 'A comparison of evaluations and assessments obtained using alternative standards for predicting the hazards of whole-body vibration and repeated shocks', *Journal of Sound and Vibration*, 215(4), pp. 915–926.

Linde, F., Hvid, I. and Madsen, F. (1992) 'The effect of specimen geometry on the mechanical behaviour of trabecular bone specimens', *Journal of Biomechanics*, 25(4), pp. 359–368.

Linde, F., Nørgaard, P., Hvid, I., Odgaard, A. and Søballe, K. (1991) 'Mechanical properties of trabecular bone. Dependency on strain rate', *Journal of Biomechanics*, 24(9), pp. 803–809.

Lines, J.A. and Stayner, R.M. (1999) *Ride vibration reduction of shocks arising from overtravel of seat suspension*.

Luoma, K., Riihimäki, H., Luukkonen, R., Raininko, R., Viikari-Juntura, E. and Lamminen, A. (2000) 'Low Back Pain in Relation to Lumbar Disc Degeneration', *Spine*, 25(4)

Maeda, S., Mansfield, N.J. and Shibata, N. (2008) 'Evaluation of subjective responses to whole-body vibration exposure: Effect of frequency content', *International Journal of Industrial Ergonomics*, 38, pp. 509–515.

Magnusson, M.L., Aleksiev, A., Wilder, D.G., Pope, M.H., Spratt, K., Lee, S.H., Goel, V.K. and Weinstein, J.N. (1996) 'European Spine Society —The Acromed Prize for Spinal Research 1995 Unexpected load and asymmetric posture as etiologic factors in low back pain', *European Spine Journal*, 5(1), pp. 23–35.

Malko, J.A., Hutton, W.C. and Fajman, W.A. (2002) 'An in vivo MRI study of the changes in volume (and fluid content) of the lumbar intervertebral disc after overnight bed rest and during an 8-hour walking protocol.', *Journal of spinal disorders & techniques*, 15(2), pp.

157–163. Available at: 10.1097/00024720-200204000-00012 (Accessed: 5 July 2017).

Malmivaara, A. (1987) 'Disc Degeneration in the Thoracolumbar Junctional Region', *Acta Radiologica*, 28(6), pp. 755–760.

Manchikanti, L. (2000) 'Topical Review', *Pain Physician*, 3(2), pp. 167–192.

Mandiakis, N. and Gray, A. (2000) 'The economic burden of low back pain in the United Kingdom', *Pain*, 84(1), pp. 95–103.

Mansfield, N., Huang, Y. and Thirulogasingam, T. (2016) 'Does Ultra Low Cost = Ultra Low Quality? Dynamic Performance of Budget Data Logging Accelerometers', *51st United Kingdom Conference on Human Responses to Vibration*. Gosport.

Mansfield, N.J. and Griffin, M.J. (2000) 'Non-linearities in apparent mass and transmissibility during exposure to whole-body vertical vibration', *Journal of Biomechanics*, 33, pp. 933–941.

Maritime and Coastguard Agency (2007a) '*The merchant shipping and fishing vessels (Control of vibration at work) regulations 2007*', 353(February), pp. 1–25.

Maritime and Coastguard Agency (2007b) *MGN 436 ( M + F ) WHOLE-BODY VIBRATION : Guidance on Mitigating Against the Effects of Shocks and Impacts on Small*.

McIlraith, M.L.L., Paddan, G.S. and Serrao, K.M. (2014) *Crew Exposure to Whole-Body Vibration in MOD Small Marine Craft*.

McLaughlin, R., Nielsen, L. and Waller, M. (2008) 'An Evaluation of the Effect of Military Service on Mortality: Quantifying the Healthy Soldier Effect', *Annals of Epidemiology*, 18(12), pp. 928–936.

McNamara, L.M. and Prendergast, P.J. (2007) 'Bone remodelling algorithms incorporating both strain and microdamage stimuli', *Journal of Biomechanics*, 40(6), pp. 1381–1391.

Meucci, R.D., Fassa, A.G. and Faria, N.M.X. (2015) 'Prevalence of chronic low back pain: systematic review.', *Revista de saude publica*, 49, p. 1.

Michel, M.C., Guo, X.D.E., Gibson, L.J., McMahon, T.A. and Hayes, W.C. (1993) 'Compressive fatigue behavior of bovine trabecular bone', *Journal of Biomechanics*, 26(4–5), pp. 453–463.

Miller, J.A., Schmatz, C. and Schultz, A.B. (1988) 'Lumbar disc degeneration: correlation with age, sex, and spine level in 600 autopsy specimens.', *Spine*, 13(2), pp. 173–8. Available at: 10.1097/00007632-198802000-00008 (Accessed: 6 July 2017).

Ministry of Defence (2017a) *Annual Medical Discharges in the UK Regular Armed Forces*.

Ministry of Defence (2017b) *UK Armed Forces Recovery Capability : Wounded , Injured and Sick in the recovery pathway, 1 October 2010 to 1 April 2017 Key Points and Trends*.

Miwa, T. (1967) 'Evaluation Methods for Vibration Effect: Part 1. Measurements of Threshold and Equal Sensation Contours of Whole Body for Vertical and Horizontal Vibration', *Industrial Health*, 5, pp. 183–205.

Miwa, T. (1968) 'Evaluation Methods for Vibration Effect: Part 4. Measurements of Vibration Greatness for Whole Body and Hand in Vertical and Horizontal Vibrations', *Industrial Health*, 6, pp. 1–10.

Monaghan, S.J. and Twest, D.C. Van (2004) 'WHOLE-BODY VIBRATION – REVIEW OF AUSTRALIAN AND INTERNATIONAL STANDARDS AND THE FUTURE Whole-Body Vibration History of WBV Evolution of WBV Standards', *Acoustics*., pp. 609–614.

Monnier, A., Djupsjöbacka, M., Larsson, H., Norman, K. and Äng, B.O. (2016) 'Risk factors

for back pain in marines; a prospective cohort study', *BMC Musculoskeletal Disorders*, 17(1) BMC Musculoskeletal Disorders, p. 319.

Montez, J.K., Hummer, R.A. and Hayward, M.D. (2012) 'Educational Attainment and Adult Mortality in the United States: A Systematic Analysis of Functional Form', *Demography*, 49(1), pp. 315–336.

Moore, T.L.A. and Gibson, L.J. (2002) 'Microdamage accumulation in bovine trabecular bone in uniaxial compression.', *Journal of biomechanical engineering*, 124(1), pp. 63–71.

Moore, T.L.A. and Gibson, L.J. (2003a) 'Fatigue microdamage in bovine trabecular bone.', *Journal of biomechanical engineering*, 125(December), pp. 769–776.

Moore, T.L.A. and Gibson, L.J. (2003b) 'Fatigue of Bovine Trabecular Bone', *Journal of Biomechanical Engineering*, 125(December), p. 761.

Moore, T.L.A., O'Brien, F.J. and Gibson, L.J. (2004) 'Creep does not contribute to fatigue in bovine trabecular bone.', *Journal of biomechanical engineering*, 126(3), pp. 321–329.

Morgan, E.F., Bayraktar, H.H. and Keaveny, T.M. (2003) 'Trabecular bone modulus-density relationships depend on anatomic site', *Journal of Biomechanics*, 36(7), pp. 897–904.

Morgan, E.F. and Keaveny, T.M. (2001) 'Dependence of yield strain of human trabecular bone on anatomic site', *Journal of Biomechanics*, 34, pp. 569–577.

Morgan, E.F., Yeh, O.C. and Keaveny, T.M. (2005) 'Damage in trabecular bone at small strains', *European Journal of Morphology*, 42(1–2), pp. 13–21.

Morioka, M. and Griffin, M.J. (2010) 'Magnitude-dependence of equivalent comfort contours for fore-and-aft, lateral, and vertical vibration at the foot for seated persons', *Journal of Sound and Vibration*, 329, pp. 2939–2952.

Morrison, J. and Robinson, D. (2001) The evaluation of human spinal response to vibration with mechanical shocks of 0.5 to 4 G amplitude *Canadian Acoustics*. Available at: http://jcaa.caa-aca.ca/index.php/jcaa/article/view/1368 (Accessed: 8 January 2015).

Mosekilde, L. (1988) 'Age-related changes in vertebral trabecular bone architecture—assessed by a new method', *Bone*, 9(4) Elsevier, pp. 247–250. Available at: 10.1016/8756-3282(88)90038-5 (Accessed: 26 September 2017).

Mosekilde, L. and Mosekilde, L. (1986) 'Normal vertebral body size and compressive strength: Relations to age and to vertebral and iliac trabecular bone compressive strength', *Bone*, 7(3), pp. 207–212.

Mostakhdemin, M., Amiri, I.S. and Syahrom, A. (2016) 'Multi-axial Fatigue of Trabecular Bone with Respect to Normal Walking', in Kumar, A. and Rao, A. A. (eds.) *Forensic and Medical Bioinformatics*. Springer, p. 61.

Murakami, Y. (1988) 'Correlation between strain singularity at crack tip under overall plastic deformation and the exponent of the Coffin-Manson law', *ASTM special technical publication*, , pp. 1048–1065.

Nachemson, A. (1966) 'The load on lumbar disks in different positions of the body', *Clin Orthop Relat Res.*, (45), pp. 107–122.

Nachemson, A., Lewin, T., Maroudas, A. and Freeman, M.A.R. (1970) 'In Vitro Diffusion of Dye Through the End-Plates and the Annulus Fibrosus of Human Lumbar Inter-Vertebral Discs', *Acta Orthopaedica Scandinavica*, 41(6), pp. 589–607.

Nagaraja, S., Couse, T.L. and Guldberg, R.E. (2005) 'Trabecular bone microdamage and microstructural stresses under uniaxial compression', *Journal of Biomechanics*, 38, pp. 707–716.

Navy Command Secretariat FOI Section (2016) *Secretary of States in Defence of MOD derogation regulations within this legislation period*

Nawayseh, N. and Griffin, M.J. (2005) 'Non-linear dual-axis biodynamic response to fore-and-aft whole-body vibration', *Journal of Sound and Vibration*, 282, pp. 831–862.

Nesterets, Y.I., Gureyev, T.E. and Dimmock, M.R. (2018) '*Optimisation of a propagation-based x-ray phase-contrast micro-CT system*', IOP Publishing

Niebur, G.L., Feldstein, M.J., Yuen, J.C., Chen, T.J. and Keaveny, T.M. (2000) 'High-resolution finite element models with tissue strength asymmetry accurately predict failure of trabecular bone', *Journal of Biomechanics*, 33, pp. 1575–1583.

Nissen, L.R., Marott, J.L., Gyntelberg, F. and Guldager, B. (2014) 'Deployment-Related Risk Factors of Low Back Pain: A Study Among Danish Soldiers Deployed to Iraq', *Military Medicine*, 179(4), pp. 451–458.

O'Hanlon, J.F. and McCauley, M.E. (1974) 'Motion Sickness Incidence as a Function of the Frequency and Acceleration of Vertical Sinusoidal Motion', *Aerospace Medicine*, 45(4), pp. 366–369.

Oborne, D.J. (1983) 'Whole-Body Vibration and International Standard ISO 2631: A Critique', *Human Factors : The Journal of the Human Factors and Ergonomics Society*, 25(1), pp. 55–69.

Oborne, D.J. (1978) 'The stability of equal sensation contours for whole-body vibration.', *Ergonomics*, 21(January 2015), pp. 651–658.

Oftadeh, R., Perez-Viloria, M., Villa-Camacho, J.C., Vaziri, A. and Nazarian, A. (2015) 'Biomechanics and Mechanobiology of Trabecular Bone: A Review.', *Journal of biomechanical engineering*, 137(1), pp. 1–15.

Ogata, K. and Whiteside, L.A. (1981) '1980 Volvo award winner in basic science. Nutritional pathways of the intervertebral disc. An experimental study using hydrogen washout technique.', *Spine*, 6(3), pp. 211–6.

Öhman, C., Baleani, M., Perilli, E., Dall'Ara, E., Tassani, S., Baruffaldi, F. and Viceconti, M. (2007) 'Mechanical testing of cancellous bone from the femoral head: Experimental errors due to off-axis measurements', *Journal of Biomechanics*, 40(11), pp. 2426–2433.

Olausson, K. and Garme, K. (2015) 'Prediction and evaluation of working conditions on high-speed craft using suspension seat modelling', *Proceedings of the Institution of Mechanical Engineers, Part M: Journal of Engineering for the Maritime Environment*, 229(3), pp. 281–290.

Paajanen, H., Lehto, I., Alanen, A., Erkintalo, M. and Komu, M. (1994) 'Diurnal fluid changes of lumbar discs measured indirectly by magnetic resonance imaging', *Journal of Orthopaedic Research*, 12(4), pp. 509–514. Available at: 10.1002/jor.1100120407 (Accessed: 4 July 2017).

Pal, S. (2014) 'Design of artificial human joints & organs', *Design of Artificial Human Joints & Organs*, 9781461462, pp. 1–419.

Pape, R.W., Becker, F.F., Drum, D.E. and Goldman, D.E. (1963) 'Some effects of vibration on totally immersed cats', *Journal of Applied Physiology*, 18(6), p. 1193 LP-1200.

Pauwels, R., Jacobs, R., Singer, S.R. and Mupparapu, M. (2015) 'CBCT-based bone quality assessment: Are Hounsfield units applicable?', *Dentomaxillofacial Radiology*, 44(1)

Pearce, A.I., Richards, R.G., Milz, S., Schneider, E. and Pearce, S.G. (2007) 'Animal models for implant biomaterial research in bone: A review', *European Cells and Materials*, 13(0), pp.

1–10.

Pelker, R.R., Friedlaender, G.E., Markham, T.C., Panjabi, M.M. and Moen, C.J. (1983) 'Effects of freezing and freeze-drying on the biomechanical properties of rat bone', *Journal of Orthopaedic Research*, 1(4) Wiley Subscription Services, Inc., A Wiley Company, pp. 405–411. Available at: 10.1002/jor.1100010409 (Accessed: 3 January 2018).

Petit, A., Roquelaure, Y., Seidler, A., Bergmann, A., Jäger, M., Ellegast, R., Ditchen, D., Elsner, G., Grifka, J., Haerting, J., Hofmann, F., Linhardt, O., Luttmann, A., Michaelis, M., Petereit-Haack, G., Schumann, B., Bolm-Audorff, U. and Deyo, R.A. (2015) 'Cumulative occupational lumbar load and lumbar disc disease--results of a German multi-center case-control study (EPILIFT).', *BMC musculoskeletal disorders*, 15(1), pp. 272–4.

Pfirrmann, C.W. and Resnick, D. (2001) 'Schmorl nodes of the thoracic and lumbar spine: radiographic-pathologic study of prevalence, characterization, and correlation with degenerative changes of 1,650 spinal levels in 100 cadavers.', *Radiology*, 219(2), pp. 368–374. Available at: 10.1148/radiology.219.2.r01ma21368 (Accessed: 8 September 2017).

Pfirrmann, C.W.A., Metzdorf, A., Zanetti, M., Hodler, J. and Boos, N. (2001) 'Magnetic Resonance Classification of Lumbar Intervertebral Disc Degeneration', *Spine*, 26(17), pp. 1873–1878. Available at: 10.1097/00007632-200109010-00011 (Accessed: 4 July 2017).

Pisula, P.J. (2002) *Modelling the comprehensive mechanical anisotropic material properties of human lumbar vertebral cancellous bone*. University of Strathclyde.

Poisson, R. (2015) 'The imperative of military medical research and the duty to protect, preserve, and provide advanced evidence-informed care', *Journal of Military, Veteran and Family Health*, 1(1), pp. 11–13.

Pollintine, P., Dolan, P., Tobias, J.H. and Adams, M.A. (2004) 'Intervertebral Disc Degeneration Can Lead to "Stress-Shielding" of the Anterior Vertebral Body: A Cause of Osteoporotic Vertebral Fracture?', *Spine*, 29(7)

Pope, M.H. and Hansson, T.H. (1992) 'Vibration of the spine and low back pain.', *Clinical orthopaedics and related research*, (279), pp. 49–59.

Poumarat, G. and Squire, P. (1993) 'Comparison of mechanical properties of human, bovine bone and a new processed bone xenograft.', *Biomaterials*, 14(5), pp. 337–40. Available at: http://www.ncbi.nlm.nih.gov/pubmed/8507776 (Accessed: 9 January 2018).

Putz-Anderson, V., Bernard, B. and Burt, S. (1997) 'Musculoskeletal disorders and workplace factors', *National Institute for Occupational Safety and Health*, 97–141(July 1997), pp. 1-1-7–11.

Radebold, A., Cholewicki, J., Panjabi, M.M. and Patel, T.C. (2000) 'Muscle Response Pattern to Sudden Trunk Loading in Healthy Individuals and in Patients with Chronic Low Back Pain', *Spine*, 25(8)

Rantaharju, T., Mansfield, N.J., Ala-Hiiro, J.M. and Gunston, T.P. (2015) 'Predicting the health risks related to whole-body vibration and shock: a comparison of alternative assessment methods for high-acceleration events in vehicles', *Ergonomics*, 58(7), pp. 1071–1087.

Rapillard, L., Charlebois, M. and Zysset, P.K. (2006) 'Compressive fatigue behavior of human vertebral trabecular bone.', *J Biomech*, 39, pp. 2133–2139.

Read, C. and Pillay, J. (2000) 'Injuries sustained by aircrew on ejecting from their aircraft.', *Journal of accident & emergency medicine*, 17(5), pp. 371–373.

Regulations, A.O.F. (2005) *HEALTH AND SAFETY The Control of Vibration at Work Regulations 2005*. UK Statutory Instruments,

Reilly, D.T. and Burstein, A.H. (1975) 'The elastic and ultimate properties of compact bone tissue', *Journal of Biomechanics*, 8(6), pp. 393–405.

van Rietbergen, B., Weinans, H., Huiskes, R. and Odgaard, a. (1995) 'A new method to determine trabecular bone elastic properties and loading using micromechanical finite-element models', *Journal of Biomechanics*, 28(1), pp. 69–81.

Roffey, D.M., Wai, E.K., Bishop, P., Kwon, B.K. and Dagenais, S. (2010a) 'Causal assessment of workplace manual handling or assisting patients and low back pain: results of a systematic review.', *The spine journal : official journal of the North American Spine Society*, 10(7) Elsevier Inc, pp. 639–51. Available at: 10.1016/j.spinee.2010.04.028 (Accessed: 20 September 2014).

Roffey, D.M., Wai, E.K., Bishop, P., Kwon, B.K. and Dagenais, S. (2010b) 'Causal assessment of awkward occupational postures and low back pain: results of a systematic review.', *The spine journal : official journal of the North American Spine Society*, 10(1) Elsevier Inc, pp. 89–99. Available at: 10.1016/j.spinee.2009.09.003 (Accessed: 22 September 2014).

Roffey, D.M., Wai, E.K., Bishop, P., Kwon, B.K. and Dagenais, S. (2010c) 'Causal assessment of occupational pushing or pulling and low back pain: results of a systematic review.', *The spine journal : official journal of the North American Spine Society*, 10(6) Elsevier Inc, pp. 544–53. Available at: 10.1016/j.spinee.2010.03.025 (Accessed: 6 October 2014).

Roffey, D.M., Wai, E.K., Bishop, P., Kwon, B.K. and Dagenais, S. (2010d) 'Causal assessment of occupational sitting and low back pain: results of a systematic review.', *The spine journal : official journal of the North American Spine Society*, 10(3) Elsevier Inc, pp. 252–61. Available at: 10.1016/j.spinee.2009.12.005 (Accessed: 17 September 2014).

Roffey, D.M., Wai, E.K., Bishop, P., Kwon, B.K. and Dagenais, S. (2010e) 'Causal assessment of occupational standing or walking and low back pain: results of a systematic review.', *The spine journal : official journal of the North American Spine Society*, 10(3) Elsevier Inc, pp. 262–72. Available at: 10.1016/j.spinee.2009.12.023 (Accessed: 6 October 2014).

Roman, J. (1958) Effect of severe whole-body vibration on mice and methods of protection from vibration injury *WADC Technical Report*. ASTIA Document No. AD 15107,

Rüegsegger, P., Elsasser, U., Anliker, M., Gnehm, H., Kind, H. and Prader, A. (1976) 'Quantification of Bone Mineralization Using Computed Tomography', *Radiology*, 121(1) The Radiological Society of North America , pp. 93–97. Available at: 10.1148/121.1.93 (Accessed: 1 February 2018).

Sandover, J. (1983) Dynamic Loading as a Possible Source of Low-Back Disorders *Spine*.

Sandover, J. (1998) 'The FATIGUE APPROACH TO VIBRATION AND HEALTH: IS IT A PRACTICAL AND VIABLE WAY OF PREDICTING THE EFFECTS ON PEOPLE?', *Journal of Sound and Vibration*, 215, pp. 699–721.

Schneider, C.A., Rasband, W.S. and Eliceiri, K.W. (2012) 'NIH Image to ImageJ: 25 years of image analysis', *Nature Methods*, 9 Nature Publishing Group, a division of Macmillan Publishers Limited. All Rights Reserved., p. 671.

Schram-Bijkerk, D. and Bogers, R.P. (2011) *Cancer incidence and cause-specific mortality following Balkan deployment*.

Schultz, D.S., Rodriguez, A.G., Hansma, P.K. and Lotz, J.C. (2009) 'Mechanical profiling of intervertebral discs', *Journal of Biomechanics*, 42(8) NIH Public Access, pp. 1154–1157. Available at: 10.1016/j.jbiomech.2009.02.013 (Accessed: 4 July 2017).

Schust, M., Kreisel, A., Seidel, H. and Bluthner, R. (2010) 'Examination of the Frequency-weighting Curve for Accelerations Measured on the Seat and at the Surface Supporting the

Feet during Horizontal Whole-body Vibrations in x- and y-Directions', *Industrial Health*, 48(5), pp. 725–742.

Seidel, H. (1993) 'Selected health risks caused by long-term, whole-body vibration', *American Journal of Industrial Medicine*, 23(4), pp. 589–604.

Seidel, H. (2004) *Effects and Evaluation of Whole-Body Vibration - Biological Aspects. (German)*. Germany

Seidel, H., Blüthner, R. and Hinz, B. (2001) 'Application of finite-element models to predict forces acting on the lumbar spine during whole-body vibration.', *Clin Biomech (Bristol, Avon)*, 16 Suppl 1, pp. S57–S63.

Seidel, H., Blüthner, R., Hinz, B. and Schust, M. (1998) 'ON THE HEALTH RISK OF THE LUMBAR SPINE DUE TO WHOLE-BODY VIBRATION—THEORETICAL APPROACH, EXPERIMENTAL DATA AND EVALUATION OF WHOLE-BODY VIBRATION', *Journal of Sound and Vibration*, 215, pp. 723–741.

Seidel, H. and Heide, R. (1986) 'Long-term effects of whole-body vibration: a critical survey of the literature.', *International archives of occupational and environmental health*, 58(1), pp. 1–26. Available at: http://www.ncbi.nlm.nih.gov/pubmed/3522434 (Accessed: 7 October 2014).

Seidel, H., Hinz, B., Blüthner, R., Menzel, G., Hofmann, J., Gericke, L., Schust, M., Kaiser, H. and Mischke, C. (2007a) 'Annex 19 to Final Technical Report: Prediction of spinal stress in drivers from field measurements', *FP5 Project No. QLK4-2002-02650*, , pp. 1–86.

Seidel, H., Hinz, B., Blüthner, R., Menzel, G., Hofmann, J., Gericke, L., Schust, M., Kaiser, H. and Mischke, C. (2007b) '*Annex 18 to Final Technical Report: Whole-body vibration experimental work and biodynamic modelling*', , pp. 1–68.

Seidel, H., Hinz, B., Blüthner, R., Menzel, G., Hofmann, J., Gericke, L., Schust, M., Kaiser, H. and Mischke, C. (2007c) 'Annex 19 to Final Technical Report: Prediction of spinal stress in drivers from field measurements', *FP5 Project No. QLK4-2002-02650*, , pp. 1–86.

Seref-Ferlengez, Z., Kennedy, O.D. and Schaffler, M.B. (2015) 'Bone microdamage, remodeling and bone fragility: how much damage is too much damage?', *BoneKEy Reports*, 4 Springer Nature Available at: 10.1038/bonekey.2015.11 (Accessed: 10 January 2018).

Serrao, K.M. and Paddan, G.S. (2013) 'Measuring whole-body vibration on high speed military craft: procedures, issues and complications', *48th United Kingdom Conference on Human Responses to vibration*. Ascot, pp. 175–184.

Sheng, S.R., Wang, X.Y., Xu, H.Z., Zhu, G.Q. and Zhou, Y.F. (2010) 'Anatomy of large animal spines and its comparison to the human spine: A systematic review', *European Spine Journal*, 19, pp. 46–56.

Shirazi-Adl, A. and Parnianpour, M. (1999) 'Effect of Changes in Lordosis on Mechanics of the Lumbar Spine-Lumbar Curvature in Lifting.', *Clinical Spine Surgery*, 12(5)

Showalter, B.L., Beckstein, J.C., Martin, J.T., Beattie, E.E., Espinoza Orías, A.A., Schaer, T.P., Vresilovic, E.J. and Elliott, D.M. (2012) 'Comparison of animal discs used in disc research to human lumbar disc: torsion mechanics and collagen content.', *Spine*, 37(15) NIH Public Access, pp. E900-7. Available at: 10.1097/BRS.0b013e31824d911c (Accessed: 6 December 2017).

Silva, M.J. and Gibson, L.J. (1997) 'Modeling the mechanical behaviour of vertebal trabecular bone: Effects of age-related changes in microstructure', *Bone*, 21(2), pp. 191–199.

Smith, L., Westrick, R., Sauers, S., Cooper, a., Scofield, D., Claro, P. and Warr, B. (2016)

'Underreporting of Musculoskeletal Injuries in the US Army: Findings From an Infantry Brigade Combat Team Survey Study', *Sports Health: A Multidisciplinary Approach*, 8(6), pp. 507–513.

Snell, R.S. (1986) *Clinical Anatomy for Medical Student*s. 3rd edn. .

Spurrier, E., Singleton, J. a. G., Masouros, S., Gibb, I. and Clasper, J. (2015) 'Blast Injury in the Spine: Dynamic Response Index Is Not an Appropriate Model for Predicting Injury', *Clinical Orthopaedics and Related Research*, 473(9), pp. 2929–2935.

Stayner, R.M. (2001) *333/2001 Whole body vibration and shock: A literature review*.

Stech, E. and Payne, P. (1969) *Dynamic Models of the Human Body*. Wright-Patterson Air Force Base, Ohio.

Takala, E.-P. (2010) 'Lack of "statistically significant" association does not exclude causality.', *The spine journal : official journal of the North American Spine Society*, 10(10) Elsevier Inc., p. 944; author reply 944-5. Available at: 10.1016/j.spinee.2010.07.008 (Accessed: 6 October 2014).

Talmage, J. (2010) 'So why does my back hurt doc?', *The spine journal : official journal of the North American Spine Society*, 10(1) Elsevier Inc., pp. 73–5. Available at: 10.1016/j.spinee.2009.11.011 (Accessed: 3 December 2014).

Taylor, M., Cotton, J. and Zioupos, P. (2002) 'Finite Element Simulation of the Fatigue Behaviour of Cancellous Bone', *Meccanica*, 37(4), pp. 419–429.

Thyagarajan, R., Ramalingam, J., Kulkarni, K.B. and Tardec, A. (2014) 'Comparing the Use of Dynamic Response Index (DRI) and Lumbar Load as Relevant Spinal Injury Metrics', *ARL Workshop on Numerical Analysis of Human and Surrogate Response to Accelerative Loading*., p. WD0046 Rev 4.

Ulrich, D., Van Rietbergen, B., Weinans, H. and Rüegsegger, P. (1998) 'Finite element analysis of trabecular bone structure: A comparison of image-based meshing techniques', *Journal of Biomechanics*, 31(12), pp. 1187–1192.

US Department of Health and Human Services (2004) 'Bone health and osteoporosis: a report of the Surgeon General', *US Health and Human Services*, , p. 437.

VDI (2002) '*Human exposure to mechanical vibrations: Whole-body vibration (Einwirkung mechanischer Schwingungen auf den Menschen: Ganzkörper-Schwingungen)*', (December)

van der Veen, A.J., van Dieën, J.H., Nadort, A., Stam, B. and Smit, T.H. (2007) 'Intervertebral disc recovery after dynamic or static loading in vitro: Is there a role for the endplate?', *Journal of Biomechanics*, 40(10), pp. 2230–2235. Available at: 10.1016/j.jbiomech.2006.10.018 (Accessed: 3 July 2017).

van der Veen, A.J., Mullender, M., Smit, T.H., Kingma, I. and van Dieën, J.H. (2005) 'Flow-related mechanics of the intervertebral disc: the validity of an in vitro model.', *Spine*, 30(18), pp. E534-9.

Vernon-Roberts, B. and Pirie, C.J. (1977) 'Degenerative changes in the intervertebral discs of the lumbar spine and their sequelae', *Rheumatology*, 16(1) Oxford University Press, pp. 13–21. Available at: 10.1093/rheumatology/16.1.13 (Accessed: 20 October 2017).

VIBRISKS (2007a) '*Risks of Occupational Vibration Exposures (VIBRISKS) Final Technical Report*'

VIBRISKS (2007b) *Risks of Occupational Vibration Exposures (VIBRISKS) Project Summary*.

Volinn, E. (1997) 'The epidemiology of low back pain in the rest of the world. A review of surveys in low- and middle-income countries.', *Spine*, 22(15), pp. 1747–54. Available at:

http://www.ncbi.nlm.nih.gov/pubmed/9259786 (Accessed: 19 September 2014).

Wachtel, E.F. and Keaveny, T.M. (1997) 'Dependence of trabecular damage on mechanical strain', *Journal of Orthopaedic Research*, 15(5), pp. 781–787.

Wahner, H., Dunn, W., Brown, M., Morin, R. and Riggs, B. (1988) 'Comparison of dual-energy x-ray absorptiometry and dual photon absorptiometry for bone mineral measurements of the lumbar spine.', *Mayo Clin Proc.*, 63(11), pp. 1075–1084.

Wai, E.K., Roffey, D.M., Bishop, P., Kwon, B.K. and Dagenais, S. (2010a) 'Causal assessment of occupational bending or twisting and low back pain: results of a systematic review.', *The spine journal : official journal of the North American Spine Society*, 10(1) Elsevier Inc, pp. 76–88. Available at: 10.1016/j.spinee.2009.06.005 (Accessed: 21 September 2014).

Wai, E.K., Roffey, D.M., Bishop, P., Kwon, B.K. and Dagenais, S. (2010b) 'Causal assessment of occupational carrying and low back pain: results of a systematic review.', *The spine journal : official journal of the North American Spine Society*, 10(7) Elsevier Inc, pp. 628–38. Available at: 10.1016/j.spinee.2010.03.027 (Accessed: 6 October 2014).

Wai, E.K., Roffey, D.M., Bishop, P., Kwon, B.K. and Dagenais, S. (2010c) 'Causal assessment of occupational lifting and low back pain: results of a systematic review.', *The spine journal : official journal of the North American Spine Society*, 10(6) Elsevier Inc, pp. 554–66. Available at: 10.1016/j.spinee.2010.03.033 (Accessed: 23 September 2014).

Walsh, K., Varnes, N., Osmond, C., Styles, R. and Coggon, D. (1989) 'Occupational causes of low-back pain.', *Scandinavian journal of work, environment & health*, 15(1), pp. 54–9. Available at: http://www.ncbi.nlm.nih.gov/pubmed/2522238 (Accessed: 7 October 2014).

Wang, X., Bank, R.A., Tekkopele, J.M. and Mauli Agrawal, C. (2001) 'The role of collagen in determining bone mechanical properties', *Journal of Orthopaedic Research*, 19(6), pp. 1021–1026.

Wang, X. and Niebur, G.L. (2006) 'Microdamage propagation in trabecular bone due to changes in loading mode', *Journal of Biomechanics*, 39, pp. 781–790.

Waterman, B.R., Belmont, P.J. and Schoenfeld, A.J. (2012) 'Low back pain in the United States: Incidence and risk factors for presentation in the emergency setting', *Spine Journal*, 12(1) Elsevier Inc, pp. 63–70.

Watson, K.D., Papageorgiou, A.C., Jones, G.T., Taylor, S., Symmons, D.P.M., Silman, A.J. and Macfarlane, G.J. (2003) 'Low back pain in schoolchildren: The role of mechanical and psychosocial factors', *Archives of Disease in Childhood*, 88(1), pp. 12–17.

Weinstein, J.N., Tosteson, T.D., Lurie, J.D., Tosteson, A.N.A., Blood, E., Hanscom, B., Herkowitz, H., Cammisa, F., Albert, T., Boden, S.D., Hilibrand, A., Goldberg, H., Berven, S., An, H. and SPORT Investigators, S. (2008) 'Surgical versus nonsurgical therapy for lumbar spinal stenosis.', *The New England journal of medicine*, 358(8) NIH Public Access, pp. 794–810. Available at: 10.1056/NEJMoa0707136 (Accessed: 18 October 2017).

Weißgraeber, P., Leguillon, D. and Becker, W. (2016) 'A review of Finite Fracture Mechanics: crack initiation at singular and non-singular stress raisers', *Archive of Applied Mechanics*, 86(1–2) Springer Berlin Heidelberg, pp. 375–401.

Whitehouse, W.J. (1974) 'The quantitative morphology of anisotropic trabecular bone', *Journal of Microscopy*, 101(2), pp. 153–168. Available at: 10.1111/j.1365-2818.1974.tb03878.x (Accessed: 5 July 2017).

Wikström, B.-O., Kjellberg, A. and Landström, U. (1994) 'Health effects of long-term occupational exposure to whole-body vibration: A review', *International Journal of Industrial Ergonomics*, 14(4), pp. 273–292.

Wikström, B.O. (1993) 'Effects from twisted postures and whole-body vibration during driving', *International Journal of Industrial Ergonomics*, 12(1–2), pp. 61–75.

Wilcox, R.K. (2007) 'The influence of material property and morphological parameters on specimen-specific finite element models of porcine vertebral bodies', *Journal of Biomechanics*, 40(3), pp. 669–673.

Wilder, D.G., Woodworth, B.B., Frymoyer, J.W. and Pope, M.H. (1982) 'Vibration and the Human Spine', *Spine*, 7(3)

Wilke, H.J., Neef, P., Caimi, M., Hoogland, T. and Claes, L.E. (1999) 'New in vivo measurements of pressures in the intervertebral disc in daily life.', *Spine*, 24(8), pp. 755–62. Available at: http://www.ncbi.nlm.nih.gov/pubmed/10222525 (Accessed: 13 October 2017).

Wolff, J. (1892) 'Das Gesetz der Transformation der Knochen (Berlin A. Hirchwild). Translated as: The Law of Bone Remodeling', *Springer-Verlag, Berlin*

Yalla, S. V and Campbell-Kyureghyan, N.H. (2010) '*Does frequency effect fatigue fracture of spine motion segments during repetitive loading?*',

Yan, Y.-B., Qi, W., Wang, J., Liu, L.-F., Teo, E.-C., Tianxia, Q., Ba, J. and Lei, W. (2011) 'Relationship between architectural parameters and sample volume of human cancellous bone in micro-CT scanning', *Medical Engineering & Physics*, 33(6) Elsevier, pp. 764–769. Available at: 10.1016/J.MEDENGPHY.2011.01.014 (Accessed: 4 January 2018).

Yingling, V.R., Callaghan, J.P. and McGill, S.M. (1999) The porcine cervical spine as a model of the human lumbar spine: an anatomical, geometric, and functional comparison *Journal of Spinal Disorders & Techniques*. Available at: http://www.ncbi.nlm.nih.gov/pubmed/10549707 (Accessed: 6 December 2017).

Yingling, V.R., Callaghan, J.P. and McGill, S.M. (1997) 'Dynamic loading affects the mechanical properties and failure site of porcine spines', *Clinical Biomechanics*, 12(5), pp. 301–305.

Zhu, T., Ai, T., Zhang, W., Li, T. and Li, X. (2015) 'Segmental quantitative MR imaging analysis of diurnal variation of water content in the lumbar intervertebral discs', *Korean Journal of Radiology*, 16(1) Korean Society of Radiology, pp. 139–145. Available at: 10.3348/kjr.2015.16.1.139 (Accessed: 4 July 2017).

Zioupos, P., Cook, R.B. and Hutchinson, J.R. (2008) 'Some basic relationships between density values in cancellous and cortical bone', *Journal of Biomechanics*, 41(9), pp. 1961–1968.

Zioupos, P. and Currey, J.. (1998) 'Changes in the Stiffness, Strength, and Toughness of Human Cortical Bone With Age', *Bone*, 22(1), pp. 57–66.